

**Identification and Analysis of Clp Protease
Substrates in *C. crescentus***

Inauguraldissertation

zur
Erlangung der Würde eines Doktors der Philosophie
vorgelegt der
Philosophisch-Naturwissenschaftlichen Fakultät
der Universität Basel

von

Sherif Tawfilis

aus Melbourne, Australien

Genehmigt von der Philosophisch-Naturwissenschaftlichen Fakultät auf
Antrag von

**Prof. Dr. Urs Jenal, Prof. Dr. Thomas A. Bickle, Prof. Dr. Christoph
Dehio**
(Mitglieder des Dissertationskomitees)

Basel, den 28.09.04

Prof. Dr. Marcel Tanner
(Dekan der Philosophisch-
Naturwissenschaftlichen Fakultät)

ACKNOWLEDGEMENTS.....	I
OVERVIEW.....	II
1 INTRODUCTION.....	1
1.1 General notes.....	1
1.2 The ClpXP proteolytic machine.....	3
1.2.1 General notes.....	3
1.2.2 The ClpX chaperone.....	4
1.2.3 The ClpP serine protease.....	6
1.2.4 Substrate recognition.....	7
1.2.5 The SsrA tag.....	8
1.2.6 Dynamics of substrate unfolding and ClpX interaction with ClpP.....	10
1.3 The ClpXP protease in <i>C. crescentus</i>.....	12
1.3.1 General notes.....	12
1.3.2 ClpXP is essential for survival.....	12
1.3.3 ClpX is required for G1-to-S phase transition.....	13
1.3.4 ClpXP degrades the master regulator CtrA.....	14
1.3.5 Why is ClpXP essential in <i>C. crescentus</i> ?.....	15
AIMS OF THESIS.....	17
2 MATERIALS AND METHODS.....	18
2.1 Pulse labelling and Pulse/Chase experiments.....	18
2.2 Immunoprecipitation.....	18
2.3 Scintillation counting.....	20
2.4 Protein preparation and two dimensional gel electrophoresis.....	20
2.5 Data Processing and Analysis.....	22
2.6 DNA manipulation and construction of plasmids and mutant alleles.....	23
2.6.1 Construction of a M2-tagged <i>clpX</i> _{ATP} allele.....	23
2.6.2 Constructs for 2D gel target evaluation.....	24
2.6.3 Construct for CC2323 chromosomal M2 tagging and deletion.....	28
2.6.4 Constructs for overexpression of the CC2323 protein.....	29
2.6.4 Constructs for SsrA tagged FlbD.....	30
2.6.5 Transfer of <i>flbD</i> tail sequences from motile suppressor mutants to wild-type cells.....	32
2.7 Microscopy.....	33
2.8 Strains and plasmids used in study.....	33

3 IDENTIFICATION OF NOVEL SUBSTRATES OF THE ClpXP PROTEASE IN *C. CRESCENTUS* 45

Abstract 45

3.1 Generation and analysis of a conditional dominant lethal allele of *clpX*..... 47

3.1.1 Construction of the *clpX*_{ATP} allele 47

3.1.2 *clpX*_{ATP} is a dominant lethal allele 49

3.1.3 ClpX_{ATP} monomers physically interact with wild-type ClpX to form mixed oligomers 50

3.1.4 ClpX_{ATP} synthesis results in filamentous cell morphology, cell death and rapid stabilisation of CtrA 51

3.2 Identification of novel ClpXP substrates in *C. crescentus* using a proteomic approach 58

3.2.1 Identification of protein spots with altered behaviour upon ClpX_{ATP} induction 59

3.2.2 Protein identification by mass spectrometry 69

3.2.3 Target validation: use of an in vivo assay to test the dependence of candidate proteins on ClpXP for degradation 75

3.3 Functional analysis of CC2323, a novel ClpXP substrate in *C. crescentus* 80

3.3.1 Expression and stability of CC2323 83

3.3.2 The product of the CC2323 gene is not essential 86

3.3.3 Overexpression phenotype of CC2323 87

3.4 DISCUSSION 91

3.4.1 The *clpX*_{ATP} allele and ClpX inactivation 91

3.4.2 Identification of ClpX substrates in *C. crescentus* 96

3.4.3 CC2323, a potential novel ClpXP substrate 98

3.5 CONCLUDING REMARKS 104

4 FUNCTIONAL ANALYSIS OF SSRA-DEPENDENT DEGRADATION IN *C. CRESCENTUS*..... 106

Abstract 106

4.1 FlbD_{Δ13}-SsrA is a substrate for the ClpXP protease 108

4.2 Cells containing SsrA-tagged FlbD are non-motile and readily give rise to motile suppressors 112

4.3 Cells bearing an undegradable version of SsrA-tagged FlbD are non-motile 124

4.4 DISCUSSION 129

4.4.1 SsrA-tagged FlbD variants as targets for the ClpXP protease 129

4.4.2 Degradation determinants in the SsrA tag 129

4.4.3 Motile suppressors with an intact SsrA tag 131

4.4.4 Novel FlbD C-termini and motility 132

4.5 CONCLUDING REMARKS.....	137
5 IDENTIFICATION OF THE PROTEASE AND THE TURNOVER SIGNAL RESPONSIBLE FOR CELL CYCLE-DEPENDENT DEGRADATION OF THE <i>CAULOBACTER</i> FLIF MOTOR PROTEIN.....	139
REFERENCES.....	151

ACKNOWLEDGEMENTS

To thank all the people who have helped me over the past few years of this PhD would simply not be feasible in a page. Suffice to say that I'll send a hearty "thank you" into the universe at large with the inner irrational certainty that it will karmically find you. There. I should like to thank Urs for his help, supervision and showing me what good science is about. Since I came to the Biocentre, I've seen around two-and-a-bit generations of budding Jeanl-ists, and I'd like to thank them in a more or less chronological order: Björn and Gaby, who, aside from the small fact of being great colleagues, have been my 2D gel teachers; Magne for being a super supervisor in the first few months I was here and teaching me the ropes about pretty crescentoid things; Martin for his help with the statistical part of my thesis; and Thomas for advice and beer. Then came the second lot. Wanda for offering the feminine element, with all its insight, in predominantly male-filled Rm. 403. Thanks for the friendship, support and the scientific discussions, without which, in times of scientific troughs, I would have gone outback and raised chickens somewhere; Assaf and Simon for being two of the most fun and interesting people I've ever met; and all three for the mindless fun, and (the strangely regular) philosophical engagements, we had. Other people/things I'd like to thank: Alex for being of great help when I needed it; the originators of kebabs and coca cola for offering brain food in those late hours; the serial-smoking and coffee-drinking strange man in the building opposite Rm. 403 for providing us with hours of speculative fun as to the nature of his life's purpose; and of course, my very close friends, especially Dolly, for support, being genuine, true, honest and caring. Rare qualities, I dare venture. If it hadn't been for you, life would have been drier, colder, *exceedingly* mundane and without much spice. Ta very much!

OVERVIEW

Proteolysis is an irreversible regulatory mechanism by which cells can remove a protein whose function is no longer required or if its presence in a particular cellular compartment and/or at a certain time is harmful to the cell. Degradation of cytoplasmic proteins is energy dependent, and in prokaryotic cells is carried out by five ATP-dependent proteases, namely, ClpXP, ClpAP, FtsH, Lon and HslUV (Gottesman and Maurizi 1992). Protein degradation has been shown to be of crucial importance for a variety of cellular processes such as stress response, DNA damage repair and cell cycle progression (Jenal and Fuchs 1998; Jenal and Hengge-Aronis 2003; Straus et al. 1988; Sutton et al. 2000).

A critical event occurring during the cell cycle progression of *C. crescentus* is the degradation of the essential master cell cycle regulator, CtrA, during the G1-to-S phase transition (Quon et al. 1996). CtrA belongs to the response regulator superfamily of proteins and aside from directly controlling the expression of about 100 genes (Laub et al. 2002; Laub et al. 2000) it suppresses DNA replication initiation by binding to several sites in the origin of replication (Quon et al. 1998). CtrA is degraded in a ClpXP-dependent manner as depletion of ClpXP results in its stabilisation. Furthermore, in the absence of ClpXP, cells are arrested at the G1 phase of the cell cycle, become filamentous and lose viability (Jenal and Fuchs 1998). A similar phenotype is observed in cells expressing a stable and constitutively active variant of CtrA (Domian et al. 1997). Inhibition of CtrA degradation alone does not cause a G1 cell cycle block, suggesting that the G1 arrest observed in cells depleted for ClpXP is not due to CtrA stabilisation. This suggests that the ClpXP-dependent

degradation of one or several additional proteins is essential for cell cycle progression and survival.

The primary aim of this work was to identify novel substrates of the ClpXP protease, particularly those whose timed degradation is critical for G1-to-S phase transition. This task is of crucial importance as previous work by Grünenfelder et al. (2001) has shown that a large fraction of the cell's proteins is rapidly degraded and differentially synthesised during the cell cycle. It is likely that a subset of these proteins is involved in cell cycle progression and control. In the first part of this thesis (Chapter 3) we created a vector that allowed the conditional expression of the dominant negative allele of *clpX*, *clpX_{ATP}*, for use in a global proteomics screen to identify ClpXP substrates. In this screen, proteins that became stable upon disruption of ClpX activity were to be identified. The rationale behind our generating the conditional *clpX_{ATP}* allele was to create a system wherein ClpX activity can be rapidly disrupted in cells. The original ClpX depletion strain created by Jenal and Fuchs (1998) required at least four hours before the ClpX protein is undetectable in cells. Since the result of ClpX depletion is ultimately cell death, use of this mutant in a proteomics screen would make it difficult to distinguish between proteins stabilised as a direct effect of ClpX depletion and those stabilised as a consequence of cell deterioration.

We found that expression of *clpX_{ATP}*, which has mutations in the walker A motif of the ATPase domain, results in rapid CtrA stabilisation, cell elongation and cell death. We propose that this is due to ClpX_{ATP} monomers inactivating ClpX through the formation of mixed oligomers with ClpX_{wt} monomers. As this study was in progress, the crystal structure of ClpX from *H. pylori* was solved revealing that the residues we

mutated in ClpX_{ATP} contact the ATP moiety and may be involved in ATP hydrolysis (Kim and Kim 2003). Thus, our results indicate that the presence of ClpX_{ATP} disrupts ClpX activity by preventing the assembly of hexameric rings, disturbing ATP binding and/or inhibiting ATP hydrolysis by the mixed ClpX hexamers. Although the nature and oligomeric state of the mixed oligomers is not clear from our results, previous work with *clpA* alleles with similar mutations in the walker A motif has demonstrated that mixed *hexamers* do form and that monomer swapping readily occurs (Seol et al. 1995; Singh and Maurizi 1994).

Through the global comparison of protein stability between wild-type and *clpX*_{ATP} expressing cells, we found nine proteins to be stabilised as a result of ClpX inactivation. These include CtrA and CheD, both previously identified as ClpXP substrates using genetic means (Jenal and Fuchs 1998; M.R.K. Alley, unpublished). Target validation confirmed that CtrA, CheD and the product of the CC2323 gene were degraded in a ClpXP-dependent manner.

CC2323 is a protein of unknown function whose orthologues are found exclusively in alpha proteobacteria. CC2323 expression was previously found to be regulated by GcrA, a cell cycle regulator that inversely oscillates with CtrA (Holtzendorff et al. 2004). We found that CC2323 synthesis is limited to the late S-, and G2- phase of the cell cycle and that its product is rapidly degraded. As a result, the CC2323 protein is only present when it is actively synthesised and is therefore absent in SW and ST cells. Our results indicate that CC2323 may be degraded by ClpXP and that its levels during the cell cycle are controlled only through its regulated expression. Although CC2323 was found to be non-essential for growth, our results indicate that its

overproduction is deleterious for cell growth and survival. Thus, it appears that either high levels of CC2323, or its undesirable presence in certain cellular compartments and/or phases of the cell cycle, have negative effects on the cells. Future analysis will aim to address the reasons why CC2323 overproduction is harmful to cells and why its cellular concentration appears stringently controlled during the cell cycle at the levels of both expression and proteolysis.

In the second part of this thesis (Chapter 4) we defined SsrA-tagged proteins as additional targets of the ClpXP protease in *C. crescentus*, and conducted a functional examination of the SsrA tag. The SsrA is a protein tag that is attached to proteins under a variety of conditions, including starvation, and targets them for degradation by ATP-dependent proteases. In *E. coli*, ClpXP is the main protease that is responsible for SsrA-tagged substrate degradation (Gottesman et al. 1998). We constructed several fusions between FlbD, a transcriptional regulator of late flagellar genes, and the SsrA to determine if in *C. crescentus*, as in *E. coli*, ClpXP degrades SsrA tagged substrates. FlbD-SsrA was found to be highly unstable but was stabilised upon induction of the *clpX_{ATP}* allele. Similarly, FlbD-SsrA was stabilised when ClpP was depleted from cells. This indicated that ClpXP is responsible for the rapid turnover of SsrA-tagged proteins in *C. crescentus*.

SsrA-tagged FlbD variants were then used to genetically dissect the SsrA degradation pathway. We found that cells bearing FlbD-SsrA were non-motile due to the rapid degradation of FlbD and consequent lack of flagellar gene expression. To identify mutations, *cis* or *trans*, that stabilised FlbD-SsrA, a selection for motile suppressors was carried out. Our hypothesis was that cells which regained motility would have

stabilised FlbD through mutations in the SsrA tag or in an accessory component. Only two suppressors were isolated that contained amino acid substitutions in the SsrA tag, indicating that these are important residues for recognition by ClpX.

The remainder of the motile suppressors contained deletion or insertion frame-shifts by which the identity of the FlbD C-terminus was completely altered and the SsrA tag removed. In most cases, this resulted in FlbD stabilisation. However, transfer of one of those alleles into a clean genetic background suggested that the *flbD* allele alone is not able to restore motility. From this we concluded that FlbD variants with an altered C-terminus were non-functional and that a second mutation *in trans* must have occurred to restore motility. Consistent with this, FlbD fused to a stable variant of SsrA (FlbD-SsrA_{DDD}) did not support motility. Motile suppressors of strains carrying FlbD-SsrA_{DDD} had retained the nature of their SsrA tag, again suggesting that mutations *in trans* had restored motility. Those could map to components that either regulate the activity of FlbD or interact with it. It will be interesting to map these mutations as they may provide useful information about FlbD and its regulation of flagellar assembly in *C. crescentus*. The challenge for future work will be to map the second site mutation(s) and to define the exact contributions of *cis*- and *trans*-mutations for FlbD stability and/or activity.

In the third and final part of this thesis (Grünenfelder et al. 2004), we examined cell cycle-dependent FliF degradation. FliF forms the MS ring that anchors the flagellum in the inner membrane. Degradation of FliF at the G1-to-S phase transition coincides with flagellar ejection and was hypothesised to be the committing step of this developmental process (Grünenfelder et al. 2003; Jenal and Shapiro 1996). We found

that the non-essential ClpAP protease is required for the degradation of FliF as SW cells differentiate into ST cells. To define the nature of the ClpAP degradation signal, we conducted a high resolution mutational analysis of the FliF C-terminus. We found that though the degradation signal of FliF resides in the last 28 residues of the protein, no primary sequence appears to govern its turnover. Instead, our results indicate a requirement for hydrophobic residues at the C-terminus of FliF.

1 INTRODUCTION

1.1 General notes

Cells must adapt to changing conditions, both external and internal, in order to survive and proliferate. One of the main mechanisms by which cells accomplish this is to alter gene expression in response to detected changes. Another mechanism is proteolysis by which cells degrade proteins that have become misfolded and dysfunctional. This process is critical for survival under conditions of heat stress, DNA damage and starvation (Goldberg and St John 1976; Straus et al. 1988; Sutton et al. 2000).

Furthermore, proteolysis has been shown to play a key role in some complex regulatory circuits such as competence induction and sporulation in *Bacillus subtilis* (Turgay et al. 1998) and cell differentiation and cell cycle progression in *Caulobacter crescentus* (Jenal and Fuchs 1998; Wright et al. 1996). In both instances, the removal of target proteins at specific times and/or from specific cellular compartments is critical for survival or differentiation. In all cases, the degradation of target proteins is energy dependent and is carried out by different ATP-dependent proteases in prokaryotes (ClpXP, ClpAP, Lon, HslUV and FtsH) and by the 26s proteasome in eukaryotes (Gottesman 1996).

C. crescentus is one of the few bacteria that undergo cell differentiation as an integral part of the cell cycle. Cell division gives rise to two morphologically distinct daughter cells: the replication incompetent swarmer (SW) cell and the stalked (ST) cell, the

latter cell type being able to immediately initiate DNA replication and cell division (Figure 1.1). The SW cell bears a flagellum, is motile and chemotactically active. To start replication, the SW cell must first differentiate into a sessile ST cell, a process involving flagellum ejection, loss of the chemotactic apparatus and synthesis of a stalk at the pole previously occupied by the flagellum. The ST cell can then begin to replicate the chromosome and develop into a predivisional (PD) cell. Towards the end of the cell cycle, the newly replicated chromosomes are moved to the two compartments of the PD cell and a new flagellum and chemosensory apparatus are assembled at the pole opposite to the stalk.

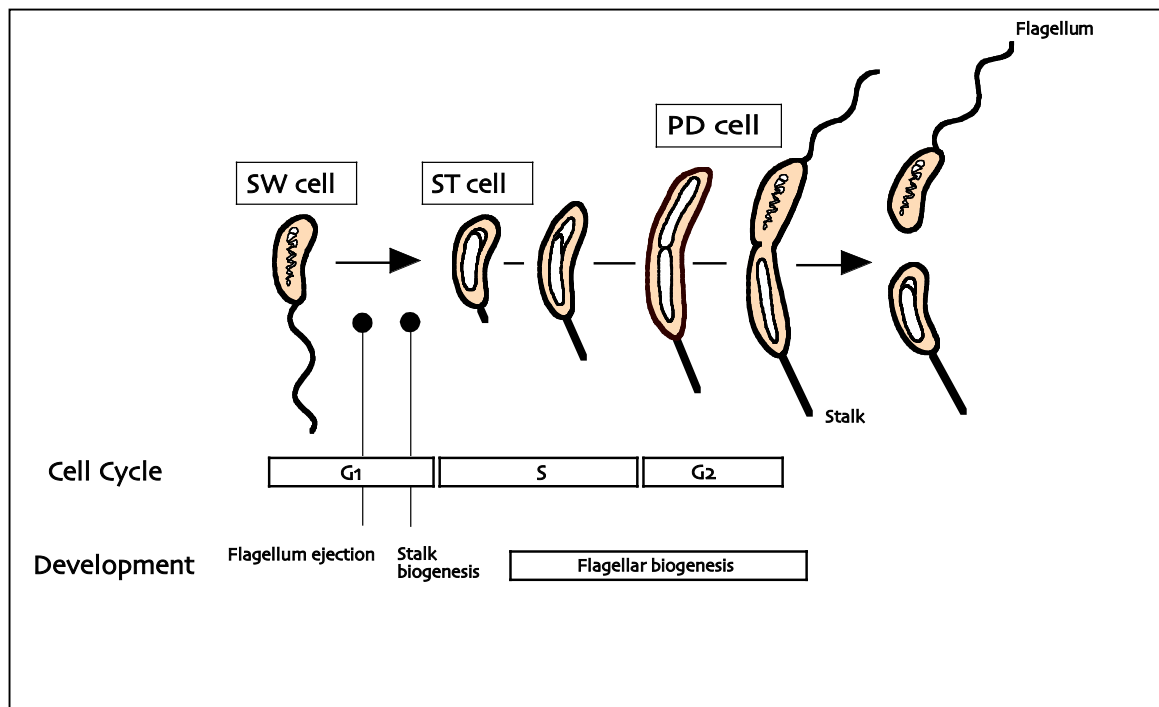


Figure 1.1. Schematic representation of the cell cycle of *C. crescentus*. Cell cycle phases are indicated (G1, S and G2) as are important developmental events. The cell cycle of *C. crescentus* is completed in approximately 90 min in complex medium (PYE) and 120 min in minimal glucose medium (M2G) (Osteras and Jenal 2000).

This unique integration of differentiation into the *Caulobacter* cell cycle makes it an excellent model organism to study the role of proteolysis cell cycle progression and development. Thus far, only a few instances of proteolysis and its biological significance in *C. crescentus* have been studied, of which three examples will be drawn. The protease ClpAP is required for degradation of the flagellar anchor protein FliF, an event either leading to or is the result of flagellar ejection (Grunenfelder et al. 2004); the Lon protease is required for cell cycle progression through timed degradation of the essential DNA methyltransferase CcrM (Wright et al. 1996); and finally, the ClpXP protease is required for the cell cycle-dependent turnover of the master regulator CtrA and, through degradation of some unknown protein(s), G1-to-S phase transition (Jenal and Fuchs 1998). ClpXP is the only protease in *C. crescentus* that is essential for growth and survival. Understanding the underlying molecular mechanisms of ClpXP's essentiality will be the major focus of this work.

1.2 The ClpXP proteolytic machine

1.2.1 General notes

The Clp (caseinolytic protease) family of proteins is well conserved throughout most prokaryotes as well as in the organelles of eukaryotes (Gottesman 2003). The first isolated members of this family were the ATP-dependent chaperone ClpA and the serine protease ClpP, where the former was found to promote the degradation of casein when complexed with the latter (Hwang et al. 1988; Katayama et al. 1988; Maurizi et al. 1990a; Maurizi et al. 1990b). ClpX was later identified as an alternative chaperone to ClpA (Gottesman et al. 1993). Alone, ClpP is able to degrade

only small peptides. Degradation of large proteins, or indeed most folded proteins, requires that they first be unfolded through ATP hydrolysis by the chaperone component.

1.2.2 The ClpX chaperone

The majority of work on ClpX has been conducted in *E. coli*. However, ClpX is highly conserved among prokaryotes and the *E. coli* ClpX shares 79% identity with that of *C. crescentus*. *C. crescentus* ClpX is also functional in *E. coli* (Osteras et al. 1999), and thus much of the basic knowledge about *E. coli* ClpX might apply to that of *C. crescentus*.

The ClpX chaperone belongs to the AAA+ (ATPases associated with diverse cellular activities) superfamily of proteins. The ClpX protein is composed of three domains (Figure 1.2): the N-terminal domain containing a Zn-binding motif (Banecki et al. 2001), a central AAA+ ATPase domain and a C-terminal domain (sensor and substrate discrimination, SSD) thus named as isolated forms thereof could interact with some substrates (Gottesman et al. 1993; Smith et al. 1999). However, it is more likely that the N-terminal domain is responsible for substrate recognition as comparison between predicted ClpX structures and the *E. coli* HslU structure revealed a strong similarity between the HslU I-domain and the N-terminal domain of ClpX (Singh et al. 2001). The I-domain of HslU has been implicated in substrate recognition and selection; furthermore, removal of the N-terminal domain of ClpX by limited proteolysis does not affect ClpX activity (Bochtler et al. 2000; Singh et al. 2001). That said, evidence also exists that the C-terminal domain may have a role in

initial substrate engagement (Joshi et al. 2003). Despite the controversy surrounding the role of the ClpX C-terminal domain, it is now known from the *H. pylori* ClpX structure that it is involved in hexamer-external contact formation between the ClpX monomers (Kim and Kim 2003) and thus has a role in hexamer formation or stabilisation. The ATPase domain of ClpX contains the classical Walker A and B motifs that are involved in binding and hydrolysis of ATP (Neuwald et al. 1999; Walker et al. 1982).

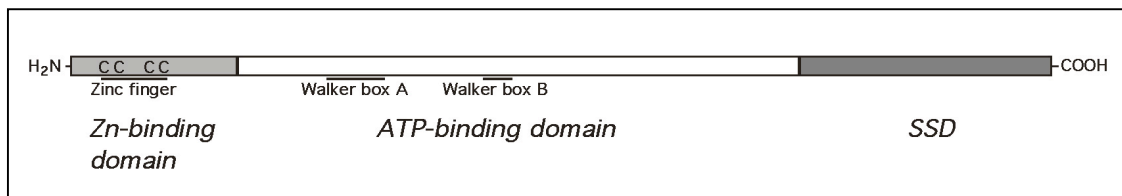


Figure 1.2. Domain organization of a ClpX monomer which in *C. crescentus* has the length of 419 AA and a molecular weight of 46 kDa.

Hexamerisation of ClpX requires ATP, Zn^{++} , Mg^{++} and a N-terminal domain with an intact Zn-binding motif (Banecki et al. 1996; Banecki et al. 2001; Singh et al. 2001). A hexamer of ClpX has an axial pore through which substrate proteins are threaded and unfolded (Figure 1.3). In combination with ClpP, the unfolded substrate is translocated directly into the pore of ClpP where it is degraded (Grimaud et al. 1998; Kim and Kim 2003). Both substrate denaturation and translocation are energy dependent processes (Hoskins et al. 2000).

The ClpX hexamer interacts with ClpP through six loops (each a tripeptide with the consensus sequence of IGF, see figure 1.3) found towards the end of the ATPase

domain (Kim and Kim 2003; Kim et al. 2001). Mutations in the IGF loops disrupt the interaction between ClpX and ClpP but do not affect ClpX activity.

1.2.3 The ClpP serine protease

The ClpP protease is composed of two heptameric rings stacked back-to-back forming a tetradecamer with a central pore that contains fourteen catalytic triads (Maurizi et al. 1990a; Maurizi et al. 1990b; Wang et al. 1997). The catalytic triads, each composed of the residues SHD, are accessible only to small peptides (20-30 AA) or unfolded proteins translocated by the chaperone component.

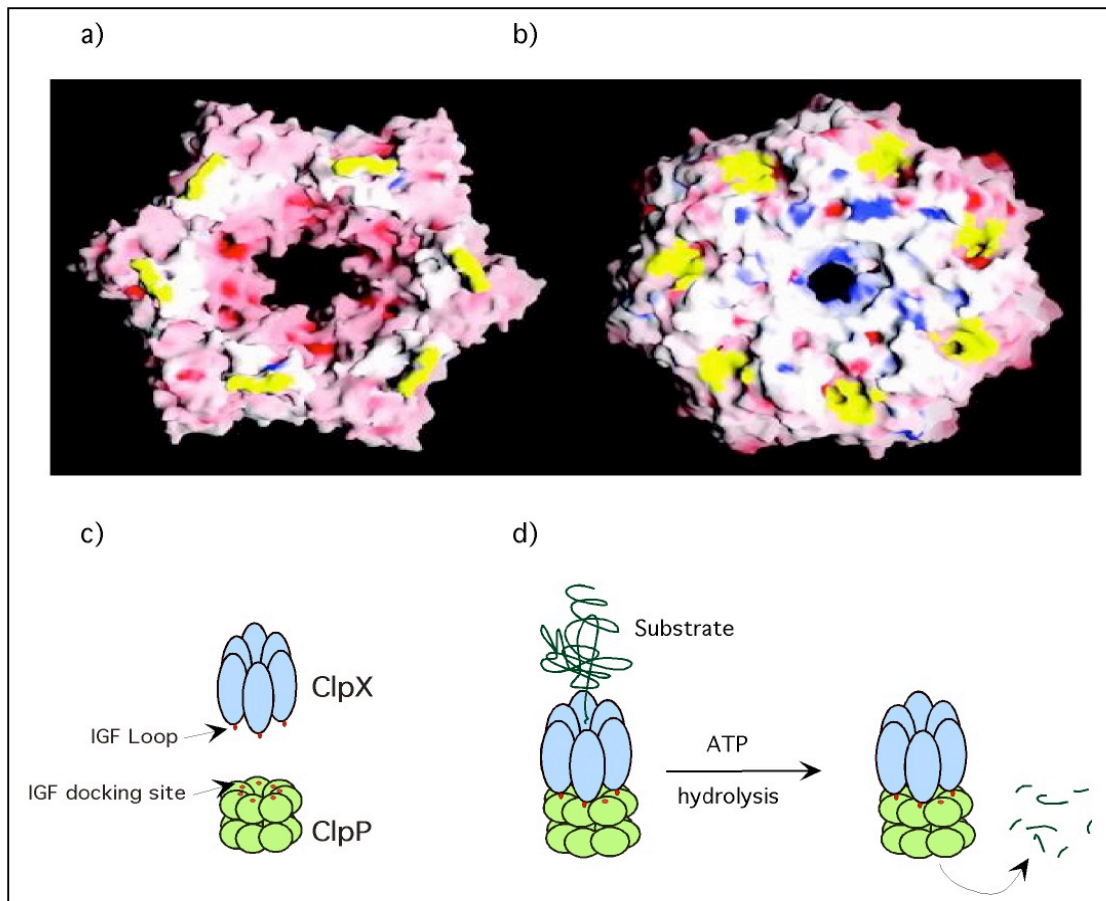


Figure 1.3. Components of the ClpXP protease. **a)** Space fill model of ClpX and **b)** ClpP crystals, derived from *H. pylori* and *E. coli*, respectively (Kim and Kim, 2003). Both molecules are shown from the contact interface. The IGF loops on individual ClpX monomers and their docking sites on ClpP are indicated in yellow. **c)** Schematic representation of the ClpX and ClpP oligomers. The ClpX IGF loops (red) interact with the IGF docking sites on ClpP (dark circles) **d)** Degradation of a substrate by ClpXP involves ATP hydrolysis, unfolding of substrate and translocation into the ClpP chamber where it is then proteolysed into small peptides, 7-10 AA in length (Thompson et al. 1994).

1.2.4 Substrate recognition

Binding of ClpX to the substrate is the first step in substrate degradation. Recognition of substrates can occur through binding to intrinsic motifs (either N- or C- terminal, or both) or introduced tags, such the SsrA tag (see section 1.2.5) (Flynn et al. 2003; Gottesman 2003). Flynn et al. (2003) have isolated fifty ClpXP substrates from *E. coli* and identified three N-terminal and two C-terminal ClpX-recognition motifs (N-M1-3 and C-M1-2, respectively). C-M1 (also termed SsrA-like motif) is the most prevalent C-motif and mostly contains the hydrophobic residues Ala, Val or Leu. The C-M2 motif is similar to that of the MuA repressor and C-M1, albeit slightly longer than the latter. Of the N-motifs, N-M1 is most strictly conserved with the consensus of polar₁-Thr-hydrophobic₂-basic₁-hydrophobic₂. N-M2 and N-M3 are less well conserved but seem to have a requirement for either hydrophobic residues, as in N-M2 or polar residues as in N-M3. In most cases, the signal required for recognition by ClpX resides solely in those motifs as their transfer to stable proteins converts them into substrates.

It is interesting to note that the C-motifs are always at the end of the protein whilst the N-motifs can be as far as four residues from the start of the protein. Although there is some evidence that terminal motifs can be recognised if grafted to internal positions (Hoskins et al. 2002; Tsai and Alley 2001) their presence at the end of the protein is more favoured as they are likely to be more accessible to ClpX.

1.2.5 The SsrA tag

The SsrA tag is the best studied ClpX-recognition sequence to date. SsrA is a highly hydrophobic protein tag added to the ends of proteins whose synthesis has been stalled at the ribosome (Keiler et al. 1996). In *E. coli*, the SsrA tag has the sequence of AANDENYALAA and the *Caulobacter* SsrA is slightly longer, yet highly similar with the sequence of AANDNFAEEFAVAA (Keiler et al. 2000). The SsrA tag is encoded by a peculiar RNA molecule that has both transfer and messenger RNA activity known as the tmRNA. Although tmRNA is universal among eubacteria, evidence suggests that it is not essential for survival (Oh and Apirion 1991) but is required for some cellular functions including proper timing of DNA replication in *C. crescentus* (Keiler and Shapiro 2003) and resistance to heat stress in *E. coli* (Komine et al. 1994) .

Keiler et al. (1996) have found that when the ribosome is stalled on a mRNA lacking a stop codon, an alanyl-tmRNA enters the empty A site of the ribosome causing the ribosome to switch from the problematic mRNA to the message encoded by the tmRNA molecule without releasing the incomplete protein. The ribosome then resumes translation hence adding the SsrA peptide to the incomplete protein. This process is known as *trans*-translation (see Figure 1.4). Proteins tagged with the SsrA peptide are targeted for degradation predominantly by the ClpXP protease, but under some conditions other proteases like FtsH and ClpAP can perform the same function (Gottesman et al. 1998; Withey and Friedman 2003). The C-terminal Ala-Ala residues are critical for SsrA recognition by ClpX, or other proteases (Gottesman et al. 1998; Keiler and Shapiro 2003). Furthermore, in *E. coli* SspB, a protein associated

with the ribosome, has been found to enhance the degradation of SsrA-tagged model substrates by ClpXP by at least ten-fold (Levchenko et al. 2000). No such factor exists in *C. crescentus*.

Ribosome stalling occurs under conditions of amino acid starvation, or at rare codons (Roche and Sauer 1999). The main function of tmRNA therefore is to release stalled ribosomes and allow the cell to recycle incomplete proteins. There is also mounting evidence that SsrA tagging has regulatory roles in cells (for review, see Withey and Friedman, 2003). For instance, *C. crescentus* strains lacking the tmRNA have a specific delay in the G1-to-S phase transition but not at other time points in the cell cycle (Keiler and Shapiro 2003). One possibility to explain this phenomenon is that in the absence of tmRNA mediated proteolysis, certain proteins inhibitory to cell cycle progression accumulate. If ClpXP is the main protease for SsrA-tagged substrates in *C. crescentus* as it is in *E. coli*, a functional link between ClpXP and the tmRNA may exist.

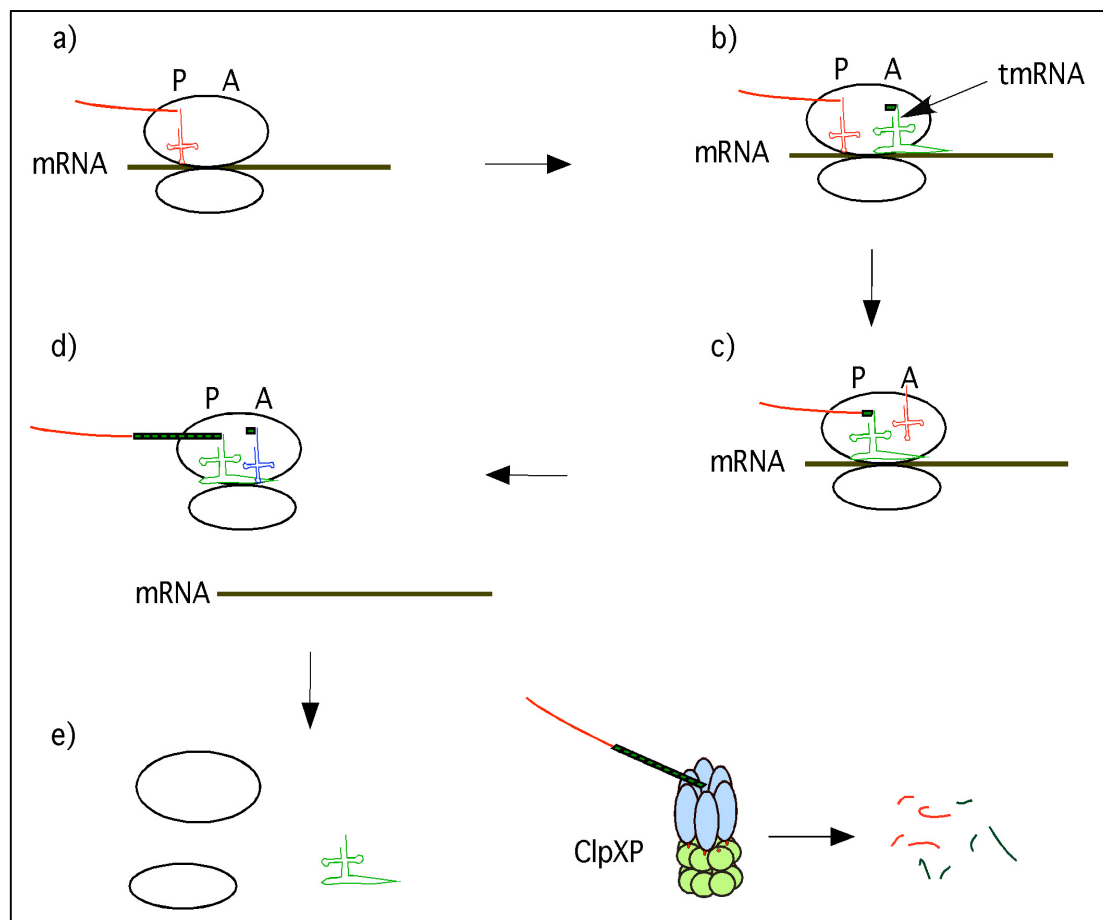


Figure 1.4. Schematic representation of the *trans*-translation process. a) A ribosome is stalled at a mRNA leaving the A site empty. b) The aminoacyl-tmRNA (green) enters the A site. c) The tmRNA moves to the P site, displaces the tRNA and adds its alanine to the incomplete peptide. d) The original mRNA is released and tmRNA becomes the template for translation resulting in the addition of the SsrA tag to the peptide (green). e) After translation is completed, the ribosomal complex dissociates and the tagged peptide is targeted for degradation by ClpXP.

1.2.6 Dynamics of substrate unfolding and ClpX interaction with ClpP

The affinity of ClpX to ClpP increases dramatically when ClpX has bound and is denaturing a substrate (Joshi et al. 2004). This is probably due to conformational changes brought about by ATP hydrolysis allowing ClpX to better contact ClpP through the IGF loops. Once the substrate is bound, ClpX applies a mechanical force

onto the substrate in order to unfold it (Burton et al. 2001). The amount of ATP required to unfold the protein can vary widely depending on how structured the recognised protein terminus is (Kenniston et al. 2003; Kim et al. 2000). As a rule, the less structured the terminus recognised, the more easily a protein can be unfolded and the less ATP is expended. Unfolding of the substrate after initial binding and engagement also reveals other sequence/structural elements less distal to the end. Those elements can determine the ease by which a protein can be unfolded and consequently its fate (Singh et al. 2000). This fact can explain why some proteins sharing similar, or identical, ClpX-recognition motifs can have vastly different stabilities. Proteins difficult to unfold slip from the grasp of ClpX and are re-engaged again in another attempt to denature them (Kenniston et al. 2003). This slipping and re-engagement serves to prevent ClpX from becoming blocked by troublesome proteins and thus allows ClpX the opportunity to denature other substrates.

The binding of ClpX can occur at one or both faces of ClpP, however translocation of substrates rarely occurs from both sides since a substrate occupying ClpP will inhibit translocation of the substrate *in trans* (Ortega et al. 2002). Furthermore, substrate denaturation by ClpX is the main rate limiting step in degradation (Kim et al. 2000) and thus the probability that both substrates are unfolded *and* translocated simultaneously into the ClpP chamber is low. This ensures that a substrate is completely degraded before the next substrate is up taken.

1.3 The ClpXP protease in *C. crescentus*

1.3.1 General notes

Although the protein levels of ClpX are relatively constant in *C. crescentus* throughout the cell cycle, its expression is controlled by three different promoters with varying strengths (Osteras et al. 1999). Similarly, ClpP, whose expression is controlled by CtrA (Laub et al. 2002), is present throughout the cell cycle (Osteras et al. 1999). Interestingly, heat shock did not induce the expression of ClpX but rather reduced its cellular level by 50% whereas it induced the expression of ClpP by two-fold (Osteras et al. 1999). In *E. coli*, the role of ClpXP is well established in the response to heat shock (Grimaud et al. 1998). A reduction of ClpX in the cells after heat shock might suggest that cells are attempting to free the available ClpP pool from ClpX. If ClpP concentrations are limiting in the cell, this could result in the formation of more active ClpAP complexes. If that is the primary reason for this decrease in ClpX after heat shock, it would imply that the role of ClpAP in *C. crescentus* is largely to cope with stress. Indeed, ClpA is not essential for *C. crescentus* growth or survival under normal growth conditions, although cells lacking the gene exhibit a slow growth phenotype and are filamentous (Grunenfelder et al. 2004).

1.3.2 ClpXP is essential for survival

Jenal and Fuchs (1998) have shown that both ClpX and ClpP are essential for growth and survival in *C. crescentus*. This contrasts with *E. coli*, where neither ClpX nor ClpP are essential, though they have important roles in coping with heat-shock (Gottesman et al. 1993). Jenal and Fuchs (1998) created conditional mutants

harbouring either the *clpX* or *clpP* gene under control of the regulatable xylose promoter (Meisenzahl et al. 1997); both strains are dependent on xylose for growth. Under restrictive conditions, cells stopped accumulating biomass after 4-7 generations (approx. 8-14 hours) subsequent to xylose removal; furthermore, the increase in viable cell count stopped after two generations (approx. 4 hours) and was reduced by five orders of magnitude after 16 hours. The fact that under restrictive conditions cells began to lose viability as early as 4 hours after the shift yet continued to accumulate biomass for prolonged periods pointed to an inhibition of cell division early on after xylose removal. Indeed, after 12 hours of the shift, most cells were found to be filamentous.

1.3.3 ClpX is required for G1-to-S phase transition

Cells depleted for ClpX were found to be arrested at the G1 phase of the cell cycle. Approximately 12 hours after xylose removal, most cells were found to contain only one chromosome as assayed by flow cytometry. This suggests that ClpX is required for the transition from G1 to S phase of the cell cycle and, perhaps indirectly, for the initiation of DNA replication. It is worth noting that this effect was more pronounced in cells depleted for ClpX as opposed to those depleted for ClpP. This may reflect that ClpP is more stable than ClpX and longer periods of time are required for its complete depletion after its synthesis is arrested (Jenal and Fuchs 1998). It is also possible that ClpX has a chaperone role, independent of ClpP, e.g. in substrate remodelling, the loss of which may contribute to this phenotype.

1.3.4 ClpXP degrades the master regulator CtrA

CtrA (cell cycle transcriptional regulator) belongs to the response regulator superfamily of proteins whose members act mostly as transcriptional regulators (Quon et al. 1996). CtrA is essential for growth of *C. crescentus* survival, and is directly involved in regulating the expression of at least 95 genes (Laub et al. 2002; Laub et al. 2000). Regulation of CtrA activity is tightly controlled in *C. crescentus* at the levels of expression, phosphorylation and proteolysis (Domian et al. 1997). CtrA binds to the origin of replication and suppresses DNA replication initiation (Quon et al. 1998). Only after activated CtrA (CtrA~P) is removed is the cell able to begin chromosome replication. CtrA is rapidly degraded at the G1-to-S phase transition of the cell cycle, and in the ST compartment of the late PD cell. As a result, CtrA is absent from ST cells, and is only present in SW cells, early PD cells and in the SW compartment of the late PD cell.

In vivo, CtrA degradation requires ClpXP (Jenal and Fuchs 1998). Analysis of the C-terminus of CtrA revealed the presence of two alanine residues that are important for its proteolysis. Mutation of those residues to Asp-Asp completely abolished proteolysis resulting in a stable CtrA protein (Domian et al. 1997). However, it is unclear how CtrA could be selectively degraded by ClpXP when the latter is present in both cell types at constant levels throughout the cell cycle. An attractive possibility is the existence of a regulatory factor whose expression or activation is tightly regulated, and that can mediate or suppress the proteolysis of CtrA. Recently, a second signal required for regulated CtrA proteolysis was found to reside in the first half of the receiver domain of CtrA (Ryan et al. 2002) offering a binding site for this hypothetical factor.

1.3.5 Why is ClpXP essential in C. crescentus?

Since CtrA blocks DNA replication initiation, one can imagine that the G1-to-S phase block observed in the absence of either ClpX or ClpP is due to CtrA stabilisation. However, work by Domian et al. (1997) showed that cells expressing a stable variant of *ctrA* (*ctrA-AA* → *ctrA-DD*) have no such G1 arrest, although they are somewhat filamentous. Only cells conditionally expressing a stable *and* constitutively active *ctrA* variant exhibit a G1 arrest, indicating that CtrA can either be inactivated through de-phosphorylation or removed by degradation. Thus, only the disruption of both pathways would lead to a G1 arrest (Domian et al. 1997)

These data lead one to discount CtrA proteolysis as the main reason for ClpX's absolute requirement in *C. crescentus*. It is tempting to speculate that ClpXP could be involved not only in the removal of CtrA but also in the degradation of protein(s) involved in regulating the activity of CtrA.

Thus far, only three other ClpXP substrates have been identified in *C. crescentus* including the chemoreceptors McpA, McpB (Potocka et al. 2002; Tsai and Alley 2001) and the chemotaxis protein CheD (Alley, M., unpublished results). Stabilisation of none of these proteins can explain the essential nature of ClpXP or its requirement in the G1-to-S phase transition. Therefore, we hypothesise that other ClpXP substrates must exist whose regulated proteolysis is essential for cell cycle progression and survival.

Recent proteomic analysis has shown that of 979 proteins reproducibly detectable on two-dimensional electrophoretic gels (2D gels), 48 proteins are rapidly degraded in the course of one cell cycle (Grünenfelder et al. 2001). Interestingly, the synthesis of

26 of those proteins was found to be under cell cycle control. The fact that more than 50% of degraded proteins are also differentially synthesised during the cell cycle suggests that carefully controlled levels of these proteins might be important for the execution of cell cycle processes. Thus, uncovering the identity of these proteins, their possible role in cell cycle progression and the regulatory significance of their degradation is a key step in understanding the control of cell proliferation in *C. crescentus*.

AIMS OF THESIS

The main aim of this work was to identify novel substrates of the ClpXP protease in *C. crescentus*. To date, no substrate protein has been identified that could either account for the essential nature of ClpXP in *C. crescentus*, or explain the role that ClpXP plays in G1-to-S phase transition. A major goal was to find substrates whose degradation would allow the cells to progress to S phase. This task becomes more important when one considers the relatively high number of rapidly degraded proteins that are also synthesised differentially during the cell cycle. It is an intriguing possibility that ClpXP could be responsible for the degradation of at least a subset of these proteins.

In the second part of this work, we aimed to study the function of C-terminal signals in proteolysis. As a first model, we analysed the SsrA tag as an example of an added proteolysis signal. The protease responsible for SsrA-tagged substrate degradation in *C. crescentus* is unknown, and it was one of our aims to find it. Furthermore, we wanted to dissect the SsrA tag and define the specific molecular determinants that are recognised by the respective protease. Finally, we aimed to study the C-terminus of FliF as an example of an intrinsic degradation signal. It has been shown earlier that cell cycle-dependent degradation of FliF relies on a C-terminal degradation signal (Jenal and Shapiro 1996). We wanted to define the exact nature of this degradation signal and identify the protease responsible for FliF degradation during the cell cycle.

2 MATERIALS AND METHODS

DNA manipulation, SDS-PAGE electrophoresis, *E. coli* growth media, general PCR and cloning techniques were carried out as described in Sambrook et al. (1989) unless otherwise stated. *C. crescentus* was grown as described previously (Johnson and Ely 1977).

2.1 Pulse labelling and Pulse/Chase experiments

Caulobacter cells were grown to the desired OD₆₆₀ in M2G, 5 ml collected in a pre-warmed 50 ml Falcon tube to which 20 µCi/ml ³⁵S-met/cys (NEG-772, NEN) was added. Cells were grown with shaking for 5 min at 30 °C and if a chase was required, 50 µl of a solution of 0.2% tryptone, 1 mM methionine, and 0.02 mM cysteine was added. At the desired time points, a 1 ml aliquot was removed; cells were harvested by centrifugation and snap frozen in liquid nitrogen. If the experiment was to be carried out on SW cells, *C. crescentus* was synchronized by density centrifugation as previously described (Johnson and Ely 1977), and isolated cells released in fresh M2G media and aliquots were pulse labelled at the desired time.

2.2 Immunoprecipitation

Labelled cells were thawed at room temperature (RT) for 2-4 min and lysed with 50 µl SDS-lysis buffer (4% SDS, 100 mM EDTA, 50 mM Tris/Cl pH7.5). Following lysis for 10 min after thorough resuspension, 1.3 ml of K2 low salt buffer (50 mM

Tris 7.5, 100 mM NaCl, 50 mM EDTA, 1% Triton X-100) was added along with 30 μ l of protein A-agarose (Roche). After mixing, extracts were centrifuged for 15 min at RT, the supernatant transferred to a new tube and scintillation counting performed (see section 2.3). The volume corresponding to 10^6 cpm of extract was removed and placed in a new tube with the appropriate volume of antibody and 40 μ l of protein A-agarose. Extracts were incubated for 20 min – 1 hr at 4 °C in a rotating wheel after which they were centrifuged for 1 min, washed once with K2 low salt buffer and twice with K2 high salt buffer (50 mM Tris 7.5, 500 mM NaCl, 50 mM EDTA, 1% Triton X-100). The pellet was then resuspended in 40 μ l 2x Laemmli buffer (Sambrook et al. 1989), boiled for 5 min, centrifuged and supernatant loaded on a SDS-PAGE gel.

For immunoprecipitation using anti-FLAG M2 affinity gel (Sigma, A2220), the same procedure was followed with minor modifications. Removal of proteins that could non-specifically bind to the matrix was unnecessary as the gel is saturated with covalently bound anti-FLAG antibodies. Thus, the first centrifugation in K2 low salt buffer was conducted solely to remove cell debris and unlysed cells. Generally, 5-10 μ l of anti-FLAG M2 affinity gel was washed 3x in K2 low salt buffer and added to the extract. The rest of the procedure is as stated above.

For immunoprecipitations under native conditions using anti-FLAG M2 affinity gel, cells were harvested from 1.5 ml of culture at OD₆₆₀ 0.3-0.5 and resuspended in 200 μ l cold column buffer (50mM Tris/Cl pH7.5, 200mM KCl, 50mM MgCl₂). Cells were lysed at 4°C in a sonication bath (8 x 30 seconds at 25MHz) followed by a 30 minutes centrifugation at 13000 rpm at 4°C to remove cell debris. The supernatant was

incubated with 10 μ l of anti-M2 affinity gel for 30 min at 4°C in a rotating wheel. After centrifugation, the precipitate was washed twice with cold column buffer and resuspended in 40 μ l 2x Laemmli buffer. After 5 min boiling, the gel matrix was centrifuged and supernatant loaded on a SDS-PAGE gel.

2.3 Scintillation counting

Depending on the volume of extract produced from cell lysis, an aliquot (usually 20-50 μ l), was removed and mixed with 100 μ l BSA (1 mg/ml) and 2ml ice cold 10% trichloroacetic acid (TCA) in a glass tube, and incubated on ice for 30 min – 1 hr. The mixture was then loaded on a fibreglass filter (Whatman, GF/C 1822 025) pre-wet with 10% TCA, in a vacuum filter manifold (Millipore, XX2702550). The filter was washed once with 2 ml 10% TCA and once with 3ml 96% ethanol after which it was dried at RT for 20 min, placed in a plastic counting bottle containing 2 ml Scintillation fluid (Packard) and counted in a liquid scintillation analyser (Packard, 2200CA).

2.4 Protein preparation and two dimensional gel electrophoresis

For analytical gels, and some preparative gels, proteins were prepared and electrophoresed as previously described in Grünenfelder et al. (2001). To enrich for proteins within a desired molecular mass range, generally between 20-50 kDa, we employed the Bio-Rad Prep Cell 491. The manufacturer's protocol was used with no alterations. Briefly, a 500 ml culture of *C. crescentus* was washed once in PO₄ buffer (245 mM Na₂HPO₄*2H₂O; 156 mM KH₂PO₄) and lysed by French press as described

previously (Grünenfelder et al., 2001). The lysate was ultra centrifuged at 40,000 rpm for 30 min at 4 °C. The supernatant was then removed and an appropriate volume of 3x Laemmli buffer was added to a final volume of 20 ml, which was then boiled for 10 min. Alternatively, a smaller amount of cells was harvested from 100-200 ml of growing culture and after washing in PO₄ buffer, was directly resuspended in 20 ml 3x Laemmli buffer and boiled for 10 min. The Prep Cell was set to have the cooling recirculation pump at 80-100 ml/min with the tubes immersed in an ice bucket. The protein extract was loaded on a 7 cm long, 8% polyacrylamide gel in the wide chamber. The chamber was run at 40mA constant current and when the dye front had migrated to the bottom of the resolving gel, 2.5 ml fractions were collected at a flow rate of 0.5 ml/min.

An aliquot of every fifth fraction was removed and run on SDS-PAGE, and stained with coomassie brilliant blue (CBB) to establish the size range of proteins collected. Fractions containing the desired size range of proteins were pooled and concentrated using Amicon ultrafiltration filters (YM10, #13622). The proteins were concentrated and re-diluted 2x in order to remove most salt remaining from electrophoresis. As the amount of SDS used in the electrophoresis and elution buffer (0.1%) could interfere with the first dimension, care was taken to reduce the SDS concentration to 0.01% or less in the final amount of protein loaded.

To some preparative gels, prepared by either methodology, we added a “spike” of radioactively labelled proteins in order to locate faint spots and better match the analytical gels to the preparative gel patterns. The spike normally consisted of 10⁶

cpm of protein labelled as described above (see section 2.1) and prepared as described in Grünenfelder et al. (2001).

Spots of interest were excised and the gel particles sent to the mass spectrometry (MS) department at the Biozentrum. Peptide mass fingerprinting (PMF) was carried out using the Mascot Search matrix available on the ExPasy proteomics server.

2.5 Data Processing and Analysis

Analytical gels were processed as described previously using the PDQuest software (Bio-Rad) (Grünenfelder et al. 2001). Briefly, the spot intensities were normalized to ppm based on the total counts present on each gel image. Gels produced in this work were matched to the analytical master gel produced previously by Grünenfelder et al. (2001). Relative spot intensities were exported to an Excel sheet (Microsoft) and organized as appropriate for the SAS statistical analysis software (Version 8.2). An analysis of variance (ANOVA) test was conducted (Wonnacott and Wonnacott 1990). Briefly, the ANOVA test conducted takes into account 3 factors: 1) the difference in the mean of a spot intensity at a time point *between* the different strains; 2) the difference in the mean of a spot between time points in the pulse chase *within* each strain; and importantly, 3) the variation introduced by the experimenter on different occasions when the experiment was repeated. It is this third point that could eliminate extraneous variation introduced purely by experimental repetition. As a result, spots that would ordinarily be discarded by t-test or simple ANOVA analysis would be maintained.

2.6 DNA manipulation and construction of plasmids and mutant alleles

2.6.1 Construction of a M2-tagged $clpX_{ATP}$ allele

To establish if $ClpX_{ATP}$ monomers formed mixed oligomers with $ClpX_{wt}$ monomers, we created pST-1, a plasmid with a C-terminally M2-tagged copy of $clpX_{ATP}$. To do this, we employed the λ -Red recombinase system as previously described (Datsenko and Wanner 2000). Firstly, plasmid pMO88 ($P_{xyI}::clpX_{ATP}$) was transferred by electroporation into *E. coli* LT2 strain UJ1786 that contains plasmid pKD46, which bears the λ recombinases. The resulting strain was induced with 1mM arabinose for 4 hours to express the recombinases and then made electrocompetent (Sambrook et al. 1999). A PCR was then performed on pKD3 using an annealing temperature of 50 °C with primers 635 (GCTGATCTATGCCGAGAAAAAGGGTGGGGCGGCCTCGG CCGACTACAAGGACGACGACGACAAGTAACATATGAATATCCTCCTTAG) and 636 (CTCGAGGCCAGTTATCCACGAAAAAGCGCGCCATCCGATGGTG TAGGCTGGAGCTGCTTC). The resulting PCR fragment contained the Chloramphenicol (Cm) resistance cassette flanked by the last 40 bp of $ClpX$ and the M2-tag on one side, and on the other, a 40 bp stretch of DNA homologous to the backbone of pMO88. The distance between the two stretches of homologous DNA on pMO88 was approximately 50 bp. This PCR product was then transformed into the strain containing pKD46 and pMO88 by electroporation and transformants were selected on LB-Cm plates. Three clones were picked from the plate, grown overnight in LB-Cm medium, minipreps prepared and end of $clpX$ gene sequenced to ensure the correct in-frame insertion on the M2-tag downstream. One clone was chosen and the

plasmid named pST-1 (in strain UJ2449). UJ2449 was conjugated with NA1000 cells to produce strain UJ2450.

2.6.2 Constructs for 2D gel target evaluation

As antibodies against most of the proteins to be tested were unavailable, we tagged all potential substrates with the M2 tag N-terminally and for some, C-terminally (see below) so as to allow the use of antibodies against the M2 peptide. We created a low copy vector with the M2 tag, which can be fused with any gene either N-terminally (pST-N-M2) or C-terminally (pST-C-M2). Both vectors were based on the low copy vector pMR10.

pST-N-M2 was created using the λ red recombinase system (Datsenko and Wanner 2000). Strain UJ1786 (*E. coli* LT2 with pKD46) was transformed with pMR10 and induced for 4 hours with 1mM arabinose following which the resulting strain was made electrocompetent. A PCR was performed on pKD3 using 50°C as the annealing temperature with primers 820 (ATTGTGAGCGGATAACAATTTTCACACAGGAAACAGCTATGGATTACAAGGATGACGACGATAAGACTAGTGTGTAGGCTGGAGCTGCTTC) and 821 (GTACCGGGCCCGTCGAGACTAGTCTCGACTCTAGAGCTCTCATATGAATATCCTCCTTAG). The resulting PCR fragment contained the CmR cassette flanked on one side with 40 bp of homology directly upstream of the ATG of the *lacZ* gene on one side, and on the other, by a *SpeI* site in frame with the M2 tag followed by a stretch of 40 bp homologous to a region in the backbone of pMR10. The distance between the two stretches of homology to pMR10 was 50 bp. The PCR fragment was transformed into the strain containing both

pKD46 and pMR10 and transformants selected on LB-Cm plates. Three clones were picked, grown overnight and examined by sequencing to confirm that correct insertion of the M2 tag at the desired location had occurred. One clone was picked and frozen as UJ2455. Genes cloned in this vector will have the M2 tag followed by two residues encoded by the *SpeI* site (Thr-Ser) N-terminal to the gene (Figure 2.1).

pST-C-M2 was created in the same manner but using primers 745 (CTCCTGCAGAGCTCTAGAGTCGAGACTAGTCTCGACGGGCGTGTTAGGCTG GAGCTGCTTC) and 746 (TAACGCCAGGGTTTTCCCAGTCACGACGTTGTAA AACGACTTACTTATCGTCGTCATCCTTGTAATCGAATTCATATGAATATC CTCCTTAG). The *E. coli* DH10B strain containing pST-C-M2 was frozen as UJ2456. Genes to be cloned in this vector must first have their stop codon removed and replaced by an *EcoRI* site as this is present directly upstream of, and in frame with, the M2 tag. Genes cloned in this vector will be followed by the two residues encoded by the *EcoRI* site (Glu-Phe) and then the M2 tag (Figure 2.2).

Genes encoding proteins of interest were amplified by PCR from NA1000 genomic DNA with annealing temperatures chosen as appropriate for the primers used and after cloning, were verified by sequencing to ensure the absence of mutations. For cloning into either vector, primers were designed to include a *SpeI* site at the 5' end and an *EcoRI* site at the 3' end of the gene. The PCR product was cloned into the vector digested with both enzymes. Table 2.1 contains the primers used to amplify the genes, the resulting plasmid designations and strain names in both *E. coli* and *C. crescentus* UJ200 ($P_{xyl}::clpX$).

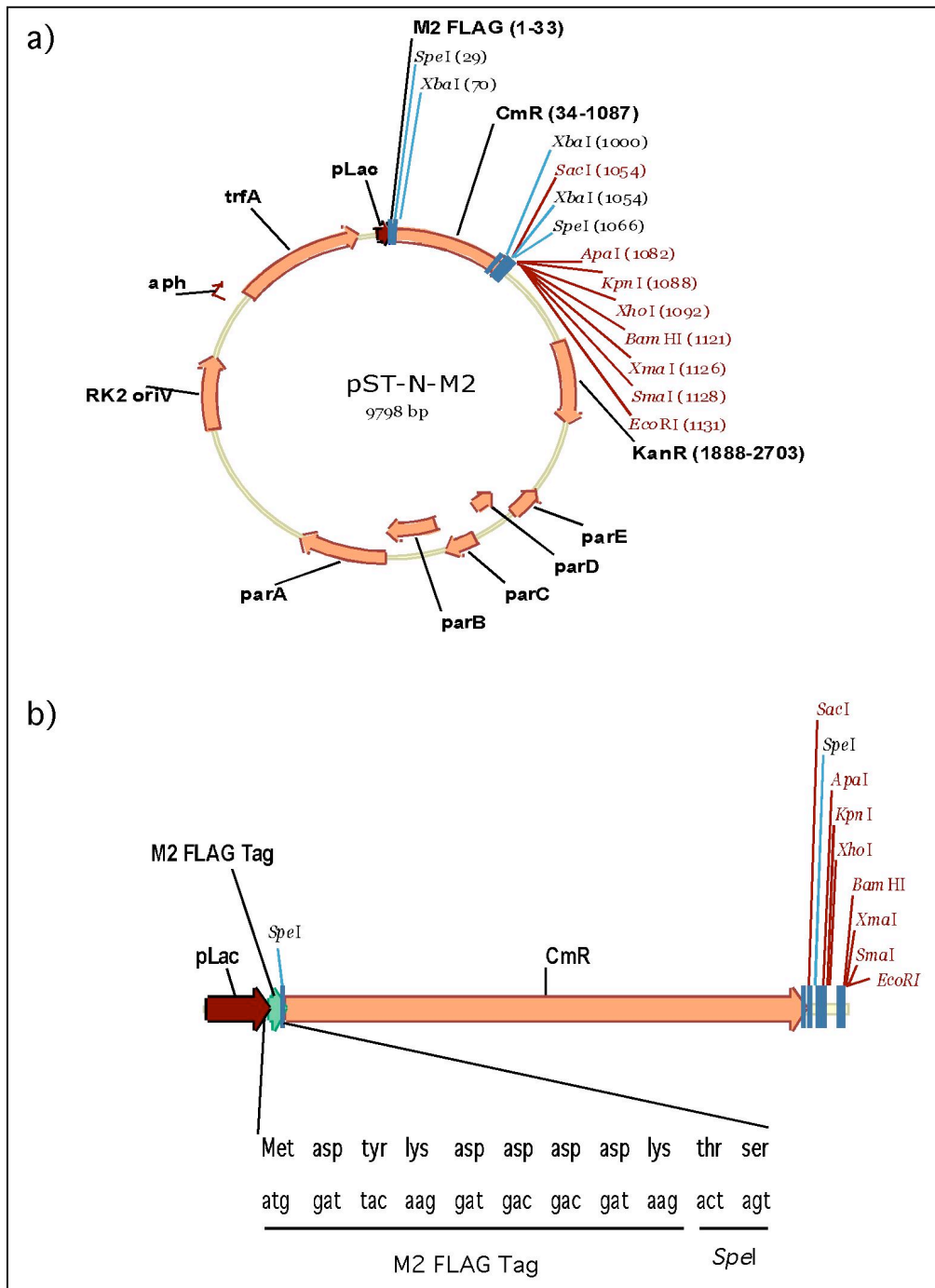


Figure 2.1. Plasmid map of pST-N-M2 (a) and magnification of area where genes of interest can be cloned (b). Digestion of the vector with *SpeI* and any one of the enzymes whose sites are located at the end of the CmR cassette will remove the latter.

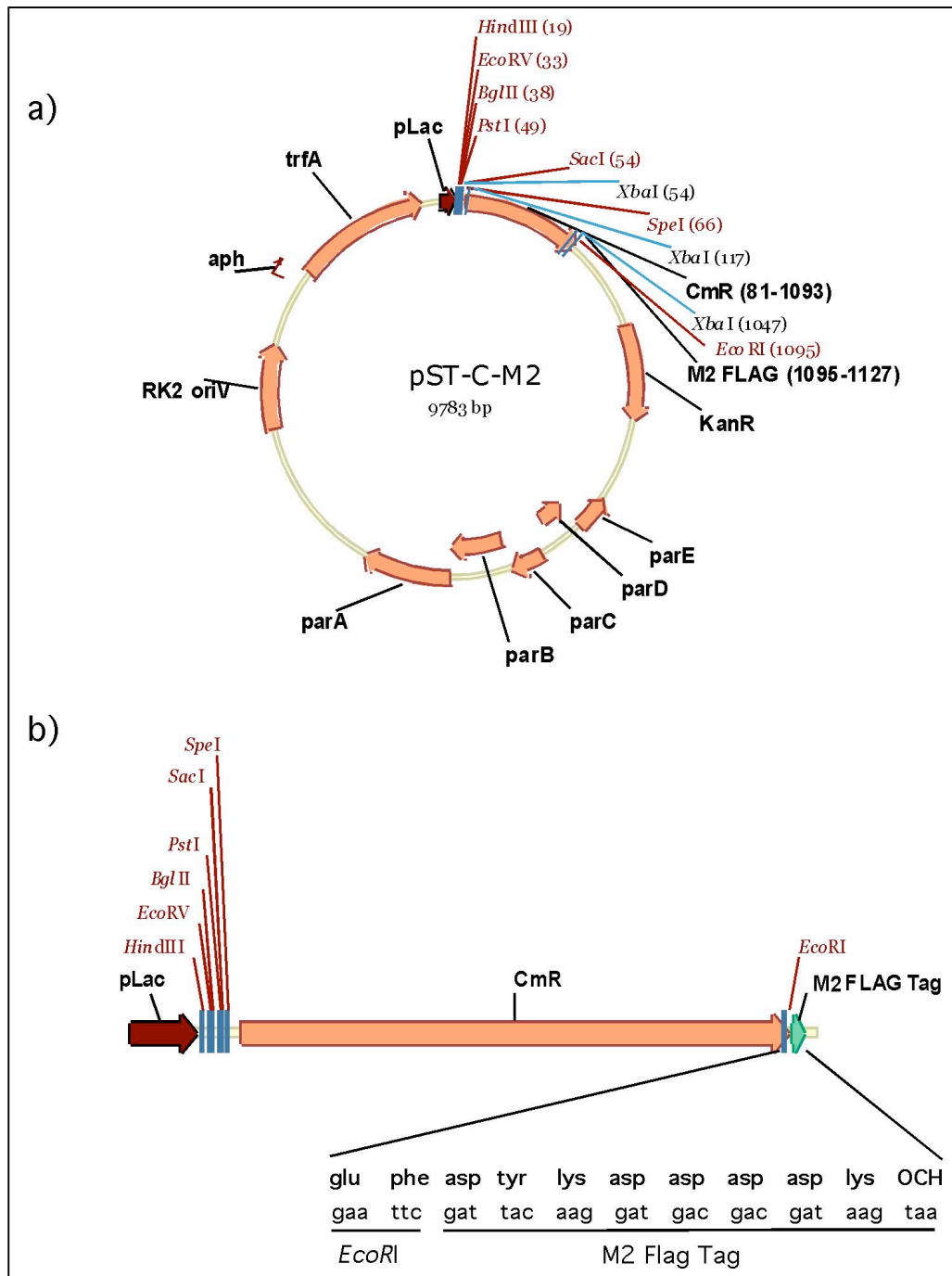


Figure 2.2. Plasmid map of pST-C-M2 (a) and magnification of the area where genes of interest can be cloned (b). Digestion of the vector with *Eco*RI and any one of the enzymes whose recognition sites precede the *CmR* cassette will remove the latter.

2.6.3 Construct for CC2323 chromosomal M2 tagging and deletion

To delete the CC2323 gene, we used the conventional two-step recombination system as outlined in Results section 3.3.2. To create the construct, two PCRs were performed. The first was with primers 756 (ATATAGAATTCCGGACTCGGCGG TCTCGG) and 757 (TATATAAGCTTGTCGGTGAGTGCTGCGCG) to generate the first fragment that contained a 1000 bp region of homology upstream of CC2323 and the first 10 AA of CC2323. The second fragment was generated with primers 758 (TATATAAGCTTGCCAGCAAGCGCCGCGCG) and 759 (TATATACTAGTC CGCAACCAGGACCGGACG) and contained the last 10 codons of CC2323 and a 1000 bp region of homology downstream of CC2323. The first fragment was digested with *EcoRI* and *HinDIII*, and the second with *HinDIII* and *SpeI*. Both fragments were joined in frame using the common *HinDIII* site, cloned into pNPTS138 using *SpeI* and *EcoRI*, transformed into *E. coli* DH10B cells and transformants selected on LB-Kan plates. Minipreps from several clones were prepared and the construct sequenced to verify that no mutations have taken place in the regions adjacent to CC2323 so as to ensure no polar effects occur. One clone with no mutations was selected (UJ2491) and used to conjugate the pNPTS138-based construct into *C. crescentus* NA1000. The two-step recombination procedure was followed as per usual (see results section 3.3.2) and 5 strains that were both Kan sensitive and able to grow on Sucrose plates were selected for further tests. A PCR was performed on genomic DNA of all 5 clones using primers 756 and 759, and the product sequenced to ensure that recombination and deletion of the central 357 AA have occurred. One strain (UJ2492) was selected for our experiments.

To create a chromosomal N-terminally M2-tagged copy of CC2323, two sets of primers were designed; 753 (ATAGACACTAGTGCGCGCTCTCGGAGAAGC) and 754 (CTTGTCGTCGTCGTCCTTG TAGTCCATGGTTCGCCCCGCTGGGAGCTA TG) to produce a fragment with a 1136 bp region of homology upstream of CC2323 followed by the M2 tag; 730 (TATATGAATTCTCAGGCCGACTGCGCGCG) and 755 (ATGGACTACAAGGACGACGACGACAAGATGGCCACCACACGCGCAG CAC) to produce a fragment containing the M2 tag and the entire ORF of CC2323 (1136bp). Both fragments were mixed at a 1:100 dilution and a PCR was conducted using the external primers 753 and 730 to amplify the full M2-tagged CC2323 gene. The resultant fragment was digested with *SpeI* and *EcoRI*, cloned into pNPTS138 and transferred into *E. coli* DH10B by electroporation. Several clones were selected, minipreps of which were sequenced to confirm there are no mutations. A clone with no mutations in the area to be replaced was selected and frozen as UJ2493. This strain was used to conjugate the pNPTS138 based construct into NA1000 and the two-step recombination procedure was carried out as outlined above. Ten Kan-sensitive and sucrose-resistant clones were selected and analysed by immunoblots using the anti-FLAG M2 antibody for the presence of a cross-reactive band with the expected size of M2-CC2323. One clone was selected and frozen as UJ2494. This strain contains the N-terminally M2-tagged CC2323 gene under control of its native promoter.

2.6.4 Constructs for overexpression of the CC2323 protein

To overexpress the CC2323 gene in the cell, we designed two plasmids: pST-10, bearing N-terminally M2-tagged CC2323 on the medium copy vector pBBR1-MCS2 and pST-11, bearing a C-terminally M2-tagged CC2323 on the low copy vector

pMR10. To produce pST-10, we performed a PCR on NA1000 genomic DNA using primers 918 (ATATCTCGAGATGGATTACAAGGATGACGACGATAAGATGGCCACCACACGCGCAGC; containing the *XhoI* site followed by the M2 coding sequence and 20 bp of homology to CC2323); and 730 (TATATGAATTCTCAGGCCGACTGCGCGCG; containing homology to the last 20 bp of CC2323 and an *EcoRI* site). The resulting PCR fragment (1169 bp) was digested with *EcoRI* and *XhoI* and cloned into pBBR1-MCS2 digested with the same enzymes; thus, the CC2323 gene in this construct is driven by the P_{Lac} . *E. coli* DH10B was transformed with the ligation mix and transformants selected on LB-Kan. Several clones were selected to sequence the insert and one correct clone was chosen and frozen as UJ2499.

To create the C-terminally M2-tagged version of CC2323, we amplified the gene from NA1000 genomic DNA using primers 730 and 917 (ATATAGAATTCTCAGGCCGACTGCGCGCGGCG). The resulting fragment (1136 bp) was cloned into vector pST-C-M2 as described above in section 2.6.2 creating pST-11. The CC2323 gene in this construct is driven by the P_{Lac} . Several clones were picked and the insert sequenced; one clone was chosen and frozen as UJ2500.

2.6.4 Constructs for *SsrA* tagged *FlbD*

To generate the *SsrA* and *SsrA*_{DDD} tagged versions of *FlbD* and *FlbD*_{Δ13} the λ red system was employed (Datensko and Wanner, 2000). For *SsrA*-tagged *FlbD*, two primers were designed; 645 (CCTGCGCAACAAGCTGAAGGAATATTCCGACGCCGGCGTGGCCGCCAACGACAACCTTCG CCGAGGAGTTCGCCG TGGCCGC

CTGACATATGAATATCCTCCTTAG) and 646 (ATGACCATGATTACG CCAAGCTTGCATGCCTGCAGGTCGAGTGTAGGCTGGAGCTGCTTC). Primer 645 contains 40 bp of the *flbD* 3' end lacking the last 39 bp of the gene, followed by the sequence coding for the *ssrA* tag and a 20 bp stretch homologous to the Cm-R cassette of pKD3. Primer 646 contains a 20 bp sequence homologous to the Cm-R cassette followed by 40 bp of homology to the pGR8 backbone, located approximately 50 bp downstream of the end of *flbD*. Both primers were used to amplify the Cm-R cassette from pKD3 at a 50 °C annealing temperature. The resulting fragment was electroporated into *E. coli* DH10B containing both pGR8 (pBGS18T containing the last 650bp of *flbD*) and pKD46, which had been induced with 1mM arabinose. Transformants were selected on LB-Cm plates and the sequence of several clones was analysed to ensure that the *ssrA* tag had been inserted correctly. Thus, in this construct, the last 13 AA of FlbD are replaced with the SsrA tag (*flbD*_{Δ13-ssrA}). One of the correct clones was chosen (pST-30), frozen as UJ2495 (DH10B, pST30, *flbD*_{Δ13-ssrA}) and conjugated into NA1000 to produce strains COH7. Another clone was also isolated that had accumulated one point mutation in the *ssrA* sequence converting the fourth residue from Asp to Val. This plasmid was named pST-39 and *E. coli* containing it were frozen as UJ2521. pST-39 was transferred to NA1000 by conjugation producing COH6.

The remaining constructs were generated similarly but replacing primer 645 with primer 668 (CCTGCGCAACAAGCTGAAGGAATATCCG ACGCCGGCGTGCC CGCCAACGACAACCTTCGCCGAGGAGTTCGCCGACGACGACTGACATATGA ATATCCTCCTTAG) for *flbD*_{Δ13-ssrA_{DDD}}; 705 (GCAGGTGC CGCCGCCCCAGGGCGGGGTCGGCGCGGCCGCTGCCGCCAACGACAACCTTC

GCCGAGGAGTTCGCCGTGGCCGCCTGACATATGAATATCCTCCTTAG) for *flbD-SsrA*; and, 722 (GCAGGTGCCGCCGCCAGGGCGGGGTCGGC GCGGCCGCTGCCGCCAACGACAACCTTCGCCGAGGAGTTCGCCGACGACG ACTGACATATGAATATCCTCCTTAG) for *flbD-SsrA_{DDD}*. Constructs verified by sequencing were frozen as UJ2496 (DH10B, pST-31, *flbD_{Δ13}-SsrA_{DDD}*); UJ2497 (DH10B, pST-32, *flbD-SsrA*); and, UJ2498 (DH10B, pST-33, *flbD-sSrA_{DDD}*). These strains were used to conjugate the plasmids into NA1000 cells to produce COH12 and 13 (from UJ2496); COH33 (from UJ2497); and, COH34 and 35 (from UJ2498).

2.6.5 Transfer of flbD tail sequences from motile suppressor mutants to wild-type cells

To establish if alterations in the *flbD* 3' end alone are responsible for the suppression of the motility defect, the *flbD* alleles of suppressor strains COH18 and COH38 were moved into NA1000 wild-type cells. To do this, we digested chromosomal DNA of both suppressors with *XhoI* and *SacII*, separated DNA fragments by electrophoresis, and excised the genomic material of 2-4 kBp in size. The genomic fragment of interest had an expected size of 3.1 kBp and contains the 3' end of *flbD* allele (as of the *SacII* site), followed by the Cm-R cassette introduced by the λ red recombinase system (see above) and most of the Kan-R gene (to the *XhoI* site) from the plasmid backbone integrated in the chromosome. The excised genomic DNA was purified and cloned into pGR8 digested with the same enzymes where the *SacII-XhoI* fragment (approximately 2 kBp) was removed. The ligation mix from this cloning step was transformed into *E. coli* DH10B cells and transformants selected on LB-Cm-Kan plates. One clone from each plate was isolated and the plasmid conjugated into *C. crescentus* NA1000 cells producing strains ST190 and ST191 (bearing the *flbD* 3' end

of COH18) and ST192 (bearing the *flbD* 3' end of COH38). PCRs and sequencing reactions were conducted on the *flbD* gene of all three strains to ensure that the 3' end of the respective *flbD* allele had been carried over faithfully to NA1000.

2.7 Microscopy

Cell morphology was observed on logarithmic-phase growing cells. At the appropriate OD₆₆₀, 2.5 µl of cells were removed and added to a poly lysine microscopy slide (Roth H884.1) with 40 µl of solidified 0.4% PYE agar. The drop of cells was distributed evenly on the agar surface and when dried (5-10 min), the slide was examined with a 100x objective on the Olympus AX70 microscope. Pictures were taken and stored using the OpenLab 3.0.9 software.

2.8 Strains and plasmids used in study

The strains and plasmids used in chapter 3 are listed in table 2.1, and those used in chapter 4 are in listed in table 2.2. All *E. coli* strains used in both studies are of the DH10B background.

Table 2.1. List of strains and plasmids used in identification of ClpX substrates and target evaluation (chapter 3).

Strain/Plasmid	Description	Reference or source
<i>Strains</i>		
<i>E. coli</i>		
DH10B	F- <i>mcrA</i> D (<i>mrr hsdRMS mcrBC</i>) F80 <i>dlacZDM15 DlacX74 endA1 recA1</i> <i>deoR</i> D (<i>ara, leu</i>) 7697 <i>araD139 galU galK</i> <i>nup GrpsL</i>	GIBCO BRL
UJ1191	DH10B::pMO88 ($P_{xyI}::clpX_{ATP}$)	M. Osteras
UJ2449	DH10B::pST-1 ($P_{xyI}::clpX_{ATP}$ -M2)	This study
UJ2455	DH10B::pST-N-M2	This study
UJ2456	DH10B::pST-C-M2	This study
UJ2457	DH10B::pST-4 (<i>M2-ctrA</i>)	This study
UJ2459	DH10B::pST-5 (<i>M2-CC2323</i>)	This study
UJ2461	DH10B::pST-6 (<i>M2-cheD</i>)	This study
UJ2463	DH10B::pST-12 (<i>M2-G3PD</i>)	This study
UJ2465	DH10B::pST-13 (<i>M2-CC2821</i>)	This study
UJ2467	DH10B::pST-14 (<i>M2-ribosomal subunit interface protein</i>)	This study
UJ2469	DH10B::pST-15 (<i>M2-murA</i>)	This study
UJ2471	DH10B::pST-16 (<i>M2-cu⁺⁺ binding protein</i>)	This study
UJ2473	DH10B::pST-17 (<i>M2-riboflavin synthetase α</i>)	This study

	<i>chain</i>)	
UJ2475	DH10B::pST-18 (<i>M2-GTP cyclohydrolase II</i>)	This study
UJ2477	DH10B::pST-19 (<i>M2-acetyl coA transferase</i>)	This study
UJ2479	DH10B::pST-20 (<i>M2-G6P 1-dehydrogenase</i>)	This study
UJ2481	DH10B::pST-21 (<i>M2-aminotransferase class II</i>)	This study
UJ2483	DH10B::pST-22 (<i>G3PD-M2</i>)	This study
UJ2485	DH10B::pST-23 (<i>murA-M2</i>)	This study
UJ2487	DH10B::pST-24 (<i>riboflavin synthetase α-chain-M2</i>)	This study
UJ2489	DH10B::pST-25 (<i>GTP cyclohydrolase II-M2</i>)	This study
UJ2491	DH10B::pST-7 (Δ CC2323)	This study
UJ2493	DH10B::pST-8 (<i>M2-CC2323</i>)	This study
UJ2499	DH10B::pST-10 (<i>M2-CC2323</i>)	This study
UJ2500	DH10B::pST-11 (<i>CC2323-M2</i>)	This study
<u><i>C. crescentus</i></u>		
UJ199	NA1000 <i>clpP</i> :: Ω <i>P_{xyI}</i> :: <i>clpP</i>	Jenal and Fuchs (1998)
UJ200	NA1000 <i>clpX</i> :: Ω <i>P_{xyI}</i> :: <i>clpX</i>	Jenal and Fuchs (1998)
UJ418	NA1000::pMR20	P. Aldridge
UJ1249	NA1000::pMO88 (<i>P_{xyI}</i> :: <i>clpX_{ATP}</i>)	M. Osteras
UJ2450	NA1000::pST-1 (<i>P_{xyI}</i> :: <i>clpX_{ATP}-M2</i>)	This study
UJ2458	UJ200::pST-4 (<i>M2-ctrA</i>)	This study
UJ2460	UJ200::pST-5 (<i>M2-CC2323</i>)	This study

UJ2462	UJ200::pST-6 (<i>M2-cheD</i>)	This study
UJ2464	UJ200::pST-12 (<i>M2-G3PD</i>)	This study
UJ2466	UJ200::pST-13 (<i>M2-CC2821</i>)	This study
UJ2468	UJ200::pST-14 (<i>M2-ribosomal subunit interface protein</i>)	This study
UJ2470	UJ200::pST-15 (<i>M2-murA</i>)	This study
UJ2472	UJ200::pST-16 (<i>M2-cu⁺⁺ binding protein</i>)	This study
UJ2474	UJ200::pST-17 (<i>M2-riboflavin synthetase α-chain</i>)	This study
UJ2476	UJ200::pST-18 (<i>M2-GTP cyclohydrolase II</i>)	This study
UJ2478	UJ200::pST-19 (<i>M2-acetyl coA transferase</i>)	This study
UJ2480	UJ200::pST-20 (<i>M2-G6P 1-dehydrogenase</i>)	This study
UJ2482	UJ200::pST-21 (<i>M2-aminotransferase class</i>)	This study
UJ2484	UJ200::pST-22 (<i>G3PD-M2</i>)	This study
UJ2486	UJ200::pST-23 (<i>murA-M2</i>)	This study
UJ2488	UJ200::pST-24 (<i>riboflavin synthetase α-chain-M2</i>)	This study
UJ2490	UJ200:: pST-25 (<i>GTP cyclohydrolase II-M2</i>)	This study
UJ2492	NA1000 Δ CC2323	This study
UJ2494	NA1000 <i>M2-CC2323</i> (chromosomal copy of CC2323 N-terminally M2 tagged)	This study
UJ2579	UJ200::pMR10	A. Schauerte
UJ2580	NA1000::pMR10	A. Schauerte
UJ2581	NA1000::pST-5 (<i>M2-CC2323</i>)	This study

Plasmids

pMR10	KanR low copy number and broad host range vector	C. Mohr and R. Roberts
pMR20	TetR low copy number and broad host range vector	C. Mohr and R. Roberts
pNPTS138	KanR suicide vector with <i>sacB</i> gene and <i>oriT</i>	M.R.K. Alley
pBBR1-MCS2	KanR medium copy and broad range vector	M.E. Kovach
pST-N-M2	pMR10 based cloning vector used for translational fusion of genes with the FLAG M2 tag N-terminally	This study
pST-C-M2	pMR10 based cloning vector used for translational fusion of genes with the FLAG M2 tag C-terminally	This study
pMO88	pMR20 based plasmid with $P_{xyl}::clpX_{ATP}$	M. Osteras
pST-1	pMO88 based plasmid with $P_{xyl}::clpX_{ATP}$ -M2	This study
pST-4	pST-N-M2 with <i>ctrA</i> (CC3035) cloned as <i>SpeI-EcoRI</i> fragment (PCR with primers 822 and 823)	This study
pST-5	pST-N-M2 with CC2323 cloned as <i>SpeI-EcoRI</i> fragment (PCR with primers 729 and 730)	This study
pST-6	pST-N-M2 with <i>cheD</i> (CC0438) cloned as <i>SpeI-EcoRI</i> fragment (PCR with primers 828 and 829)	This study
pST-7	pNPTS138 with Δ CC2323	This study

pST-10	pBBR1-MCS2 with <i>M2-CC2323</i>	This study
pST-11	pMR10 with <i>CC2323-M2</i>	This study
pST-12	pST-N-M2 with <i>G3PD (CC3248)</i> cloned as <i>SpeI-EcoRI</i> fragment (PCR with primers 735 and 736)	This study
pST-13	pST-N-M2 with <i>CC2821</i> cloned as <i>SpeI-EcoRI</i> fragment (PCR with primers 741 and 742)	This study
pST-14	pST-N-M2 with <i>ribosomal interface subunit protein (CC3597)</i> cloned as <i>SpeI-EcoRI</i> fragment (PCR with primers 743 and 744)	This study
pST-15	pST-N-M2 with <i>murA (CC2350)</i> cloned as <i>SpeI-EcoRI</i> fragment (PCR with primers 733 and 734)	This study
pST-16	pST-N-M2 with <i>cu⁺⁺ binding protein (CC0965)</i> cloned as <i>SpeI-EcoRI</i> fragment (PCR with primers 725 and 726)	This study
pST-17	pST-N-M2 with <i>riboflavin synthetase α-chain (CC0886)</i> cloned as <i>SpeI-EcoRI</i> fragment (PCR with primers 824 and 825)	This study
pST-18	pST-N-M2 with <i>GTP cyclohydrolase II (CC0887)</i> cloned as <i>SpeI-EcoRI</i> fragment (PCR with primers 826 and 827)	This study
pST-19	pST-N-M2 with <i>acetyl coA acetyltransferase (CC0510)</i> cloned as <i>SpeI-EcoRI</i> fragment	This study

	(PCR with primers 739 and 740)	
pST-20	pST-N-M2 with <i>G-6-P 1-dehydrogenase</i> (CC2057) cloned as <i>SpeI-EcoRI</i> fragment (PCR with primers 731 and 732)	This study
pST-21	pST-N-M2 with <i>aminotransferase class II</i> (CC1162) cloned as <i>SpeI-EcoRI</i> fragment (PCR with primers 737 and 738)	This study
pST-22	pST-C-M2 with <i>G3PD</i> (CC3248) cloned as a <i>SpeI-EcoRI</i> fragment (PCR with primers 735&750)	This study
pST-23	pST-C-M2 with <i>murA</i> (CC2350) cloned as a <i>SpeI-EcoRI</i> fragment (PCR with primers 733 and 749)	This study
pST-24	pST-C-M2 with <i>riboflavin synthetase α-chain</i> (CC0886) cloned as a <i>SpeI-EcoRI</i> fragment (PCR with primers 751and 824)	This study
pST-25	pST-C-M2 with <i>GTP cyclohydrolase II</i> (CC0887) cloned as a <i>SpeI-EcoRI</i> fragment (PCR with primers 752 and 826)	This study

Table 2.2. List of strains and plasmids used in studies on the SsrA tag in *C. crescentus* (chapter 4).

Strain/Plasmid	Description	Reference or source
<i>E. coli</i>		
DH10B	F- <i>mcrA</i> D (<i>mrr hsdRMS mcrB C</i>) F80 <i>dlacZDM15 DlacX74 endA1 recA1</i> <i>deoR</i> D (<i>ara, leu</i>) 7697 <i>araD139 galU galK</i> <i>nup GrpsL</i>	GIBCO BRL
UJ1252	DH10B::pGR8 (<i>flbD_{wt}</i>)	G. Rummel
UJ1255	DH10B::pGR11(<i>flbD_{Δ13}-ssrA</i>)	G. Rummel
UJ2495	DH10B::pST-30 (<i>flbD_{Δ13}-ssrA</i>)	This study
UJ2496	DH10B::pST-31 (<i>flbD_{Δ13}-ssrA_{DDD}</i>)	This study
UJ2497	DH10B::pST-32 (<i>flbD-ssrA</i>)	This study
UJ2498	DH10B::pST-33 (<i>flbD-ssrA_{DDD}</i>)	This study
UJ2502	UJ199::pGR8	This study
UJ2516	DH10B::pST-36 (pBBR1-MCS2:: <i>flbD-ssrA_{DDD}</i>)	This study
UJ2517	DH10B::pST-37 (pBBR1-MCS2:: <i>flbD-ssrA</i>)	This study
UJ2518	DH10B::pST-34 (<i>flbD_{Δ11}</i>)	This study
UJ2519	DH10B::pST-35 (<i>flbD_{Δ13}</i>) clone 1	This study
UJ2520	DH10B::pST-35 (<i>flbD_{Δ13}</i>) clone 2	This study
UJ2521	DH10B::pST-39 (<i>flbD_{Δ13}-ssrA</i>). NOTE: pST-39 contains <i>flbD</i> with a spontaneous mutation (originally from pST-30)	This study

C. crescentus

UJ1346	NA1000:: <i>flbD</i> _{wt}	G. Rummel
UJ1347	NA1000:: <i>flbD</i> _{Δ13-ssrA}	G. Rummel
COH6 (UJ2522)	NA1000:: <i>flbD</i> _{Δ13-ssrA} (from UJ2521)	This study
COH7 (UJ2523)	NA1000:: <i>flbD</i> _{Δ13-ssrA} (from UJ2495)	This study
COH12 (UJ2524)	NA1000:: <i>flbD-ssrA</i> _{DDD} (from UJ2496, #1)	This study
COH13 (UJ2525)	NA1000:: <i>flbD-ssrA</i> _{DDD} (from UJ2496, #2)	This study
COH14 (UJ2526)	Motile suppressor of COH6	This study
COH15 (UJ2527)	Motile suppressor of COH6	This study
COH16 (UJ2528)	Motile suppressor of COH6	This study
COH17 (UJ2529)	Motile suppressor of COH6	This study
COH18 (UJ2530)	Motile suppressor of COH7	This study
COH19 (UJ2531)	Motile suppressor of COH7	This study
COH20 (UJ2532)	Motile suppressor of COH7	This study
COH21 (UJ2533)	Motile suppressor of COH7	This study
COH22 (UJ2534)	Motile suppressor of COH12	This study
COH23 (UJ2535)	Motile suppressor of COH12	This study
COH24 (UJ2536)	Motile suppressor of COH12	This study
COH25 (UJ2537)	Motile suppressor of COH12	This study
COH26 (UJ2538)	Motile suppressor of COH13	This study
COH27 (UJ2539)	Motile suppressor of COH13	This study
COH28 (UJ2540)	Motile suppressor of COH13	This study
COH29 (UJ2541)	Motile suppressor of COH13	This study
COH33 (UJ2542)	NA1000:: <i>flbD-ssrA</i> (from UJ2497)	This study
COH34 (UJ2543)	NA1000:: <i>flbD-ssrA</i> _{DDD} (from UJ2498, #1)	This study

COH35 (UJ2544)	NA1000:: <i>flbD</i> - <i>ssrA</i> _{DDD} (from UJ2498, #2)	This study
COH36 (UJ2545)	Motile suppressor of COH33	This study
COH37 (UJ2546)	Motile suppressor of COH33	This study
COH38 (UJ2547)	Motile suppressor of COH33	This study
COH39 (UJ2548)	Motile suppressor of COH33	This study
COH40 (UJ2549)	Motile suppressor of COH33	This study
COH43 (UJ2550)	Motile suppressor of COH34	This study
COH44 (UJ2551)	Motile suppressor of COH34	This study
COH45 (UJ2552)	Motile suppressor of COH34	This study
COH46 (UJ2553)	Motile suppressor of COH34	This study
COH47 (UJ2554)	Motile suppressor of COH34	This study
COH48 (UJ2555)	Motile suppressor of COH35	This study
COH49 (UJ2556)	Motile suppressor of COH35	This study
COH50 (UJ2557)	Motile suppressor of COH35	This study
COH51 (UJ2558)	Motile suppressor of COH35	This study
COH52 (UJ2559)	Motile suppressor of COH35	This study
ST190 (UJ2562)	NA1000::COH18 <i>flbD</i> 3' end	This study
ST191 (UJ2563)	NA1000::COH18 <i>flbD</i> 3' end	This study
ST192 (UJ2564)	NA1000::COH38 <i>flbD</i> 3' end	This study
ST197 (UJ2565)	NA1000:: <i>flbD</i> _{Δ11} (from UJ2518)	This study
ST198 (UJ2566)	NA1000:: <i>flbD</i> _{Δ13} (from UJ2519, #1)	This study
ST199 (UJ2567)	NA1000:: <i>flbD</i> _{Δ13} (from UJ2519, #2)	This study
ST200 (UJ2568)	NA1000:: <i>flbD</i> _{Δ13} (from UJ2520, #1)	This study
ST201 (UJ2569)	NA1000:: <i>flbD</i> _{Δ13} (from UJ2520, #2)	This study

Plasmids

pBGS18T	KanR derivative of pUC18 with <i>oriT</i>	M.R.K Alley
pBBR1-MCS2	KanR medium copy and broad range vector	M.E. Kovach
pGR8	pBGS18T with the 3' 650 bp of <i>flbD</i>	G. Rummel
pGR11	pBGS18T with the 3' 650 bp of <i>flbD</i> where coding sequence of last 13 AA was changed to that of the SsrA tag	G. Rummel
pST-30	pGR8 based plasmid with <i>flbD</i> _{Δ13} - <i>ssrA</i> (PCR with primers 645 and 646)	This study
pST-31	pGR8 based plasmid with <i>flbD</i> _{Δ13} - <i>ssrA</i> _{DDD} (PCR with primers 646 and 668)	This study
pST-32	pGR8 based plasmid with <i>flbD</i> - <i>ssrA</i> (PCR with primers 646 and 705)	This study
pST-33	pGR8 based plasmid with <i>flbD</i> - <i>ssrA</i> _{DDD} (PCR with primers 646 and 722)	This study
pST-34	pGR8 based plasmid with <i>flbD</i> _{Δ11} (PCR with primers 646 and 819)	This study
pST-35	pGR8 based plasmid with <i>flbD</i> _{Δ13} (PCR with primers 646 and 818)	This study
pST-36	pBBR1-MCS2 with <i>flbD</i> - <i>ssrA</i> _{DDD} (PCR with primers 847 and 706 on genomic material of COH43)	S. Baeriswyl
pST-37	pBBR1-MCS2 with <i>flbD</i> - <i>ssrA</i> (PCR with primers 847 and 706 on genomic material of	S. Baeriswyl

	COH39)
pST-39	pST-30 with spontaneous point mutation in This study the fourth codon of <i>ssrA</i> (see text for details, COH6)

3 IDENTIFICATION OF NOVEL SUBSTRATES OF THE CLPXP PROTEASE IN *C. CRESCENTUS*

Abstract

Proteolysis is an important regulatory mechanism by which cells can degrade particular proteins in response to cues either external, such as heat stress, or internal, such as cell cycle progression. In the dimorphic bacterium *C. crescentus*, the ClpXP protease is essential for growth, survival and cell cycle progression. Depletion of ClpXP results in a block at the G1-to-S phase transition, most probably due to the stabilisation of one or several substrate proteins whose untimely presence inhibits cell cycle progression. Identification of ClpXP substrates is of crucial importance to analyse the role of ClpXP in cell cycle control. The observation that about 5% of the cell's proteins are rapidly degraded, with more than half of them also being synthesised differentially during the cell cycle, emphasised the critical role of proteolysis in cell cycle progression (Grünenfelder et al. 2001)

To identify substrates of the ClpXP protease, particularly those whose degradation is imperative to cell cycle progression, we generated a dominant negative allele of *clpX*, *clpX_{ATP}*, with a mutation in the nucleotide binding domain. Conditional expression of *clpX_{ATP}* was used in a global proteomic screen to identify proteins that were stabilised upon inactivation of ClpX. We found that ClpX_{ATP} monomers physically interact with ClpX_{wt} monomers arguing that this lead to ClpX inactivation through the formation of mixed inactive oligomers. Cells expressing *clpX_{ATP}* rapidly stabilised the only known ClpXP substrate to date, CtrA, showed a cell division block and rapidly lost

viability. Through a proteomics screen we identified nine proteins as potential ClpXP substrates, including the previously identified CtrA protein. Target validation experiments confirmed three of these proteins, namely CtrA, CheD and CC2323, as potential substrates of ClpXP.

CC2323 is a hypothetical protein found exclusively in alpha proteobacteria. We found that CC2323 is not essential for growth or survival of *C. crescentus*. However, the expression of CC2323 appears to be tightly regulated by the interplay of the cell cycle master regulators CtrA and GcrA, arguing that CC2323 is under cell cycle control. N-terminally M2-tagged CC2323 was used to follow expression and measure protein stability during the cell cycle. Expression of CC2323 is restricted to the late S and G2 phase of the cell cycle and coincides precisely with the presence of the CC2323 protein. This is consistent with the observation that the protein is rapidly degraded with a half life of approximately 60 minutes. Thus, the undesirable presence of CC2323 in certain cellular compartments and/or at particular stages of the cell cycle may have negative deleterious effects on the cells. In accordance with this, we found that overproduction of CC2323 is highly toxic. Based on this, we propose that the tight regulation of CC2323 through both expression and rapid proteolysis might be critical for *C. crescentus* cell cycle control.

3.1 Generation and analysis of a conditional dominant lethal allele of *clpX*

To identify substrates of the ClpXP protease, we intended to use a global proteomic approach (see section 3.2). Briefly, the system would require the removal of ClpX activity in the cell and, using 2D gels, ask which proteins become stabilised as a result. When this work was initiated, the only available conditional ClpX mutant was strain UJ200 that relies on depletion of ClpX upon cessation of *clpX* expression from a xylose-dependent promoter (see section 1.3.2; Jenal and Fuchs 1998). In UJ200, complete depletion of the cellular ClpX pool takes more than 4 hours after xylose removal (Jenal and Fuchs 1998). Although UJ200 could have been used for the proposed experiments, the long reaction time might make it difficult to distinguish between direct and indirect effects of ClpX depletion. An ideal system would disrupt ClpX activity in the cell rapidly so as to minimise the number of false positive candidates detected on 2D gels. It was to this end that we created the *clpX*_{ATP} allele. In this chapter, the mutant allele is described and results of its biological efficacy in disrupting ClpX activity are presented.

3.1.1 Construction of the *clpX*_{ATP} allele

We set out to construct a *clpX* mutant allele that encodes a *clpX* variant which has lost its activity but can still interact with wild-type ClpX and abolish the activity of the chaperone through the formation of mixed oligomers. Several alleles of *clpX* were constructed by site directed mutagenesis with changes in the Zn-binding motif, the

walker A box of the ATPase domain or the conserved sensor 2 motif of SSD domain (Figure 3.1).

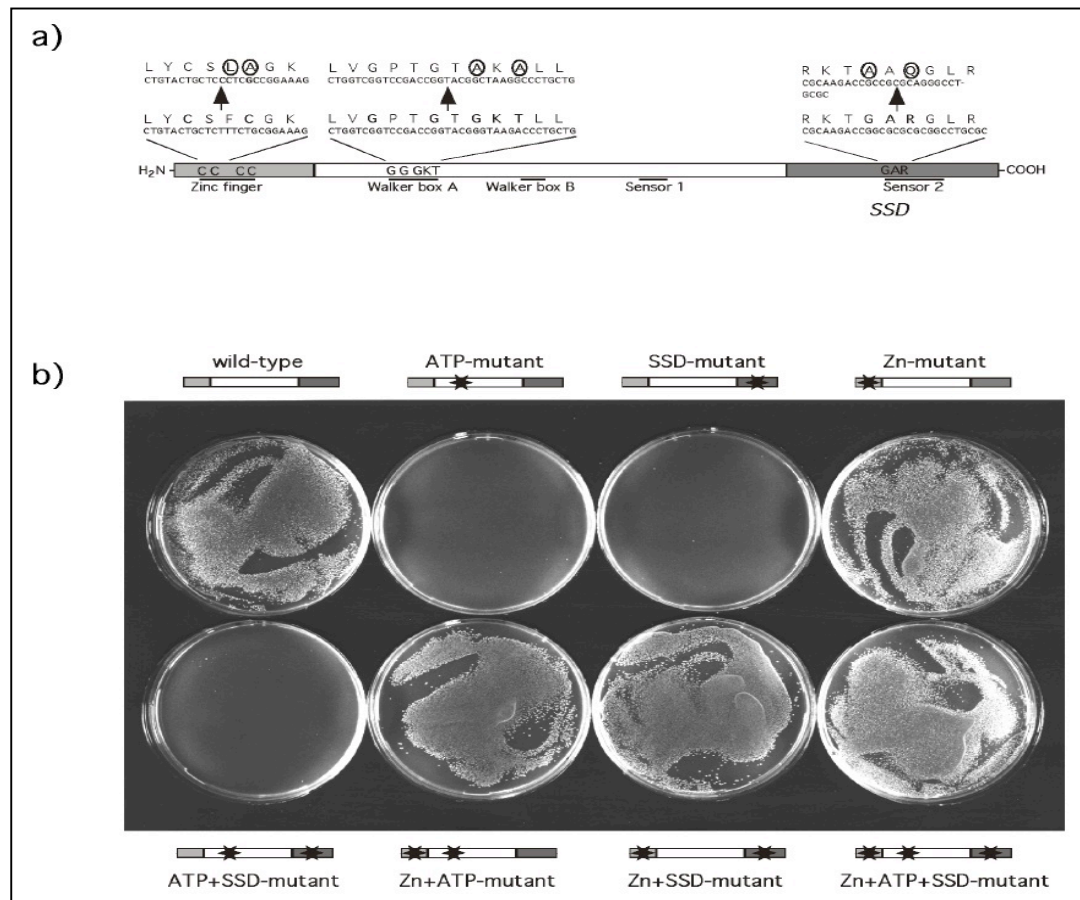


Figure 3.1. a) Site directed mutagenesis of *clpX* in conserved residues in the Zn binding motif, walker A box and sensor 2 motif of the SSD domain. b) Each allele was introduced into NA1000 cells on the medium copy vector pBBR by conjugation. Cells bearing plasmids with a mutation in the ATP or SSD domain fail to grow but can grow normally if the mutations are coupled with one in the Zn binding domain of *clpX*.

As shown in Figure 3.1, mutations in the ATP or SSD domain of *clpX* have a dominant lethal phenotype and we propose that this is due to the formation of mixed oligomers with wild-type ClpX leading to chaperone inactivation. The effects of either mutation are nullified by the presence of a second site mutation in the Zn binding motif of ClpX. This result confirms that the Zn binding domain is essential for oligomerisation (Banecki et al. 2001). We selected the *clpX* allele with the walker

A box mutation for use in our system, thereafter referred to as $clpX_{ATP}$. With the knowledge available at the onset of this study, we predicted that this allele could bind ATP and but not hydrolyse it. As discussed above in section 1.2.2, the role of the SSD domain in ClpX activity is not entirely clear, hence casting doubt on the reason for its dominant lethality. Furthermore, it has long been known that ATP is important in oligomer formation (Parsell et al. 1994; Seol et al. 1995a; Seol et al. 1995b), and thus we were more convinced that the dominant lethality of the ATP allele is more likely than that of the SSD allele to be due to direct inactivation of ClpX activity through mixed oligomer formation.

3.1.2 $clpX_{ATP}$ is a dominant lethal allele

We cloned the $clpX_{ATP}$ allele into the low copy vector pMR20 under control of the xylose dependent promoter P_{xy} and introduced the resulting plasmid (pMO88) into *C. crescentus* by conjugation. The resulting strain, UJ1249, grew normally on PYE-Glucose but could not grow on PYE-Xylose plates (Figure 3.2). This supports the notion that $clpX_{ATP}$ is a dominant negative allele whose expression is deleterious to *C. crescentus*.

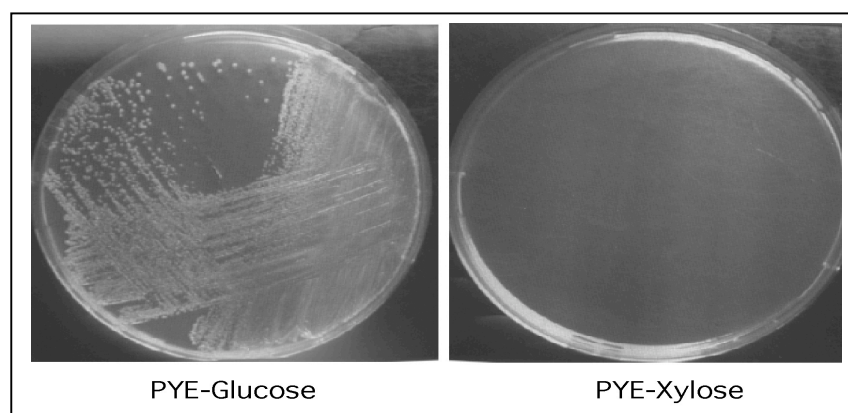


Figure 3.2. Strain UJ1249 is unable to grow on xylose containing plates (right panel) but is able to grow normally on glucose plates.

3.1.3 ClpX_{ATP} monomers physically interact with wild-type ClpX to form mixed oligomers

To demonstrate that the toxicity of ClpX_{ATP} monomers is due to their interaction with, and inactivation of, ClpX_{wt} monomers, we designed a simple biochemical assay. In this assay, a M2-tagged copy of *clpX*_{ATP} (*clpX*_{ATP}-M2) was expressed under control of *P*_{xyI} (see Materials and Methods section 2.6.1) in NA1000 (UJ2450). We reasoned that if ClpX_{ATP} can interact with ClpX_{wt}, immunoprecipitation of the former using anti-M2 antibodies should co-immunoprecipitate the slightly shorter wild-type protein.

Strain UJ2450 was induced with xylose for 2 hours, and cells were lysed under native conditions using a gentle sonication technique (see Materials and Methods section 2.2). The resulting extract was used for immunoprecipitation with anti-FLAG M2 agarose beads (see Materials and Methods section 2.2) and the precipitated fraction was analysed by SDS-PAGE. An immunoblot using anti-ClpX antibodies showed the presence of 2 bands of ClpX (Figure 3.3), the larger of which corresponds to ClpX_{ATP}-M2. This confirms that ClpX_{ATP} monomers indeed physically interact with ClpX_{wt} monomers.

As a control, we performed the same assay on uninduced cells and detected a faint band corresponding to ClpX_{wt} but no band of ClpX_{ATP} was seen. Since a weak band was also seen when NA1000 extract was used for immunoprecipitation, we assume that the anti-FLAG M2 agarose weakly cross-reacts with ClpX_{wt} (Figure 3.3). As all strains were harvested at the same OD₆₆₀ for the assay, the ClpX_{wt} band intensity between NA1000, uninduced and induced UJ2450 were directly compared using the

ImageQuant™ software (Molecular Dynamics) (not shown). This revealed that although anti-FLAG M2 agarose is not completely specific for the tag, the majority of ClpX_{wt} observed in the induced cell-IP sample must be attributed to a genuine interaction with ClpX_{ATP} monomers.

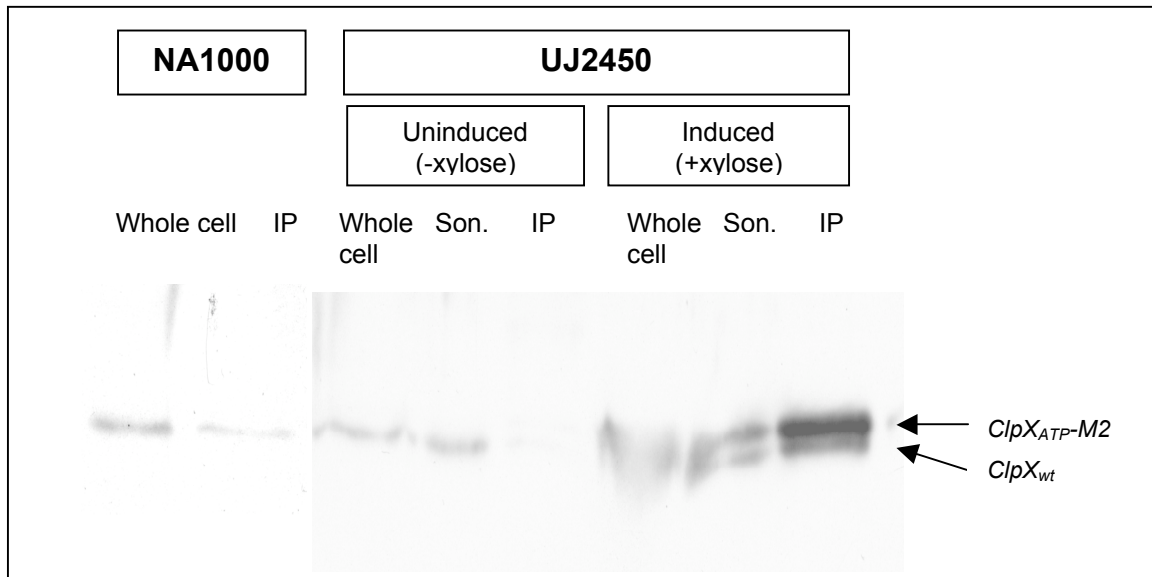


Figure 3.3. Anti-FLAG M2 agarose was used to immunoprecipitate ClpX_{ATP}-M2 from UJ2450 cells before and after induction with xylose. SDS-PAGE and western blot analysis was performed on immunoprecipitated proteins as well as on whole cell extracts and samples of the sonicated cells (Son.). Whole cell extracts show that in NA1000 cells and uninduced UJ2450 only one form of ClpX is present, whereas in induced UJ2450, 2 forms could be seen corresponding to ClpX_{wt} and ClpX_{ATP}-M2. Immunoprecipitation of ClpX_{ATP}-M2 in induced UJ2450 also brought down ClpX_{wt} (IP) demonstrating that the mutant allele physically interacts with ClpX_{wt}.

3.1.4 ClpX_{ATP} synthesis results in filamentous cell morphology, cell death and rapid stabilisation of CtrA

To address the effect of *clpX_{ATP}* expression on cell morphology, strain UJ1249 was grown in PYE-Glu or PYE-Xyl for 24 hours and analysed by light microscopy at 2, 4, 6, 12 and 24 hours after dilution into either medium (Figure 3.4). Furthermore, the growth and viability of strain UJ1249 at was assessed at both restrictive and

permissive conditions by plating dilutions of the respective culture onto PYE-Glu plates every 2 hours after sugar addition (Figure 3.5). As early as 2 hours after induction of ClpX_{ATP} production, cells began to show signs of elongation. By 4 hours, the morphological difference was obvious, and 12 hours after dilution, cells expressing *clpX_{ATP}* had become completely filamentous (Figure 3.4).

It is interesting to note the presence of some cells of wild-type appearance in the induced culture at t24 which were absent from t12 micrographs (Figure 3.4). We propose that during the severe selection, spontaneous mutants had been enriched that have either turned off or inactivated *clpX_{ATP}*, or alternatively, that have learned to cope without ClpX altogether. These suppressors could explain why the viability of induced UJ1249 cells seems to fall below detection after 8 hours of induction and climb again to high numbers (close to those observed at t4 in the uninduced controls) by 24 hours after xylose addition (not shown).

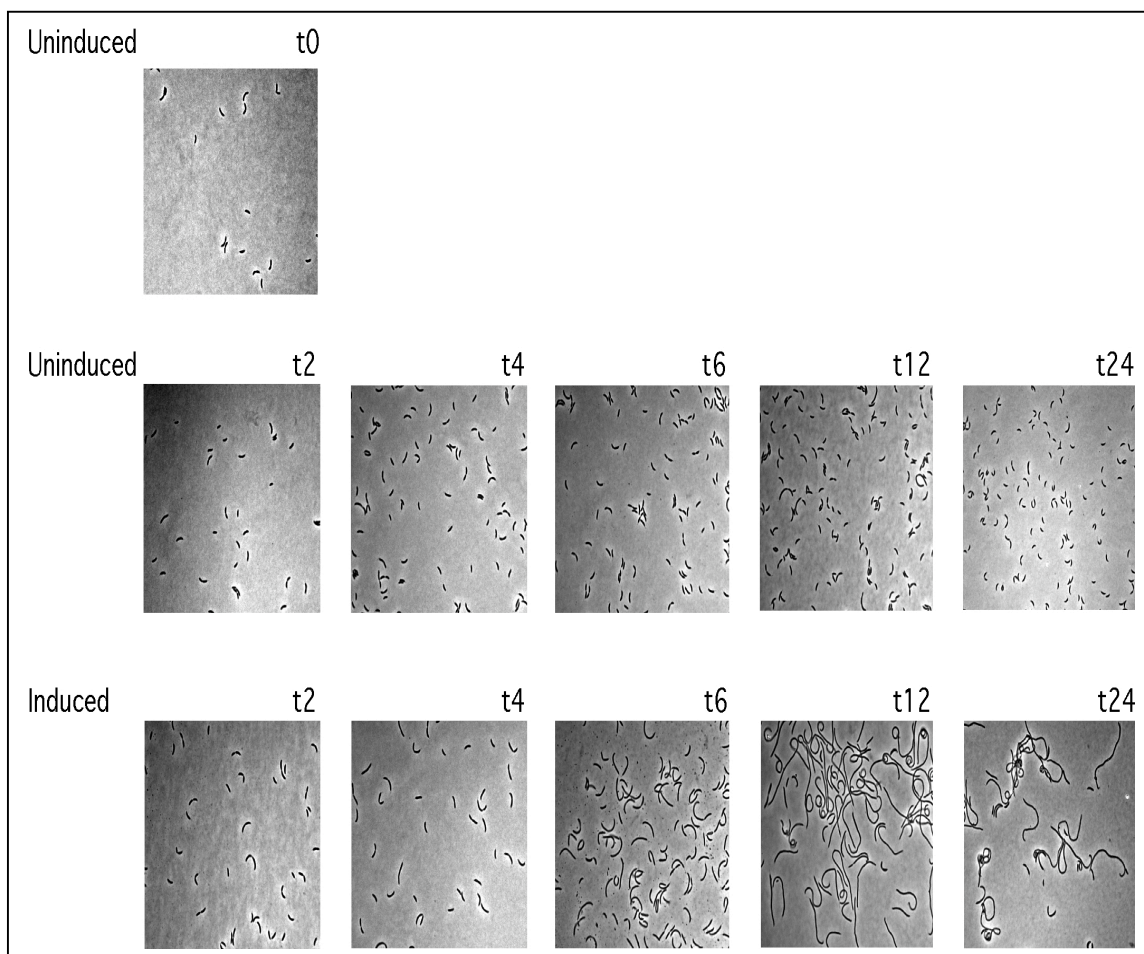


Figure 3.4. *clpX_{ATP}* expression results in cell elongation and filamentation. UJ1249 cells were resuspended in either PYE-X or PYE-G at t0 and cell morphology for a period of 24 hours was recorded using an Olympus AX70 microscope with DIC (Nomarski) optics. Cells start showing signs of elongation as early as 2 hours after xylose addition and by t12 are completely filamentous.

As previously observed for strain UJ200 (Jenal and Fuchs 1998), cells of strain UJ1249 continue to accumulate biomass for up to 8 hours (4 generations) whilst viable cell numbers plateau as early as 4 hours after induction (Figure 3.5). By 6 hours after induction, the viability of induced UJ1249 cells had dropped by one order of magnitude. This indicates that cell division is rapidly stopped upon induction of *clpX_{ATP}* while cessation of growth is much slower and probably an indirect effect of cell cycle arrest. Thus, the phenotype of strain UJ1249 grown in the presence of

xylose is comparable to that of strain UJ200 after depletion of ClpX as pertaining to cell viability, growth and morphology. This confirms that induction of *clpX*_{ATP} and cessation of *clpX* expression have the same effect on *C. crescentus* cell physiology.

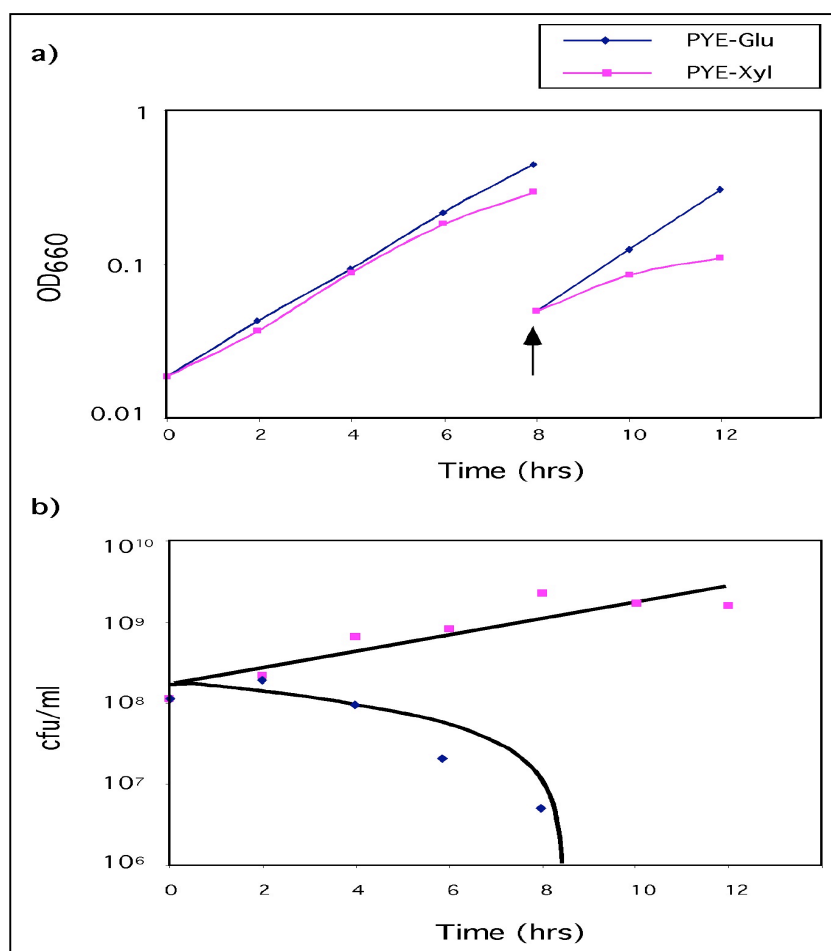


Figure 3.5. Expression of *clpX*_{ATP} is deleterious to the growth and viability of *C. crescentus*. (a) Accumulation of biomass was monitored by optical density measurement at 660nm. Both cultures were diluted to 0.05 in the respective medium upon reaching an OD₆₆₀ of about 0.5 at t8 in order to maintain logarithmic growth (arrow). (b) Viable cells at different times after sugar addition were measured as colony forming units per ml.

We next asked whether ClpX_{ATP} induction leads to stabilisation of CtrA in the same manner that repression of *clpX* expression in UJ200 does. To address this question, cells of strain UJ1249 were grown in M2G minimal medium and then induced for various periods of time with xylose, and synchronised to isolate SW cells. The SW cells were resuspended in M2GX and followed through the cell cycle. Samples were

collected every 20 minutes and CtrA levels assayed by immunoblot analysis using the anti-CtrA antibody. As expected, expression of *clpX_{ATP}* prevented CtrA degradation during the SW-to-ST cell transition even when the cells had only been induced with xylose for 2 hours (Figure 3.6).

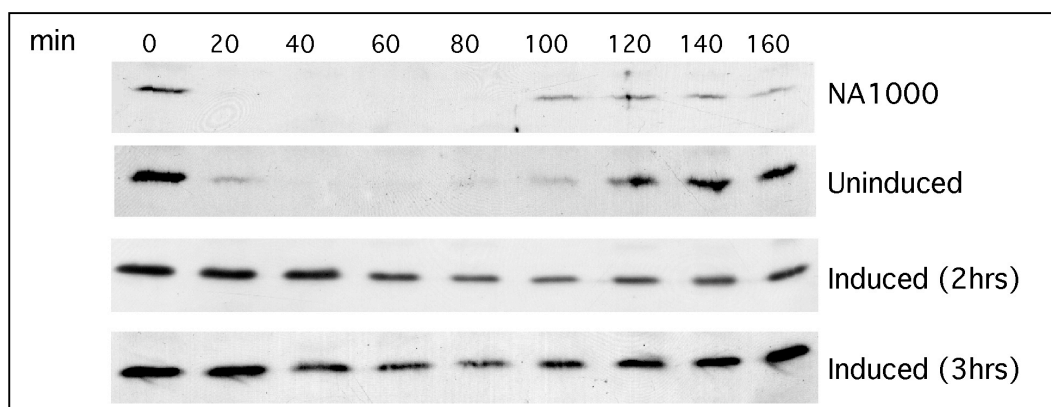


Figure 3.6. Immunoblots of synchronised UJ1249 cells to examine CtrA turnover at the SW-to-ST cell transition after induction of *clpX_{ATP}* expression. The top panel shows CtrA turnover in NA1000 cells that had been exposed to xylose for 2 hours prior to synchronisation. The lower three panels show UJ1249 cells without pre-exposure to xylose (uninduced) or induced for 2 or 3 hours, respectively, before synchronisation. While CtrA is degraded in the absence of ClpX_{ATP}, it clearly persists upon induction of the toxic ClpX allele.

To demonstrate that CtrA persistence is a function of its altered stability in induced UJ1249 cells, we conducted pulse/chase experiments. Non-synchronised UJ1249 cells were exposed to xylose for increasing periods of time, pulse labelled with ³⁵S-cys/met (NEG-772, NEN) for 5 min, then chased with an excess of unlabelled cys/met mix and samples were collected every 30 min. For these experiments, the IPs were performed using antibodies against CtrA, ClpX and ClpP at the same time (Figure 3.7). The results were quantitated using ImageQuant™ (Molecular Dynamics) in order to compare the intensities of CtrA, ClpX and ClpP bands throughout the pulse chase (Figure 3.8).

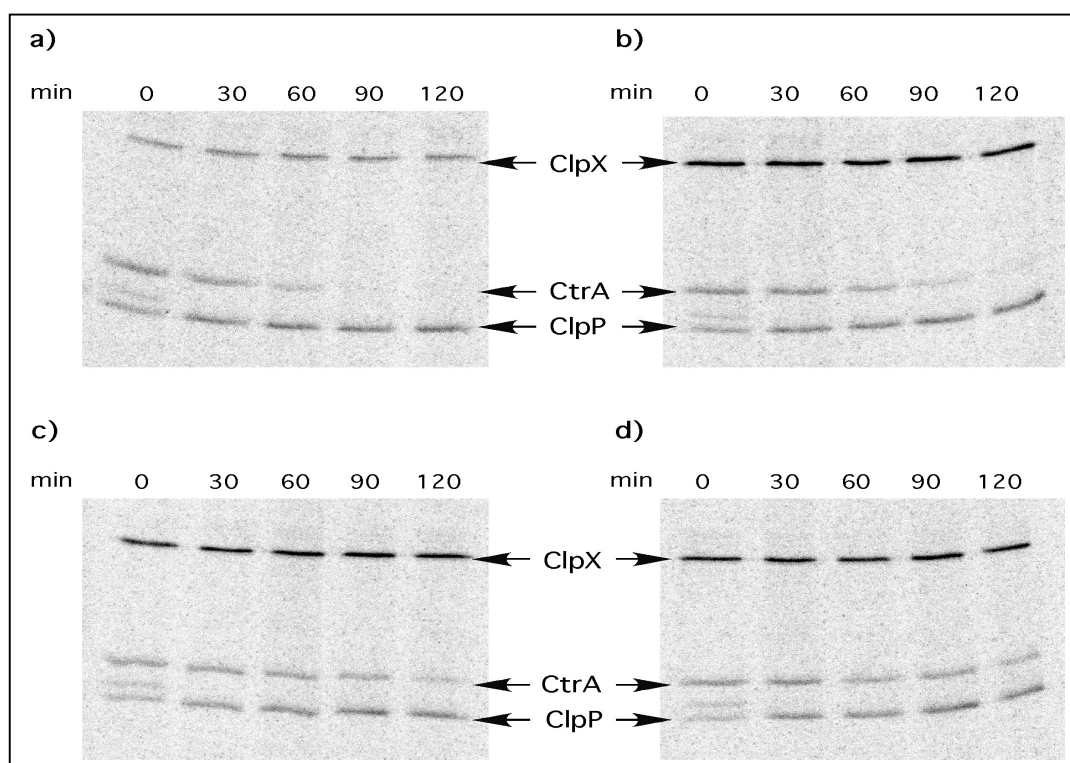


Figure 3.7. Pulse chase/immunoprecipitation of ClpX, CtrA and ClpP from UJ1249 cells before (a), after 5 min (b), 1 hr (c) and 2 hrs (d) of xylose addition. ClpX levels increase dramatically even 5 min after xylose addition (b) and CtrA stabilisation occurs coincidentally, but is better observed after 1 or 2 hrs of xylose addition. ClpP levels are unaffected by xylose addition.

ClpP levels were found to be unaffected by induction of the *clpX*_{ATP} allele (Figure 3.7a as compared to b, c and d). In uninduced UJ1249 cells, CtrA's half life was found to be about 30-45 min (Figure 3.8 b). This is slightly higher than CtrA degradation in NA1000 cells (not shown) but is most likely due to the leakiness of *P*_{xyI} and residual production of ClpX_{ATP} even in the uninduced state. To our surprise, when we added xylose at the same time as the pulse and continued the experiment as described above, ClpX levels were markedly increased to 4-6 times their value in uninduced cells, and CtrA was weakly stabilised (Figures 3.7b, 3.8). Since in pulse/chase experiments one studies the stability of proteins synthesised within the time of the pulse (in our case, 5 min) the results of this experiment suggest that ClpX levels increase very quickly upon xylose addition. As the levels of ClpX as expressed

from the chromosomal *clpX* copy gene do not respond to xylose, this increase is evidently due to the ClpX_{ATP} produced from pMO88. This rapid increase in ClpX_{ATP} in the cell is coincident with weak CtrA stabilisation (Figure 3.7b). However, CtrA stabilisation was more marked in cells exposed to xylose for 1 or 2 hours before pulsing (Figure 3.7c, d; Figure 3.8 t1, t2).

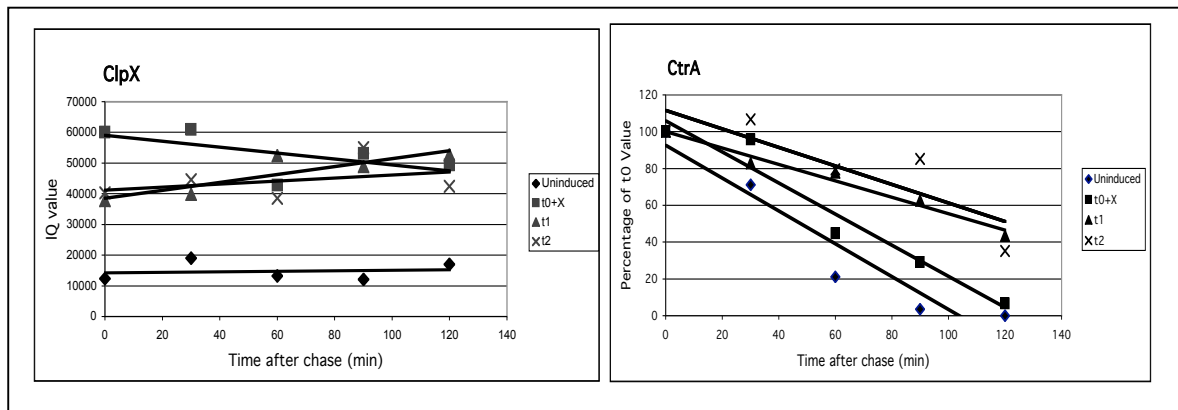


Figure 3.8. Quantitation of ClpX, ClpP and CtrA levels in cells before and 5 min, 1 hr and 2 hours after induction of *clpX*_{ATP} (see text for details)

3.2 Identification of novel ClpXP substrates in *C. crescentus* using a proteomic approach

Having established a system by which ClpX activity can be rapidly removed, we set out to identify ClpXP substrates. Using strain UJ1249, we intended on inducing the expression of *clpX*_{ATP} for 2 hours before performing a pulse/chase experiment taking samples at 0, 60 and 120 min after chase addition. From each time point, a 2D gel would be run (see Materials and Methods section 2.4). Those 2D gels would then be compared with gels prepared from a control strain that is wild-type for ClpX so as to find spots that are stabilised when ClpX activity is depleted in the cell.

Although 2D gel electrophoresis is a robust technique, problems are often encountered with pattern reproducibility and consistency in spot behaviour (Rabilloud 2000). Therefore, we decided to conduct six repeat experiments for statistical analysis. Furthermore, since UJ1249 cells are always grown in the presence of tetracycline to maintain pMO88, we decided to use strain UJ418 grown in the presence of tetracycline as our control strain. Strain UJ418 contains plasmid pMR20, which is the backbone of pMO88, and is induced with xylose for 2 hours prior to protein preparation for 2D gels. Thus, any proteins that are stabilised as a result of either tetracycline or xylose addition would be identified as false positives and be removed from our screen.

Ultimately, our plan can be summarised by the diagram shown in Figure 3.9. As mentioned in section 1.3.5, Grünenfelder et al. (2001) had found 48 spots on 2D gels to be degraded during the course of 120 min after their synthesis (Figure 3.9, open

circles in UJ418 gels). Our aim was to find the subset of these spots that is stabilised in the absence of ClpX activity (Figure 3.9, red circles in UJ1249 cells).

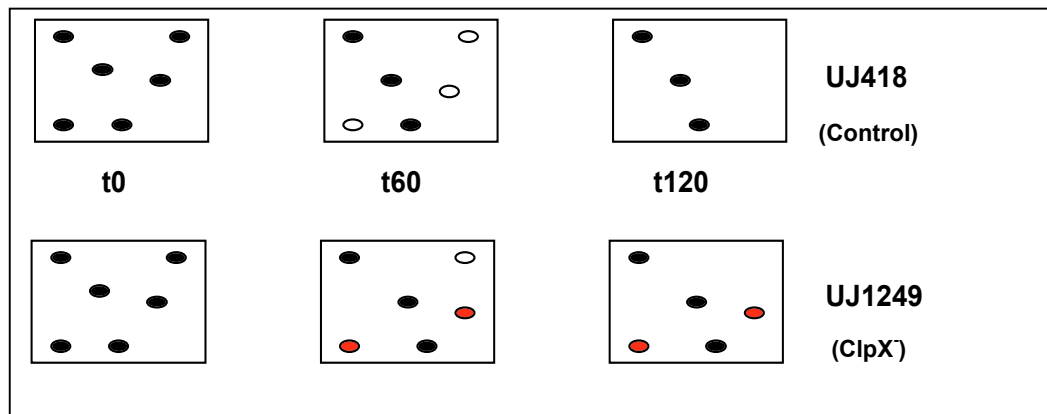


Figure 3.9. Representation of expected patterns on 2D gels of UJ418 and UJ1249 cells. Open circles represent unstable proteins and red circles represent proteins that are stabilised as a result of $clpX_{ATP}$ expression (see text) over the course of 120 min of chase.

3.2.1 Identification of protein spots with altered behaviour upon $ClpX_{ATP}$ induction

Thirty-six analytical 2D gels were prepared as described previously (Grünenfelder et al. 2001). Through data processing and analysis of the resulting autoradiograms (see Materials and Methods section 2.5) we detected a total of 59 spots (hereafter referred to as standard spot, SSPs) whose behaviour is significantly altered in the pulse/chase upon expression of $clpX_{ATP}$ (less than $\alpha_{0.05}$ using an ANOVA test). These 59 SSPs were subjected to two further tests to eliminate spots that could be false positives. The first criterion most commonly used to eliminate false positives was spot intensity. SSPs whose intensity was lower than the arbitrarily set threshold of 200 ppm in all gels, at all time points and in both strains were discarded. This intensity criterion was empirically set as SSPs with lower intensity could often be mistaken with background

noise of the gels, and tend to have high variation. The second criterion was the number of times each spot was found in the repeats and SSPs that were not found in four or more of the six repeats were discarded. However, it should be noted that both criteria were relaxed when viewing t60 and t120 gels of UJ418. This is as unstable spots would be expected to have lower intensity than our threshold and sometimes would have completely disappeared. Application of both criteria to the 59 SSPs eliminated 38 spots.

The remaining 21 SSPs were subjected to one final screen in order to find spots that are degraded in strain UJ418 but are stabilised in strain UJ1249. In this test, the spot intensity at each time point was averaged and plotted against time of chase in order to view the average intensity of the spots over time. Of these 21 SSPs, we found 6 proteins to be present in significantly higher concentration in strain UJ1249 at t0 as compared to strain UJ418. Degradation during the chase period reduced their concentrations to levels comparable to those of the control strain (Figure 3.10). These could represent proteins whose synthesis or maturation is ClpX-dependent but are degraded in a ClpX-independent manner.

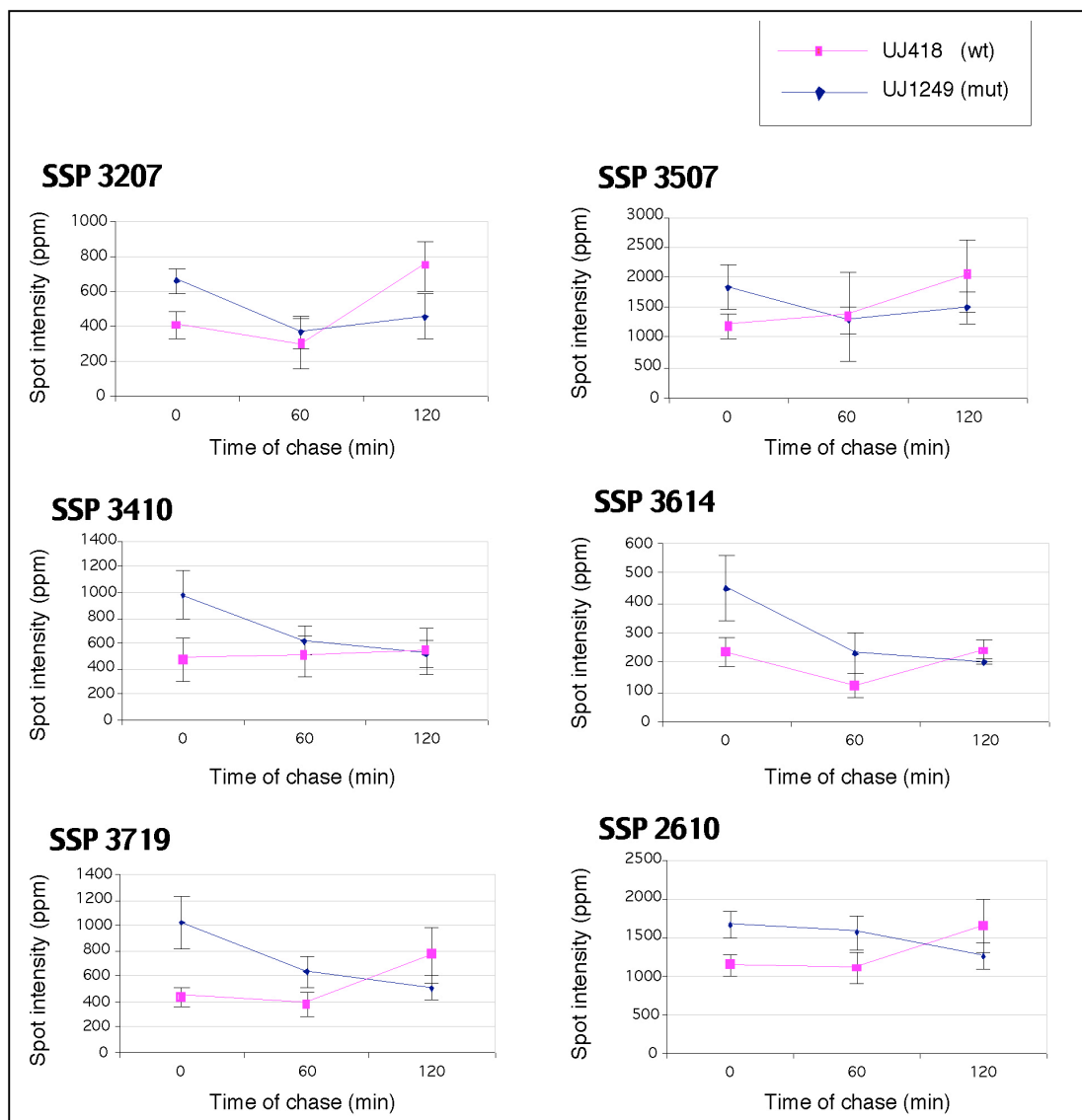


Figure 3.10. Spots that are synthesised in larger amounts in strain UJ1249. Spot intensities in strain UJ1249 are indicated in pink and for UJ418 in blue. Spots identified by mass spectrometry: SSP 3507 (Aspartate aminotransferase, CC1534), SSP 3410 (Aldo/keto reductase, CC3002) and SSP 2610 (cytosol aminopeptidase, CC1692) (identities from SWICZ: <http://proteom.biomed.cas.cz/>).

Of the remaining 15 SSPs, 2 spots were found to increase in intensity over the chase period in induced UJ1249 cells (Figure 3.11). These might be proteins that are modified or processed in a ClpX-dependent manner.

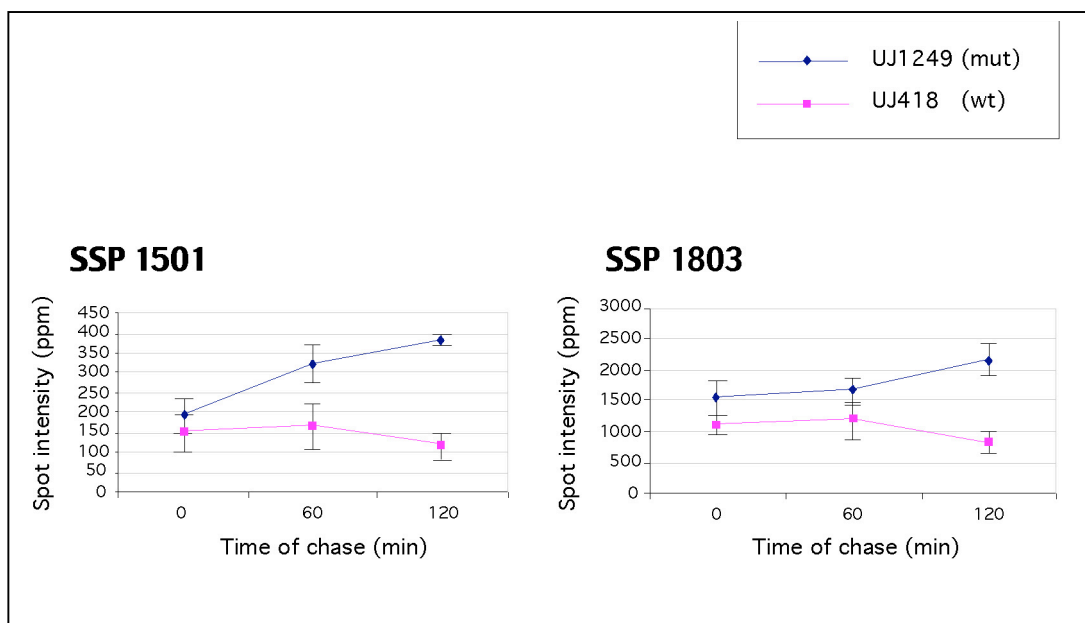


Figure 3.11. Spots whose intensity increases in strain UJ1249 during the chase period. SSP 1501 is unidentified but its synthesis is under differential cell cycle control (Grünenfelder et al. 2001). SSP 1803 was identified by mass spectrometry as Phosphoribosylformylglycinamide synthase II, (CC2500) (identity from SWICZ: <http://proteom.biomed.cas.cz/>).

Two spots were found to have their synthesis repressed in induced UJ1249 cells (Figure 3.12) and a further 2 spots did not fit into the above categories (Figure 3.13).

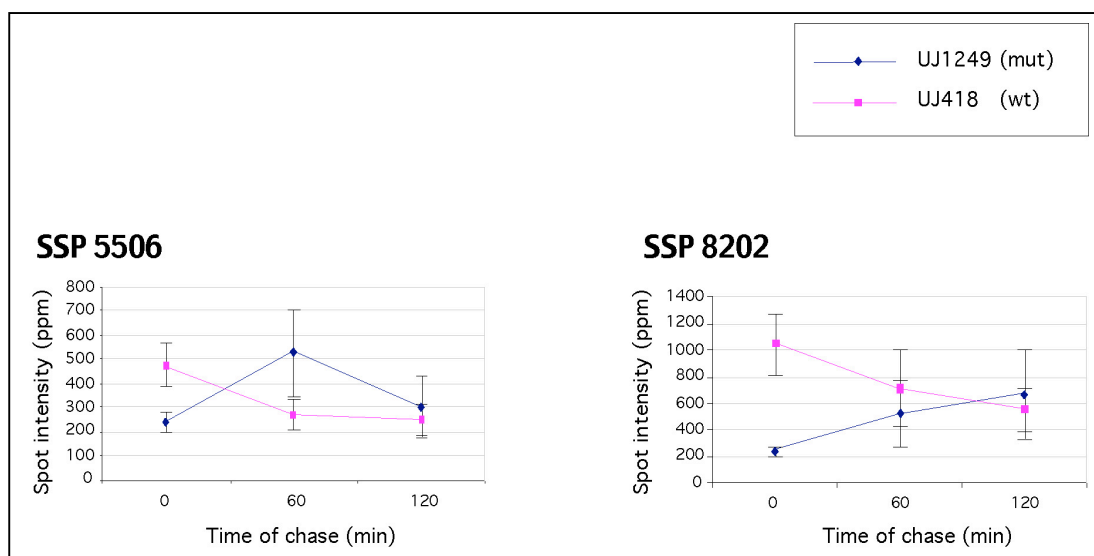


Figure 3.12 Spots whose synthesis is repressed in induced UJ1249 cells. SSP 8202 has been identified by mass spectrometry to be an ABC transporter ATP binding protein (CC1518). (Identity from SWICZ: <http://proteom.biomed.cas.cz/>).

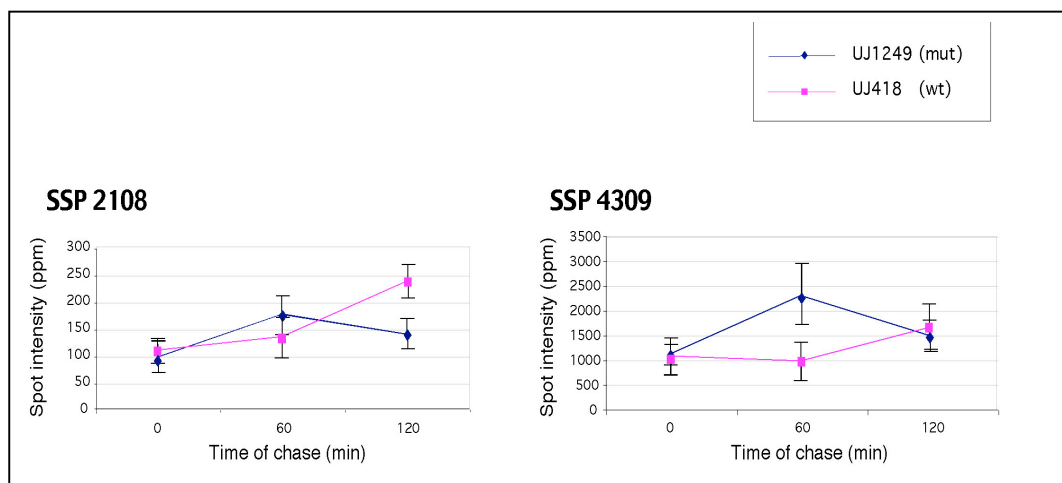


Figure 3.13 SSP 2108 and 4309 spot intensities in strain UJ1249 and UJ418 during the chase. Mass spectrometry has identified SSP 2108 as glutathione peroxidase (CC1730) and SSP 4309 as the 30s ribosomal protein (CC1923) (Identity from SWICZ: <http://proteom.biomed.cas.cz/>).

All twelve spots described above did not decrease in intensity during the chase period in the control strain and therefore were not considered potential ClpXP substrates. This is with the exception of SSP 2108 and 4309, which, upon re-analysis of the data late in the course of the study appeared to be degraded in the wild-type control (Figure 3.13). These two spots could well be counted as potential ClpXP substrates, except that their intensity in strain UJ1249 cells increases over the chase period. This contrasts with the behaviour of proteins considered to be potential ClpXP substrates (see below; Figure 3.14).

Of the 21 spots found to be significantly affected by expression of the *clpX_{ATP}* allele in UJ1249 cells, only nine SSPs passed the final criterion for consideration as potential ClpXP substrates; that is, they are degraded in UJ418 and significantly stabilised in strain UJ1249. The spot intensity profiles of the 9 spots during the chase period is shown in Figure 3.14. In order to focus on the stability of the proteins over the course

of the chase period, the spot intensities at t0 were set to 100% and the intensities at t60 and t120 expressed as a percentage of the t0 value (Figure 3.15).

As shown in Figure 3.14, the synthesis of all proteins in this category is repressed in cells of strain UJ1249 as compared to strain UJ418. This could indicate that those proteins are subject to cell cycle-dependent synthesis. However, when the spot behaviour over 120 min is compared between UJ418 and UJ1249 (Figure 3.15) it is clear that proteins in this set are degraded in the presence of ClpX but stabilised when ClpX activity is depleted. For most proteins, this is pronounced during the first 60 min of the chase. Thus we considered all nine spots as good candidate substrates for ClpXP.

As shown in Table 3.1, only four of the spots in this set have been previously identified as unstable proteins (Grünenfelder et al., 2001); and furthermore are synthesised differentially during the cell cycle. The remaining five spots are therefore novel proteins that can be added to the previously identified 48 unstable proteins. It is unclear why these proteins have previously gone undetected but it is likely to be due to differences in handling or the strain background (UJ418 in our experiments vs. NA1000 in previous work). Furthermore, we used a slightly more sensitive statistical analysis (ANOVA) which takes into consideration a variety of additional factors not previously considered (see Materials and Methods section 2.5).

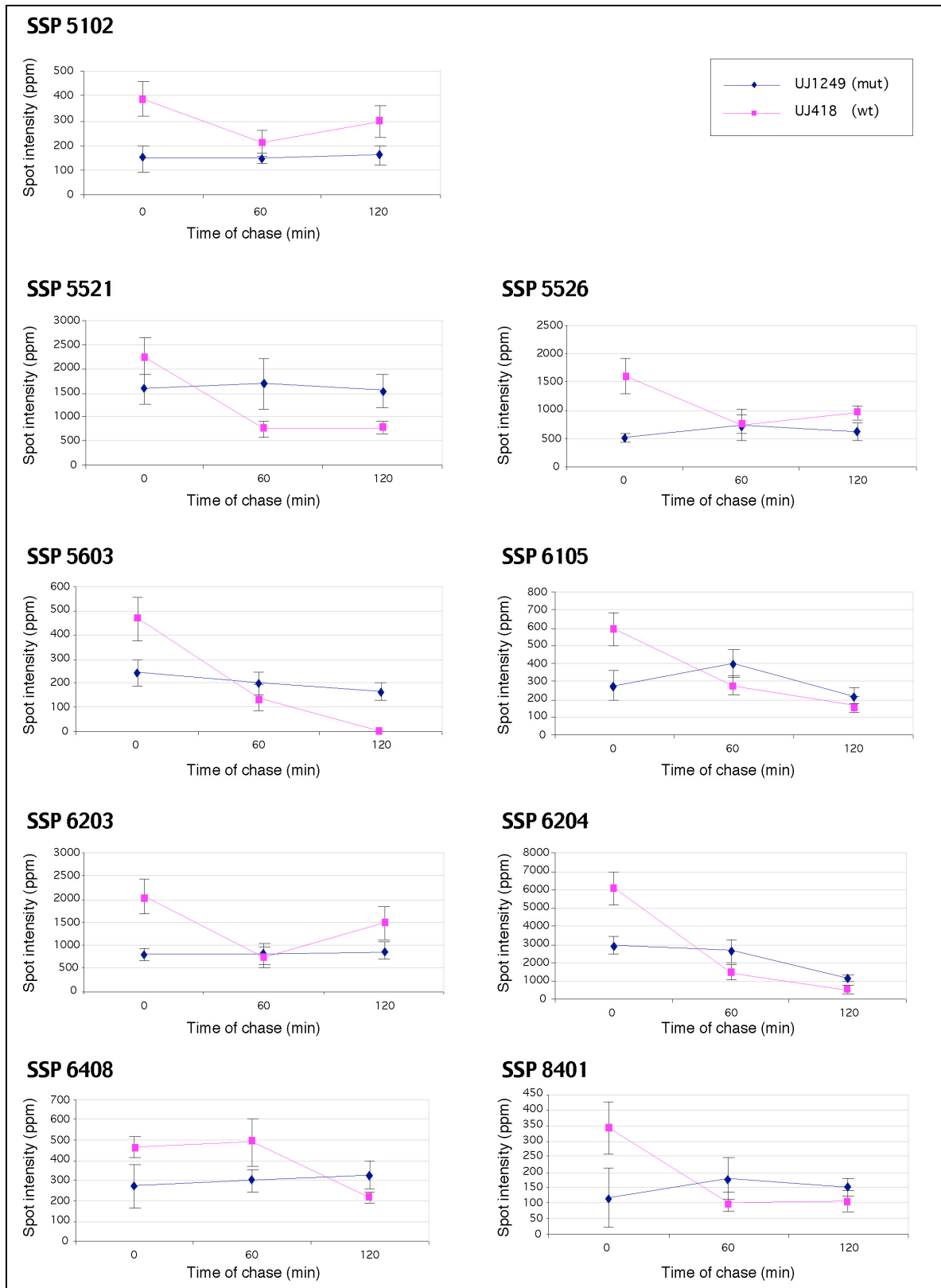


Figure 3.14. Nine spots are stabilised in UJ1249 cells upon expression of *clpX_{ATP}*. Spot intensities are shown as absolute values (ppm). See table 3.1 for further information.

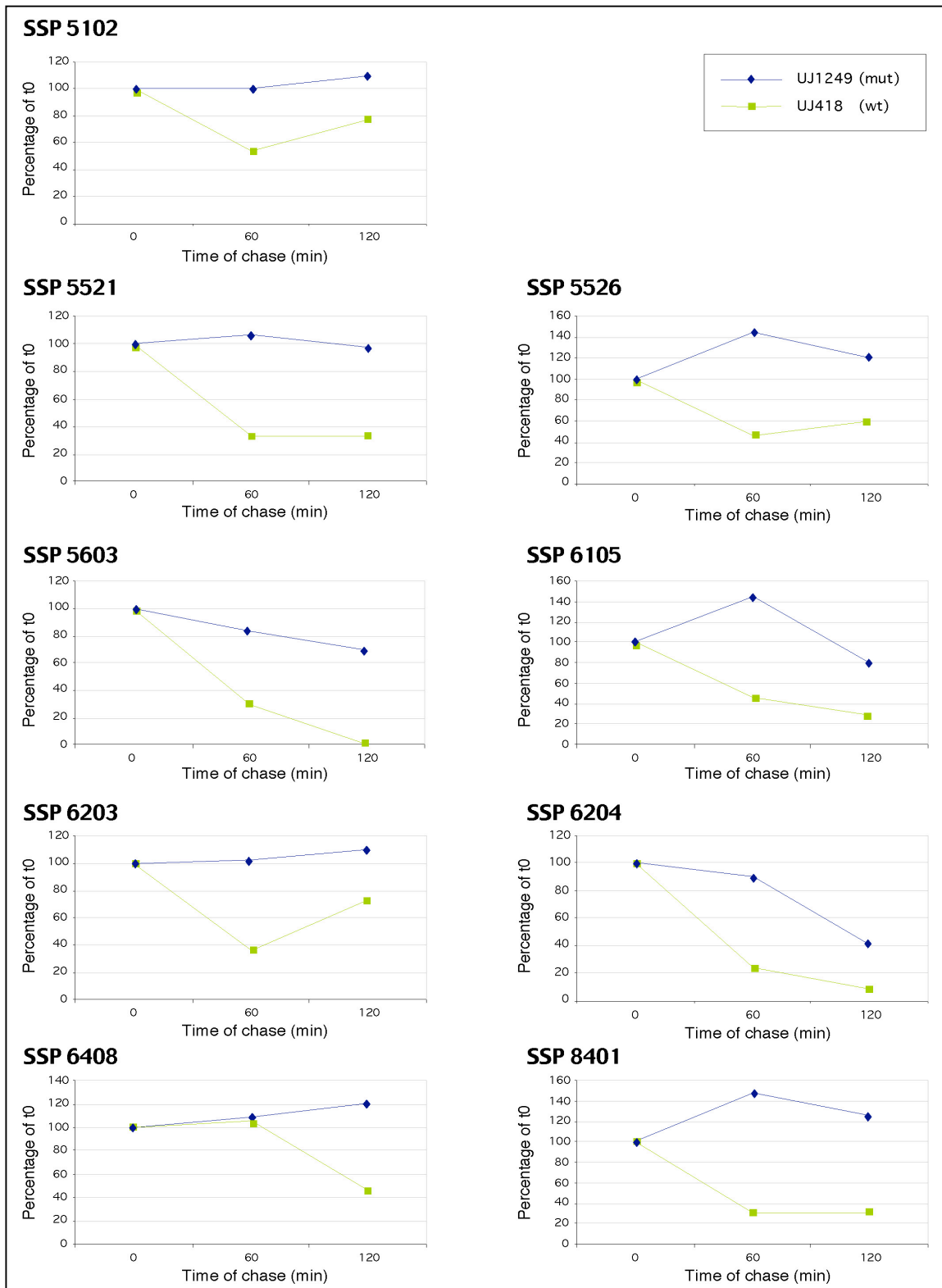


Figure 3.15 Stability profiles of nine spots found to be significantly stabilised in UJ1249 cells as compared with the wild-type control UJ418. Spot intensities are shown as relative values of the initial intensity at t0. See table 3.1 for further information.

Table 3.1. Summary of information available of the nine protein spots found to be stabilised in UJ1249 cells upon *clpX_{ATP}* expression. The Mw/pI column contains the molecular weight (kDa) and isoelectric point of each spot as estimated from their position on 2D gels by comparison with known standard proteins. The significance of spot intensity difference over the chase period between the test strains used is within a 95% confidence interval for all spots. Spots whose synthesis is under cell cycle control are highlighted in bold.

SSP	Identity and gene number	Mw/pI	Significance level (p value)	Differential protein synthesis during cell cycle?	Previously identified as unstable protein?
5102	Riboflavin synthetase α-chain, CC0886	26/5.79	0.0058	Yes	No
5521	?	43/5.78	0.0292	No	No
5526	GTP Cyclohydrolase II, CC0887	44/5.81	0.0103	Yes	No
5603	?	51/5.75	0.0022	Yes	<i>Yes</i>
6105	CheD, CC0438	22/5.98	0.0177	Yes	<i>Yes</i>
6203	?	29/5.85	0.0247	No	No
6204	CtrA, CC3035	28/5.87	0.0029	Yes	<i>Yes</i>
6408	?	40/5.88	0.0090	No	No
8401	?	41/6.76	0.0141	Yes	<i>Yes</i>

Flynn et al. (2003) also showed that ClpX itself is a substrate for the ClpXP protease. Although our screen did not find ClpX, we decided to test this possibility by conducting a simple experiment in strain UJ199. Strain UJ199 has the *clpP* gene under control of the xylose-dependent promoter and therefore is dependent on xylose for survival. We removed xylose from the growth medium of UJ199 and took samples every 2 hours. SDS-PAGE was conducted on the samples and immunoblots performed using anti-ClpX/ClpA/ClpP antibodies. As can be seen in Figure 3.16, as the levels of ClpP become depleted, both ClpA and ClpX levels increase in the cells. This could suggest that either chaperone is degraded in a ClpP-dependent manner. In

this case, degradation of ClpX in *C. crescentus* would, as in *E. coli*, be dependent on ClpP. Alternatively, depletion of ClpP from the cells may indirectly induce the expression of ClpA and ClpX. Experiments are underway to distinguish between the two possibilities.

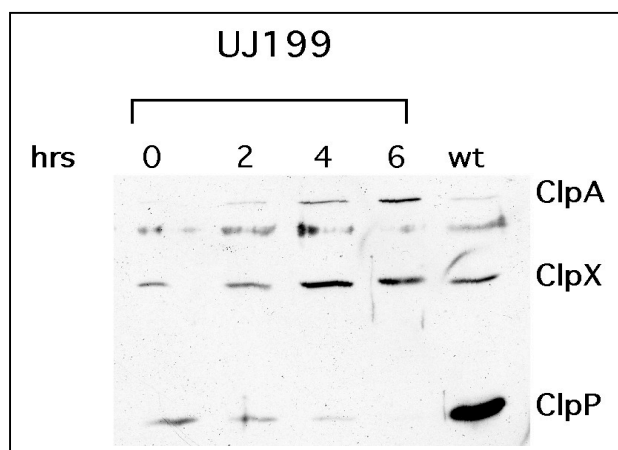


Figure 3.16. ClpA and ClpX are dependent on ClpP for degradation. Xylose was removed from the medium of the cells at t0 and by 4 hours ClpP levels were significantly depleted coincident with an increase in ClpA and ClpX levels. All samples were standardised to the same OD₆₆₀.

As mentioned earlier, unstable proteins whose synthesis is under differential cell cycle control are of most interest to understanding the role of the ClpXP protease in G1-to-S phase transition. Of the nine potential ClpXP substrates, six proteins are synthesised under cell cycle control (Table 3.1). With the exception of CtrA, the function of none of the identified spots could explain the G1-to-S arrest or indeed cell death in ClpX mutants (see section 1.3.5). SSP 5102 and 5526 are metabolic proteins involved in riboflavin synthesis, and whilst they are both synthesised under cell cycle control, it is unlikely that their stabilisation would lead to toxicity or cell cycle arrest. Identification of the function of the unknown spots could therefore shed light on this question, and is the focus of the next section of this chapter.

3.2.2 Protein identification by mass spectrometry

The experiments carried out to define ClpXP substrates were conducted using radiolabelled proteins. For analytical purposes, only small amounts of protein were separated on 2D gels. The spots to be identified are indicated by arrows on Figure 3.17, and as can be seen, their intensities are low indicating that the cellular concentration of these proteins is also low. To identify proteins by mass spectrometry (MS), preparative quantities of proteins need to be run. As a consequence of the higher protein concentrations and the altered staining procedure, spots on preparative gels often have altered mobilities and intensities therefore causing problems in matching the patterns on analytical and preparative gels (compare Figure 3.17 with Figure 3.18). A discussion of the reasons for this phenomenon can be found in many reviews but a good summary is given by T. Rabilloud (2000).

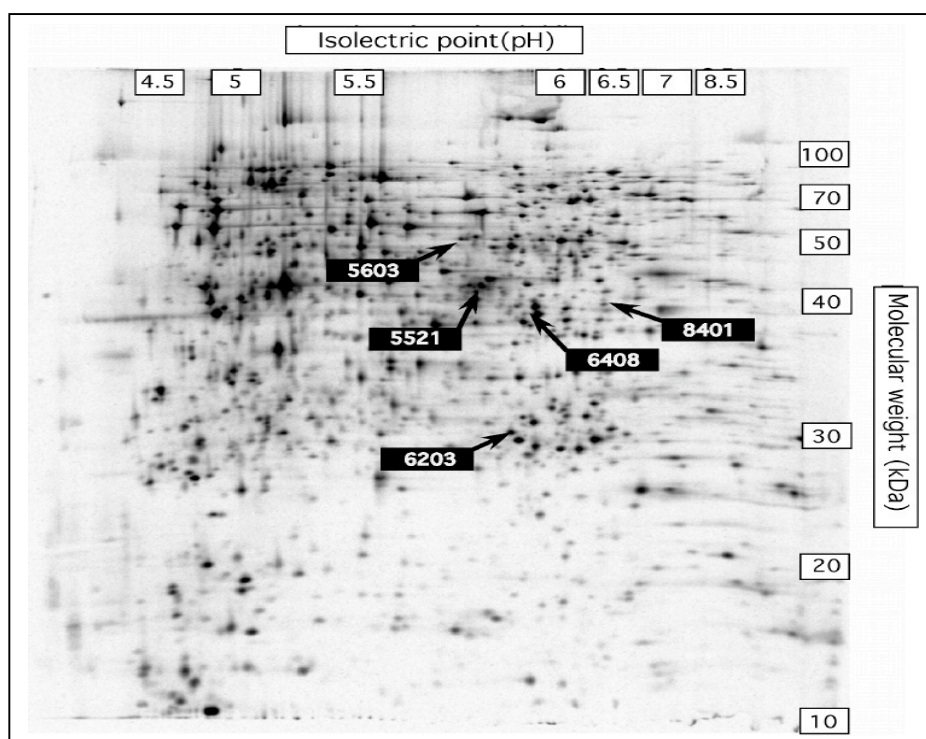


Figure 3.17. Autoradiogram of a typical analytical 2D gel used in this study. The positions of the five unidentified potential ClpXP substrates are indicated.

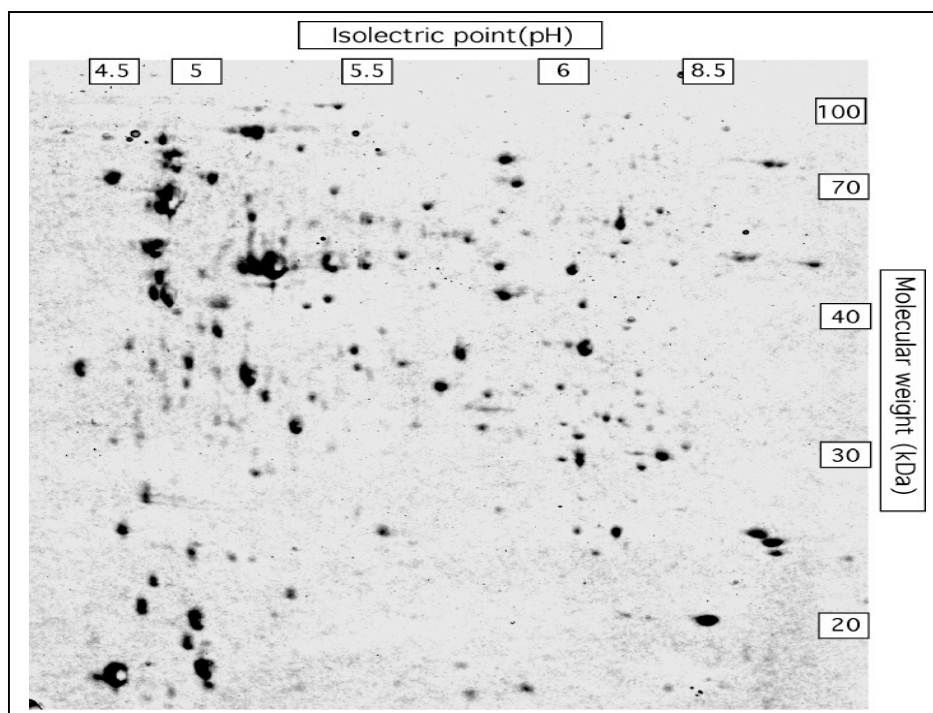


Figure 3.18. A typical example of a coomassie stained preparative 2D gel. Approximately 1 mg of total protein was separated as compared to approximately 50-100 μ g of protein in Figure 3.17.

Furthermore, preparative gels are stained with coomassie brilliant blue (CBB), the detection limit of which is much higher than for radiolabelling. As a consequence, fewer spots are seen on preparative gels than on analytical gels. To circumvent this sensitivity problem, we have “spiked” the unlabelled proteins with a small amount of radiolabelled protein prepared as per usual for analytical gels (See Materials and Methods section 2.4). An image of the CBB stained gels is taken after which the gels are dried and exposed to a phosphorimager screen to produce the autoradiogram image (Figure 3.19). The advantage of this system is that more spots are visible on the preparative gel producing a pattern that is similar to that of the analytical gels. Using those extra spots as landmarks, the autoradiographic image of the gel can then be matched to the original analytical gel. This forms the link between preparative and the analytical gels. This procedure is demonstrated in Figure 3.20 for the localisation of

and identification of SSP 6203. Though sometimes the spot of interest could be visible on the autoradiogram but not on the CBB stained image, overlaying the two images allowed the localisation of spots of interest and their isolation.

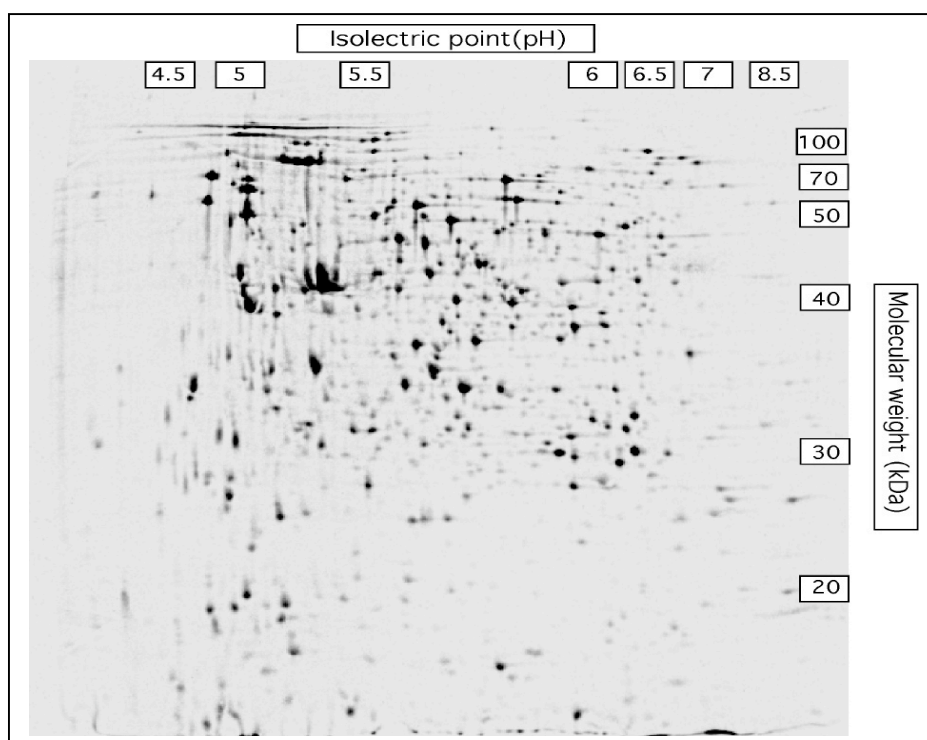


Figure 3.19. An autoradiographic image of a preparative gel spiked with 10^6 cpm of radiolabelled protein. More spots are visible on this image than on the CBB stained image resulting in a pattern more closely related to that of the analytical gels (compare with Figure 3.17).

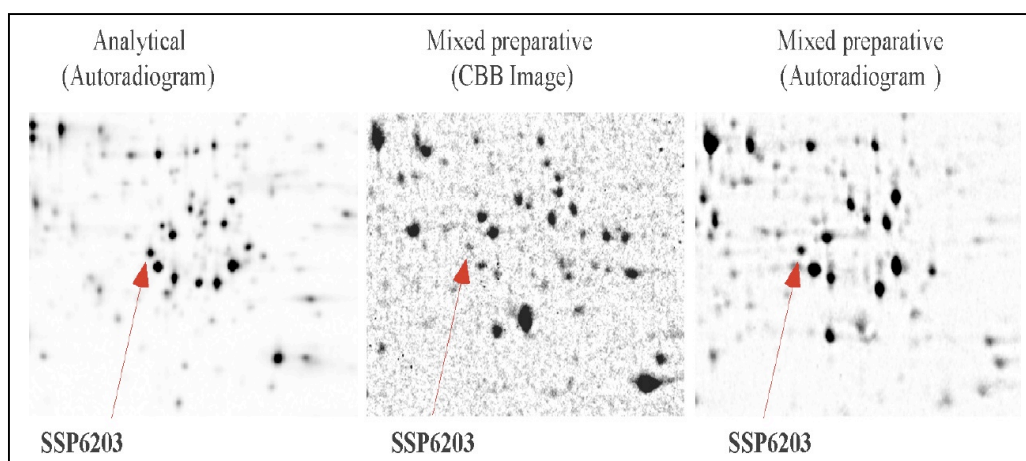


Figure 3.20. Localisation of SSP 6203 on a preparative gel. The left panel shows a magnification of the area of the analytical 2D gel image containing SSP 6203. Using the autoradiographic image of the preparative gel (right panel) the position of SSP 6203 can be discerned and matched to the CBB stained gel image (centre).

In order to maximise the yield of excised protein spots, fractions were size enriched using a Bio-Rad PrepCell (491) (See Materials and Methods section 2.4; Figure 3.21). As all proteins of interest were under 55 kDa, fractions 5-40 were pooled and applied on a 2D gel. This technique ensures that more protein in the desired size range could be run hence increasing the visibility of spots of interest and reducing interference by larger proteins. A typical CBB stained 2D gel of size-enriched proteins is shown in Figure 3.22.

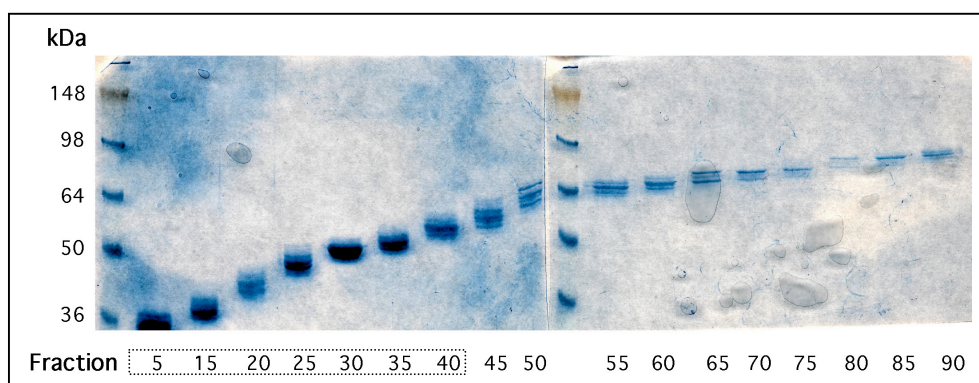


Figure 3.21. SDS-PAGE of fractions derived from Bio-Rad PrepCell 491. The spots of interest are between 20-55kDa and in this experiment, fractions 5-40 were pooled for further use.

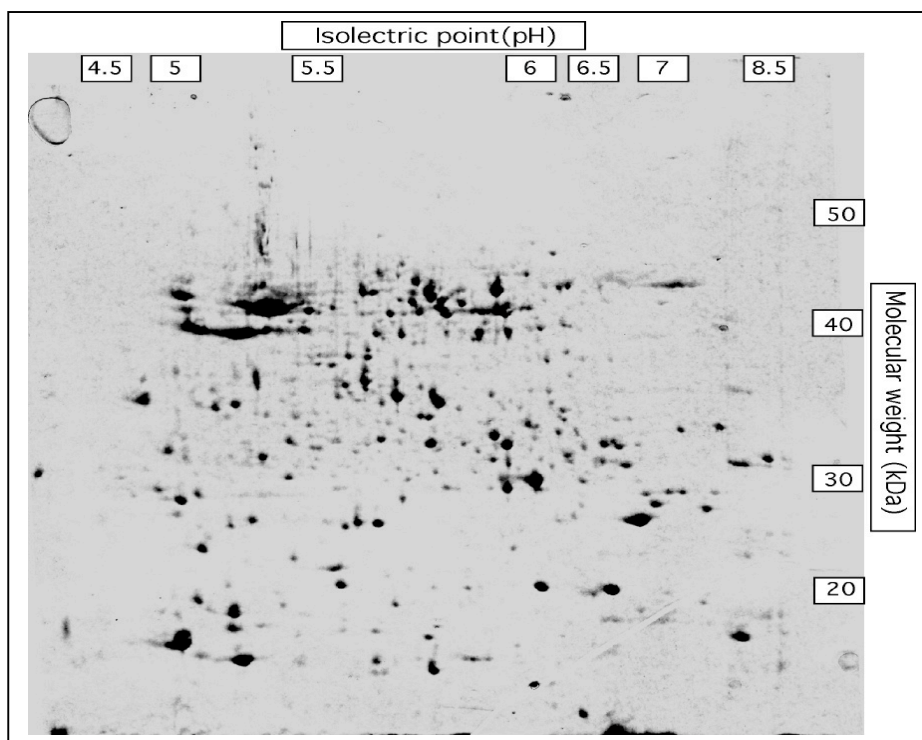


Figure 3.22. CBB stained 2D gel of size enriched proteins under 50 kDa. More proteins are visible in the size range of interest (compare this image to Figure 3.18)

A combination of these techniques was used to localise and excise the five spots of interest for mass spectrometry. The same spot was excised from four different gels and independently analysed by MS. If one or two of the spots yielded an identity that was different from remaining spots in the group, the procedure was repeated as many times as necessary to obtain at least 3 recurrent hits. The candidate genes obtained for each spot are listed in Table 3.2.

Table 3.2. Candidate genes for the 5 potential ClpXP substrates as identified by MS.

SSP	Candidate gene number	No. of peptides maximally identified and number of repeats	Annotation
8401	CC0965	8 (3x)	Copper binding protein (probable)
	CC3622	12 (2x)	Oxidoreductase, aldo/keto reductase family
	CC2323	8 (1x)	Conserved hypothetical protein
5603	CC2057	10 (5x)	Glucose-6-phosphate 1-dehydrogenase
	CC2350	5 (1x)	Enoylpyruvate transferase (MurA)
6408	CC3248	8 (6x)	Glyceraldehyde 3-phosphate dehydrogenase
5521	CC1162	9 (4x)	Aminotransferase, class II
	CC0510	13 (1x)	Acetyl-CoA acetyltransferase
6203	CC2821	7 (3x)	Hypothetical protein
	CC3597	5 (2x)	Ribosomal subunit interface protein

At least one candidate gene can be assigned to each protein spot as is evident from Table 3.2. The fact that for some spots, several genes were identified from independent experiments could result from a variety of factors that are discussed in some detail in section 3.4. To validate these targets and eliminate false-positives, we have developed an *in vivo* assay to analyse the dependence of each identified candidate protein on ClpXP for degradation. The details of this system are discussed in the following section of this chapter.

3.2.3 Target validation: use of an *in vivo* assay to test the dependence of candidate proteins on ClpXP for degradation

To determine which of the candidate proteins identified by mass spectrometry matches the original unstable spots, proteins were tagged with the FLAG M2 tag N-terminally and the corresponding genes were expressed in the conditional *clpX* mutant, strain UJ200 (see Materials and Methods section 2.6.2). We chose strain UJ200 as the *clpX* conditional mutant since pilot experiments with strain UJ1249 failed, possibly due to recombination between pMR20-based pMO88, on which the *clpX*_{ATP} allele is present, and pMR10, on which our candidate genes are cloned (not shown). The rationale was to deplete ClpX in the cells and ask whether the tagged proteins would be stabilised as a result. We tested not only candidates derived from MS but also previously identified proteins such as CtrA, CheD, riboflavin synthetase α -chain and GTP cyclohydrolase II to ensure that our *in vivo* assay works. It was uncertain at the onset of these experiments whether a N-terminal tag would interfere with degradation. However, most well studied degradation signals for ClpXP have been found to reside on the C-terminus (Gottesman 2003).

We designed vector pST-N-M2, a derivative of pMR-10 that has the *lac* promoter, after which genes of interest can be cloned in-frame with the M2 tag (see Materials and Methods section 2.6.2). Using this vector, we created thirteen constructs: pST-4-6 and pST-12-21 (Table 2.1). Each construct was transferred to strain UJ200 producing strains UJ2458, UJ2460, UJ2462, UJ264, UJ2466, UJ2468, UJ2470, UJ2472, UJ2474, UJ2476, UJ2478, UJ 2480 and UJ2482 (see Table 2.1 for description). The

protein stability in each strain was then determined in the presence and absence of ClpX.

Cells of each strain were grown overnight in M2G-Xyl and at OD₆₆₀ 0.2-0.4, cells were harvested, washed three times in fresh PYE medium and resuspended to OD₆₆₀ 0.05 in either M2G-Xyl (control) or M2G. Cells of each strain in the respective media were incubated with shaking at 30 °C for four hours (the time it takes to deplete most ClpX from cells in M2G, see section 1.3.2). A pulse/chase experiment was then performed on cells grown in either medium as per usual, followed by IP using anti-FLAG M2 agarose (see Materials and Methods, section 2.1 and 2.2). We expected that if the tagged protein is a substrate of ClpXP, it should be degraded in the presence of ClpX (+ xyl) but be stabilised in its absence (-xyl).

Of all the tagged proteins, only M2-CtrA (strain UJ2458), M2-CheD (UJ2462) and the conserved hypothetical protein of CC2323, M2-CC2323 (UJ2460) were degraded in the presence of ClpX and stabilised when ClpX was depleted (Figures 3.23 and 3.24). All other tagged proteins were stable even in the presence of ClpX (not shown). For SSP 8401, this is a positive result, as it appears that CC2323 is its source gene. However, for the other spots, this suggests that none of the candidates identified by MS are ClpX substrates; alternatively, N-terminal tagging could have interfered with degradation of the protein (see Discussion, section 3.4.2).

To address the second possibility, we tagged four of the ten candidate proteins with the FLAG M2-tag C-terminally using a similar approach to the one described above (see Materials and Methods section 2.6.2). Briefly, a pMR-10 based vector was

designed to allow in-frame fusion of the C-terminus of target genes to the M2 tag (pST-C-M2). The genes chosen for this experiment were CC3248 (Glyceraldehyde 3-phosphate dehydrogenase, for SSP 6408, strain UJ2484), CC2350 (MurA, for SSP 5603, strain UJ2486), CC0886 (Riboflavin synthetase α -chain, strain UJ2488) and CC0887 (GTP cyclohydrolase 2, strain UJ2490). None of the resulting fusion proteins were degraded in the presence of ClpX leaving open both possibilities alluded to above (not shown).

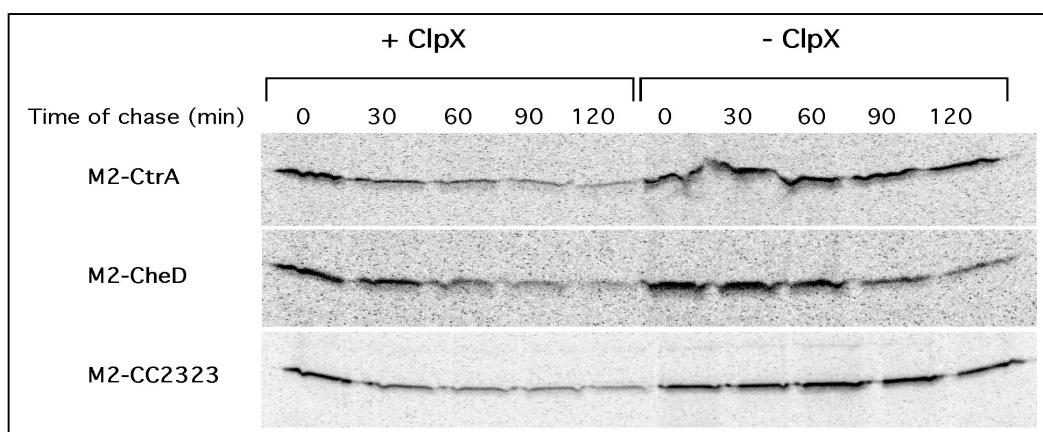


Figure 3.23. Degradation of N-terminally M2-tagged CtrA, CheD and CC2323 is dependent on ClpXP. A PC/IP was performed with anti-FLAG M2 agarose on strains UJ2458 (M2-CtrA), UJ2462 (M2-CheD) and UJ2460 (M2-CC2323) grown with xylose (+ ClpX), or four hours after they were washed and shifted to medium lacking xylose (- ClpX). In each case, depletion of ClpX results in a marked stabilisation of the fusion protein.

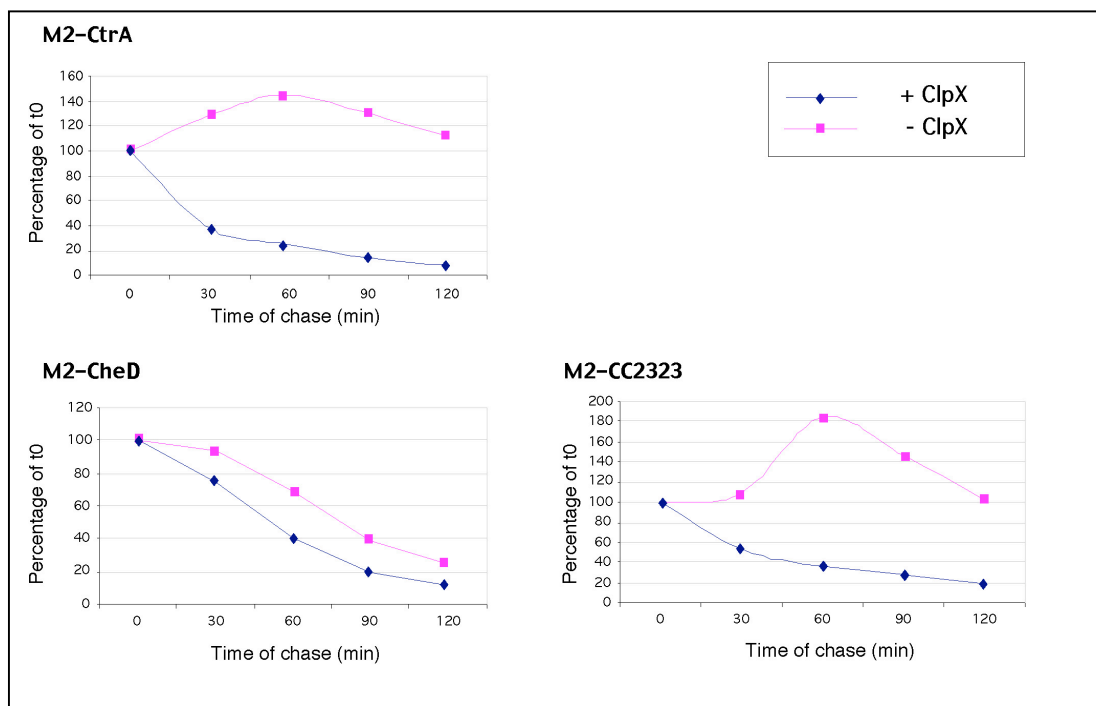


Figure 3.24. Stability of M2-tagged CtrA, CheD and CC2323 in the presence or absence of ClpX. The bands in Figure 3.23 were quantitated using ImageQuantTM and are shown as a percentage of the synthesised quantity at t0 for each strain under either condition.

It should be noted that the stabilities of both M2-CtrA (SSP 6204) and M2-CC2323 (SSP 8401) shown in Figure 3.24 are concordant with the stabilities determined on 2D gel (Figure 3.15). This indicates that the proteomic approach produced accurate results. The exception to this is M2-CheD (SSP 6105) which, though stabilised somewhat in the absence of ClpX, is still degraded more than was previously observed by proteomic analysis.

Due to time constraints, we were unable to further investigate the reasons why most of the candidate proteins tested negative in this target validation assay. We concentrated our efforts on understanding the role of CC2323 in *C. crescentus* as it is not only rapidly degraded, but also synthesised in a cell cycle dependent manner. CC2323 encodes a conserved hypothetical protein that may provide the link between

ClpXP function and G1-to-S transition. The details of our work on CC2323 are presented in section 3.3.

3.3 Functional analysis of CC2323, a novel ClpXP substrate in *C. crescentus*

As shown in section 3.2, the product of the gene CC2323 (SSP 8401) is a novel substrate of the ClpXP protease in *C. crescentus*. The C-terminus of CC2323 ends with QSA, a motif that bears homology to C-motif 1 coined by Flynn et al. (2003). SSP 8401 has been previously identified as an unstable protein spot whose synthesis is controlled in a cell cycle dependent manner (Figure 3.25; Grünenfelder et al. 2001).

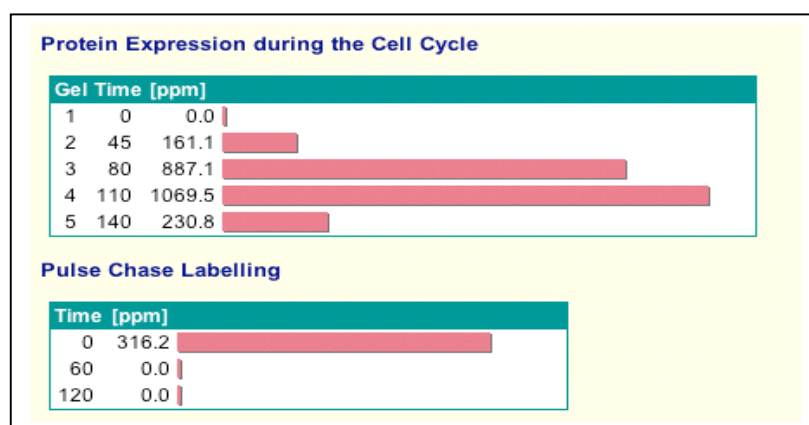


Figure 3.25. Stability and synthesis profile of SSP 8401 in *C. crescentus*. The protein synthesis data was produced by pulse experiments conducted during the cell cycle (Grünenfelder et al., 2001) whereas the stability data was from a non-synchronous population. Adapted from the SWICZ: <http://proteom.biomed.cas.cz/>.

Examination of the protein synthesis profile of SSP 8401 reveals that its synthesis peaks toward the end of the cell cycle before cytokinesis (late PD stage). Within 60 minutes of its synthesis, the protein is largely cleared from the cell. Rapid degradation of CC2323 and absence of its synthesis in SW cells could suggest that the presence of CC2323 in SW cells is undesirable for the cell. This possibility is examined in this chapter (see Results section 3.3.3).

The CC2323 ORF encodes a 377 amino acid protein with a predicted mass of 41.4 kDa. CC2323 is a conserved hypothetical protein and has at least 24 homologues, all of which are found exclusively in alpha proteobacteria and share the greatest homology between amino acid 70 and 140 (Figures 3.26). All those proteins are also of unknown function and most belong to COG5330 (Cluster of orthologues) whose members are found solely in alpha proteobacteria. *C. crescentus* also contains two paralogues of CC2323, namely CC2637 and CC0948, the former of which is more closely related in sequence to CC2323 (Figure 3.27). This conservation of CC2323 and its homologues in alpha proteobacteria could point to a conserved role it plays in the cell cycle, much like CtrA and GcrA whose orthologues are similarly conserved in the alpha-purple group.

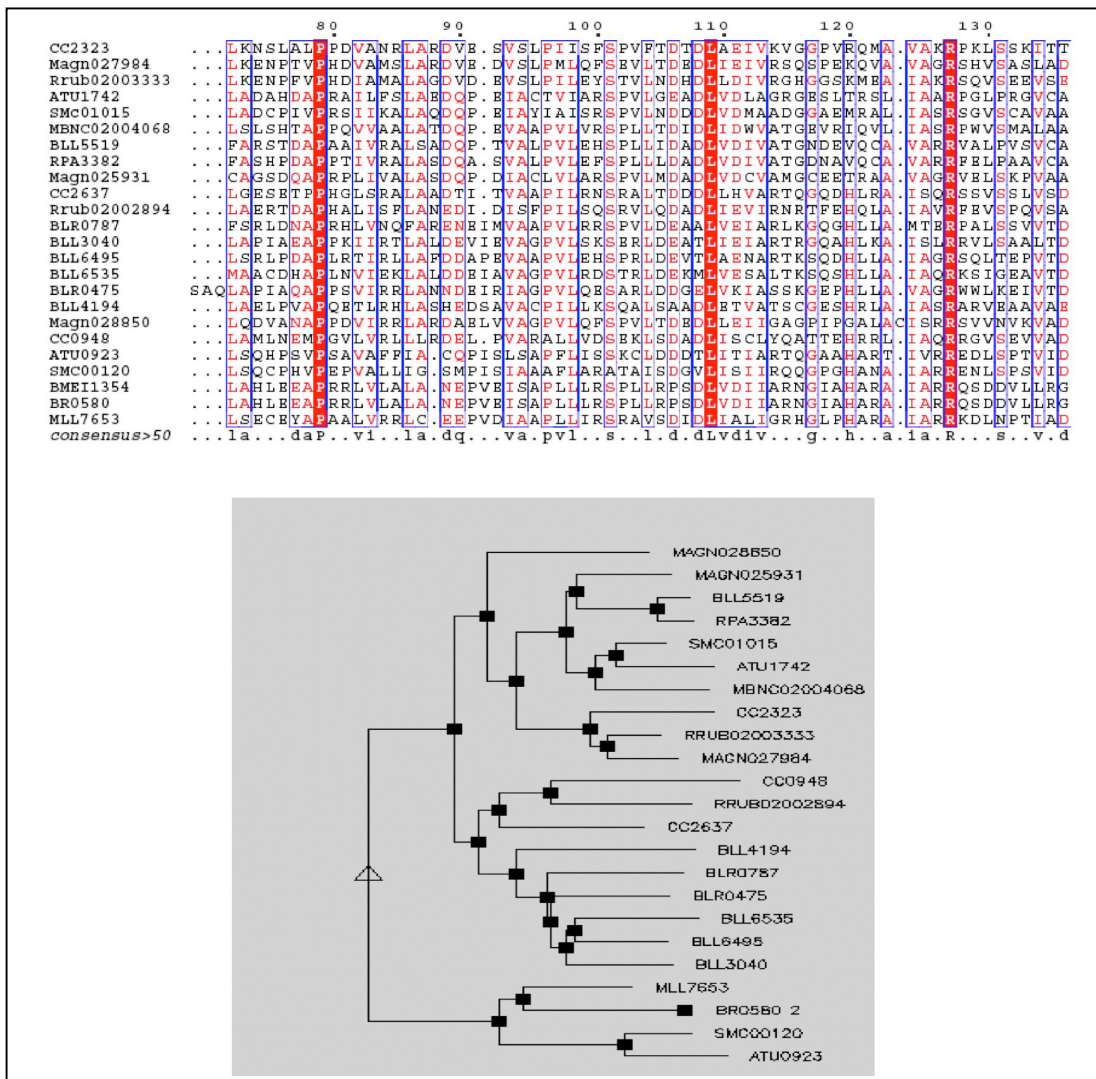


Figure 3.26. Orthologues of CC2323. The top panel shows the most highly conserved region of the 25 homologues. The bottom panel is a phylogenetic tree showing the relationship between the individual ortho- and paralogues. Both figures were created using the INRA online software at the ExPASy proteomics server (<http://prodes.toulouse.inra.fr/multalin/multalin.html>).

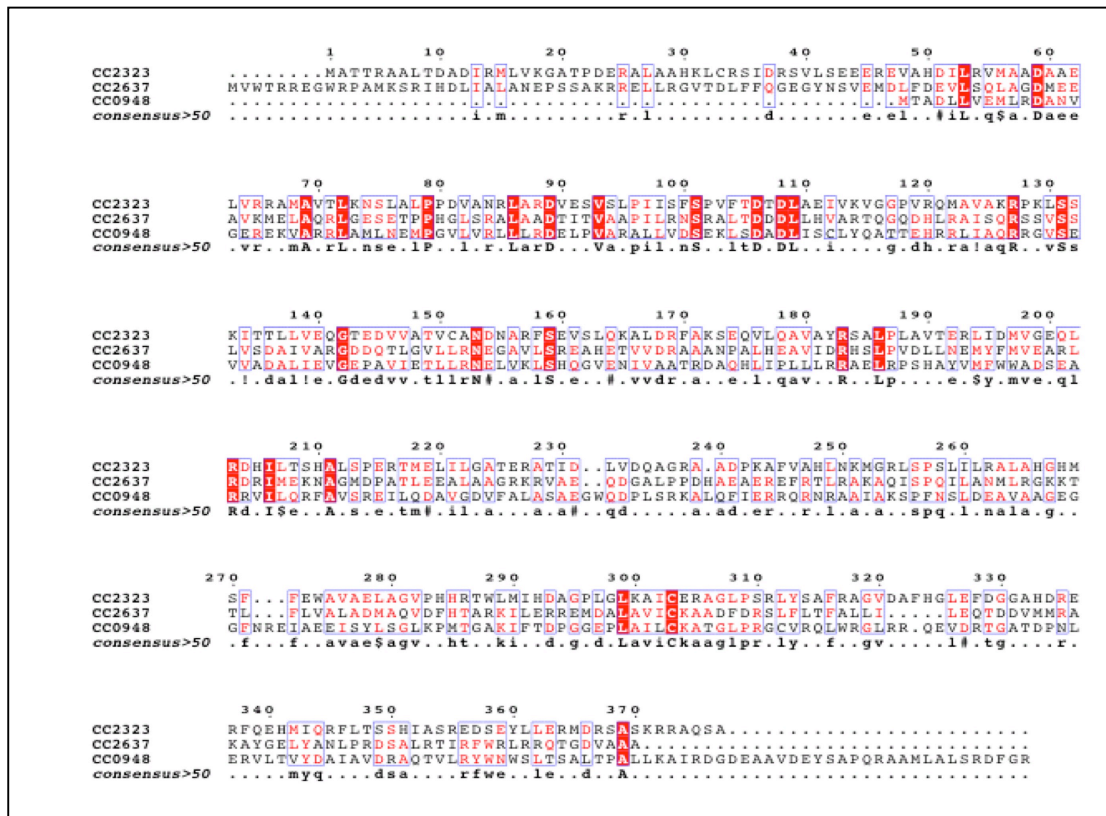


Figure 3.27. Paralogues of CC2323 in *C. crescentus*. Alignment produced by INRA online software at the ExPasy proteomics homepage (<http://prodes.toulouse.inra.fr/multalin/multalin.html>) CC2637 and CC0948 share approximately 25% and 20% identity with CC2323, respectively, but are more closely related to one another than to CC2323.

3.3.1 Expression and stability of CC2323

To confirm that the product of CC2323 is indeed unstable and synthesised in a cell cycle controlled manner, we created strain UJ2494, which has the chromosomal copy of CC2323 tagged N-terminally with the FLAG-M2 tag (see material and Methods section 2.6.3). This copy of CC2323 is present in its native chromosomal locus and is under control of its own promoter. Strain UJ2494 was grown overnight in M2G medium and at OD₆₆₀ 0.6, cells were synchronised and SW cells isolated. Every 20 min after SW cell resuspension, a sample was taken and pulsed with ³⁵S-met/cys mix (NEG-772, NEN) for 5 min, cells pelleted and frozen. Immunoprecipitations were then conducted using the anti-FLAG M2 coupled protein A-agarose matrix (Roche).

In addition, samples for immunoblot analysis were collected every 20 minutes in order to assess total CC2323 protein levels in the cell cycle. Finally, on a non-synchronous culture of UJ2494, a pulse/chase experiment was conducted to assess protein stability. The results of these experiment are shown in Figure 3.28. The band intensities of M2-CC2323 were also quantitated using the ImageQuant™ Software (Molecular Dynamics) (Figure 3.29). From the data presented, it is clear that CC2323 is expressed and the protein synthesised in PD cells prior to cytokinesis. However, a weak band corresponding to CC2323 is present at t140 (Figure 3.28 a and b). This could be due to contaminating PD cells that have not completed cell division by t140. CC2323 is not a strongly synthesised protein as evidenced by the length of exposure time in the phosphoimager screen necessary for the bands in Figure 3.28 (a and c) to be visible (7 days). This is concordant with our 2D gel results where SSP 8401 was a faint spot and had low intensity (100-350 ppm; see Figure 3.14). The half life of CC2323 is approximately 45-60 min as calculated from this experiment (Figure 3.29). This is slightly longer than the half-life observed for untagged CC2323 (SSP 8401) on 2D gels (approximately 30-45 min; Figure 3.15) suggesting that the M2 tag may alter the stability of CC2323.

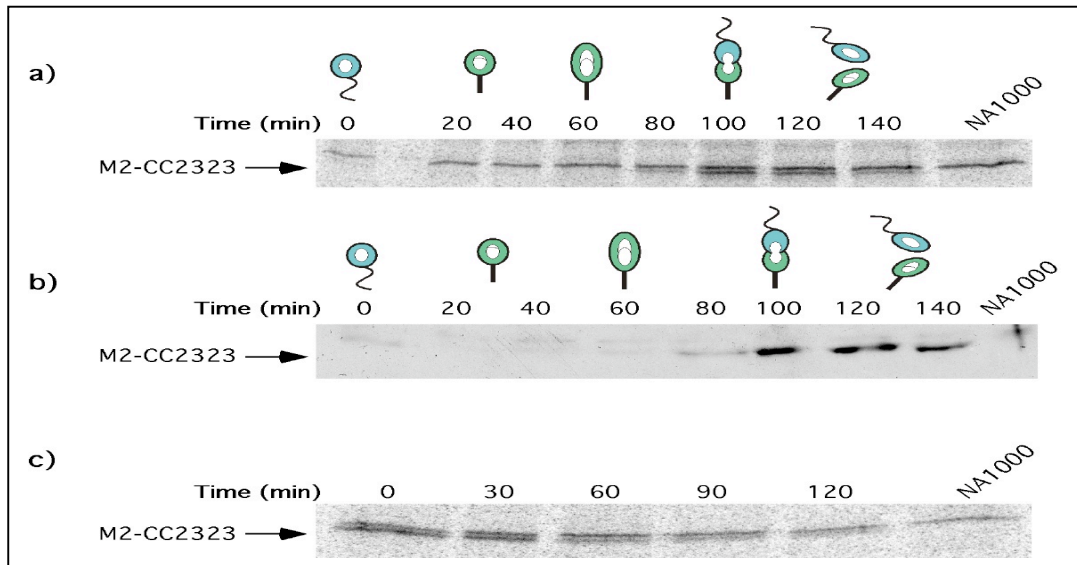


Figure 3.28. CC2323 is an unstable protein whose synthesis is cell cycle regulated and that is present only in PD cells. a) Immunoprecipitation of M2-CC2323 from synchronised cells reveals that it is synthesised specifically in late PD cells. b) Immunoblot analysis of CC2323 during the cell cycle shows that CC2323 is only present in PD cells. c) Pulse/Chase and immunoprecipitation of M2-CC2323 from non-synchronised cells of strain UJ2494. CC2323 is almost completely degraded by 120 min after it is synthesised. In all cases, the M2-CC2323 band is the lower of the two as the anti-M2 antibody-conjugated matrix cross-reacts with a protein of a size similar to M2-CC2323 in NA1000 cells.

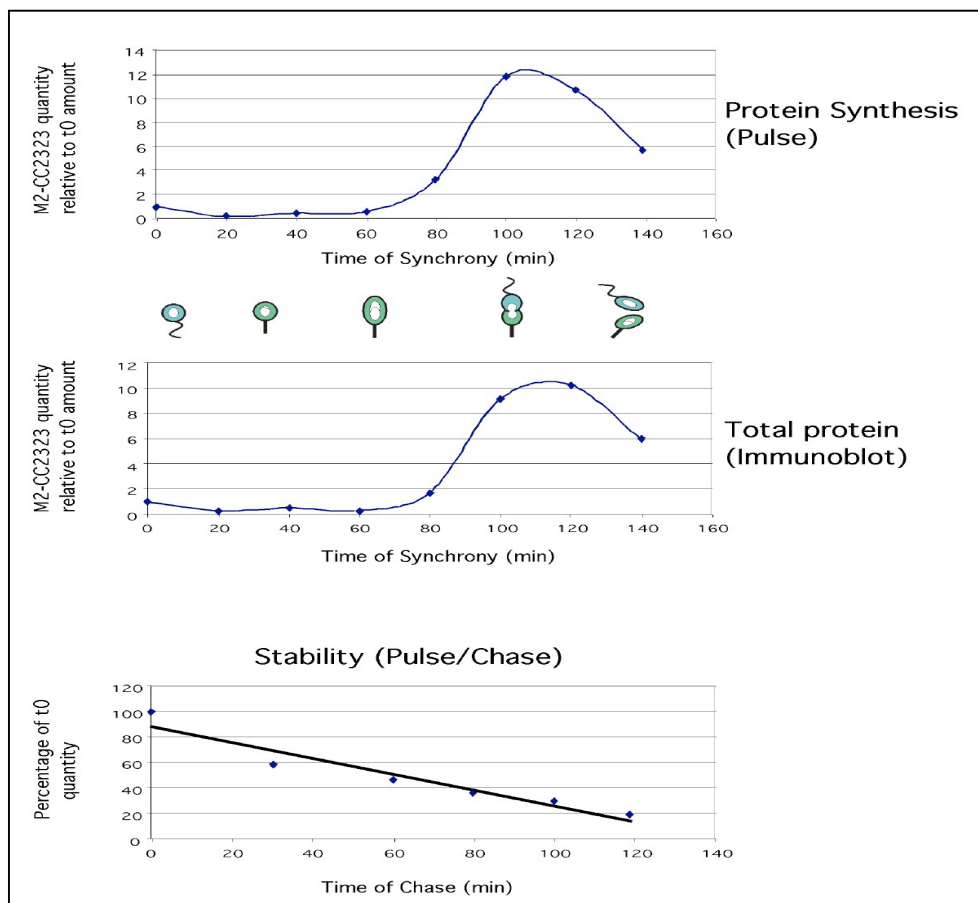


Figure 3.29. Quantitation of M2-CC2323 bands in the gels shown in Figure 3.28 using the ImageQuant™ software (Molecular Dynamics).

3.3.2 The product of the CC2323 gene is not essential

As a first step in investigating the function of CC2323, we generated a null mutation in CC2323 (see Materials and Methods section 2.6.3). We created plasmid pST-7 that is based on the *sacB* containing suicide vector pNPTS138. pST-7 has a fragment with only the 10 C-terminal and 10 N-terminal CC2323 residues flanked by 1kb of chromosomal sequence on either side. After the first recombination event, five kan-resistant clones were grown overnight in PYE in order to allow the second recombination to occur. Dilutions of those overnight cultures were plated on 3% sucrose containing PYE plates to select for the loss of pST-7 via a second step of

recombination. Of the clones growing on sucrose plates, 10 of each parental origin were selected and replica plated on PYE and PYE-Kan plates in order to establish if any of the clones had mutations in the *sacB* gene and had not undergone the second recombination. None of the clones tested contained pST-7 and therefore had performed the second recombination to delete CC2323. To ensure that these clones were indeed deletion mutants of CC2323, we performed PCR on five clones from each original parental origin and found that all had deleted CC2323 (not shown). Sequencing analysis confirmed this observation and one of the clones sequenced in this region was frozen as UJ2492. Strain UJ2492 had normal cell morphology as examined by light microscopy (not shown). The fact that deletion mutants in CC2323 were readily obtained suggested to us that CC2323 is not essential for cell growth and viability.

3.3.3 Overexpression phenotype of CC2323

As discussed previously, depletion of ClpX from cells results in a G1 cell cycle arrest. It is hypothesised that this is due to stabilisation of substrates whose presence is required at certain points in the cell cycle but disruptive to others downstream. As CC2323 was found to be dispensable for growth, we tested whether cells could tolerate its overexpression. The following observation suggested that accumulation of CC2323 in cells could impair cell growth and result in cell elongation. When pST-5 (pMR10 based vector with P_{lac} driving the expression of a N-terminally M2-tagged copy of CC2323) was introduced into UJ200 (strain UJ2460), cells were found to be slightly filamentous and slow growing as compared to the parent strain UJ200 (Figure 3.30). We hypothesised that strain UJ200 might have slightly lower levels of ClpX

than wild-type cells, and as a result, ClpXP could be limiting in this background. Thus, in strain UJ2460 not only are the levels of CC2323 increased due to its constitutive expression from P_{lac} on pST-5, but the levels of its protease might also be reduced. The combination of both elements could result in the accumulation of CC2323 to levels that negatively affect cell growth and division. Whether it is the increased levels of CC2323, or its untimely/undesirable expression in certain cell compartments that results in this phenotype is unknown and still under investigation.

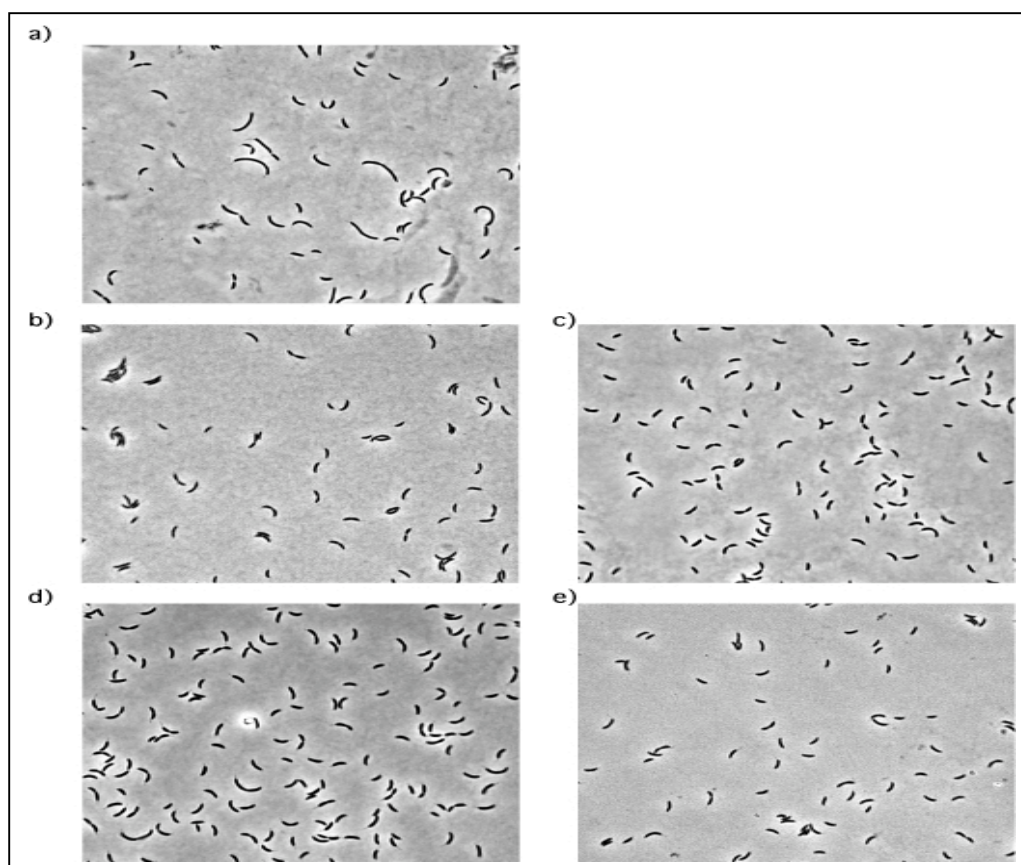


Figure 3.30. Mild overexpression of CC2323 from the low copy plasmid pST-5 results in cell filamentosity in strain UJ200 but not in NA1000. Micrograph images of: a) strain UJ2460 (UJ200::pST-5); b) strain UJ2579 (UJ200::pMR10) as a control for the vector backbone in strain UJ200; c) strain UJ200; d) strain UJ2581 (NA1000::pST-5) to control for pST-5 effects in a wild-type background; and, e) strain UJ2580 (NA1000::pMR10) as a control for the vector backbone in NA1000.

To investigate the effects of genuine CC2323 overexpression on the cells, we used vector pBBR1-MCS2 to create pST-10 that carries a copy of CC2323 with a N-terminal M2-tag, driven by P_{lac} . In addition, we used pMR10 to create pST-11 that has the M2-tag on the C-terminus of the protein, also driven by P_{lac} . We reasoned that as CC2323 ends with a QSA, a motif similar to C-motif 1 identified by Flynn et al. (2003) addition of a M2-tag to its C-terminus could disturb recognition by ClpX and result in stabilisation and consequent protein accumulation in the cell.

Plasmids pST-10 and pST-11 were moved from *E. coli* strains UJ2499 and UJ2500, respectively, to *C. crescentus* NA1000 by conjugation. As controls for the mating efficiency, the vector backbones (pBBR1-MCS2 for pST-10 and pMR10 for pST-11) were also transferred into NA1000. Dilutions of each conjugation mix were plated (50 μ l of 1:10, 1:100 and 1:1000) in order to quantitate the efficiency of transfer. The selective PYE-Nal-Kan plates from the conjugation of either plasmid contained mostly very small colonies that formed a lawn. This lawn was not observed in the respective controls. When examined by light microscopy, cells in the lawn were found to be of irregular shape, many having misplaced stalks, and were somewhat granulated suggesting that they are dead. Scattered amongst this lawn, were larger colonies that were considered as true conjugants (Table 3.3). This suggested that overexpression of CC2323, or production of a C-terminally M2-tagged variant thereof- which we predict to be stable- dramatically reduces conjugation frequency. This suggests that increased cellular levels of CC2323 are deleterious to cell growth and viability. Further, the few larger clones obtained are likely to be suppressors that have either learned to live with high amounts of CC2323, or have somehow

modulated amounts, or activity, of the plasmid expressed copy. This assumption is realistic in light of the fact that the conjugation frequencies of pST-10 and pST-11 are reduced about 1000-fold as compared to the controls.

Table 3.3. Conjugation frequencies of pST-10 and pST-11 in NA1000 cells.

* Number of transconjugants per mother cell.

	pST-10	pBBR1-MCS2	pST-11	pMR-10
Conjugation Frequency*	1×10^{-6}	3.7×10^{-4}	7.4×10^{-7}	3.5×10^{-4}

Due to time constraints, we were unable to further examine the suppressors and establish their nature. However, our observations thus far allude to the exciting possibility that increased levels of CC2323 are toxic for cell growth, suggesting that its ClpXP dependent removal during the cell cycle might be obligatory in *C. crescentus*.

3.4 DISCUSSION

3.4.1 The *clpX_{ATP}* allele and ClpX inactivation

The data presented in this chapter indicate that *clpX_{ATP}* is a dominant negative allele whose expression rapidly inactivates ClpX activity in *C. crescentus* leading to cell cycle arrest and cell death. The phenotype observed could be due to ClpX_{ATP} homo-oligomer formation and competition with ClpX_{wt} oligomers for ClpP binding, though our data discount this as the sole reason for the toxicity of the *clpX_{ATP}* allele. Instead, our data suggest that this toxicity is most likely due to a physical interaction between ClpX_{wt} and ClpX_{ATP} monomers that leads to the formation of inactive mixed oligomers (section 3.1.3). From the experiments conducted, it cannot be judged how many inactive monomers are present in each mixed oligomer, or how many are required to disrupt ClpX activity; for this, gel filtration experiments would have to be conducted. However, given that the levels of ClpX_{ATP} in the cell reach approximately 4-6 times those of chromosomally expressed ClpX_{wt} in xylose induced UJ1249 cells (Figure 3.8), it is safe to assume that mixed oligomers formed *de novo* after induction of *clpX_{ATP}* contain a relatively high fraction of inactive monomers. The stability and exchange dynamics of ClpX hexamers are unknown. Experiments with the related chaperone, ClpA, have shown that mutant monomers with a similar change in the walker A motif of the first nucleotide binding domain (NBD) can form mixed oligomers with pre-formed wild-type ClpA hexamers (Seol et al. 1995a). In accordance with this, we have observed that within five minutes after *clpX_{ATP}*

induction, some CtrA stabilisation occurs (Figures 3.6-3.8), suggesting that monomers are exchanged dynamically and swapping can readily occur.

Since marked CtrA stabilisation occurs only after 1 or 2 hours after xylose addition, the effects of *clpX*_{ATP} expression are clearly time dependent. It is worth noting that at both time points, CtrA is still degraded to some degree, though it is 40% more stable than in uninduced UJ1249 cells by 120 minutes after its synthesis (Figure 3.8). Although the overwhelming majority of ClpX in the cells consists of toxic ClpX_{ATP} monomers, ClpX_{wt} synthesis still occurs. It is possible that the residual ClpX activity results from the occasional *de novo* formation of wild-type hexamers. Alternatively, it is possible that a mixed ClpX oligomer can tolerate one or several inactive monomers without loss of activity. Previous studies on the chaperone GroEL have shown that a minimum of three *consecutive* active monomers are necessary for the GroEL heptamers to maintain wild-type levels of activity (Farr et al. 2000). If the same applies to ClpX hexamers, residual ClpX activity in xylose induced strain UJ1249 could result from mixed oligomers that have sufficient numbers of ClpX_{wt} monomers- in a favourable arrangement- to bring about substrate unfolding and delivery.

ATP binding to monomers of the related chaperone ClpA has been found to be required for hexamer formation (Maurizi 1992). Further investigation revealed that ClpA has two NBDs, each with near identical walker motifs, with each motif serving a different function. Whereas the first NBD has a low ATP hydrolysis activity and is responsible for ClpA hexamer formation, the second is largely responsible for ATP hydrolysis and consequently, substrate unfolding (Seol et al. 1995a; Singh and Maurizi 1994). Both of these studies have relied on mutating the conserved Lys

residue in the walker A motif to establish the roles of the two NBDs in ClpA. Unlike ClpA, ClpX has only one NBD and it is likely that this single NBD is responsible for both hexamerisation *and* substrate unfolding. Thus, it is unclear which of these activities the mutation in the *clpX*_{ATP} allele actually impairs. Recently, the crystal structure of ClpX in *H. pylori* has been solved revealing that both the conserved Lys residue mutated by Seol et al. (1995a) and Singh et al. (1994), and the Thr-126 residue mutated in our ClpX_{ATP} variant contact the ATP moiety (Kim and Kim 2003; Figure 3.31). This suggests that the mutation in ClpX_{ATP} may impair nucleotide binding. Furthermore, through pilot studies on strains with conditional *clpX*_{SSD} expression, we have observed a phenotype identical to that of *clpX*_{ATP} expressing cells. Also, ClpX_{SSD} monomers have been shown to form mixed oligomers with ClpX_{wt} monomers (not shown). The mutation in the SSD domain of ClpX replaced Arg-367, a conserved residue contacting the ATP moiety of ClpX (Kim and Kim 2003; Figure 3.31). Thus, our results confirm the role of the SSD domain of ClpX in ATP binding and/or hydrolysis, and the necessary cooperation of both NBD and SSD domains for assembly and activity of ClpX hexamers.

As we do not yet know the nature of the mixed ClpX oligomers in cells expressing *clpX*_{ATP} and *clpX*_{SSD}, it remains possible that at least part of the phenotype observed could be due to titration of active ClpX_{wt} monomers resulting in a ClpX ring assembly block. We do not favour this possibility as previous work has demonstrated the existence of mixed hexamers consisting of ClpA mutant monomers- with changes in the walker A motif- and wild-type ClpA monomers (Seol et al. 1995a; Singh and Maurizi 1994). A summary of the possible effects of expressing the *clpX*_{ATP} allele is

schematically represented in Figure 3.32. For all the scenarios drawn, it is easy to rationalise the observed residual activity of ClpXP.

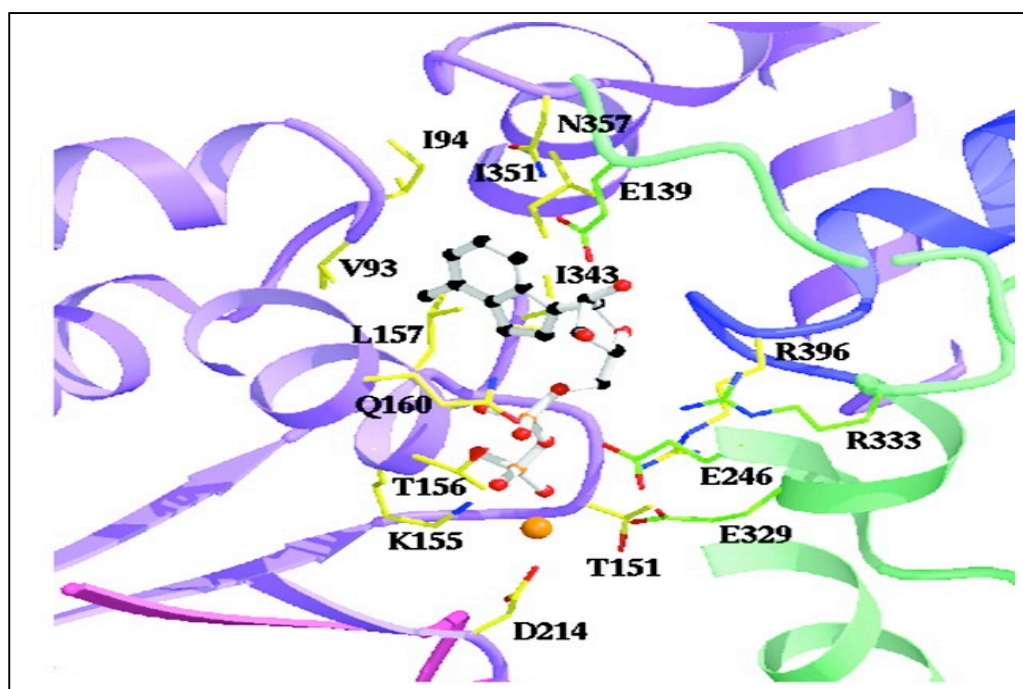


Figure 3.31. The nucleotide binding region of *H. pylori* ClpX (Kim and Kim 2003). The ATPase domain of one monomer is shown in magenta and the SSD domain of the adjacent monomer is indicated in green. The equivalents of T156 and R396 in *C. crescentus* have been mutated to create *clpX_{ATP}* and *clpX_{SSD}*. Both residues contact the bound ATP molecule (stick and ball figure), although the proposed γ -phosphate binding site is closer to T156 (indicated by the orange ball).

Though strain UJ1249 seemingly maintains some ClpX activity even in the induced state, it has a similar phenotype to strain UJ200, the original *clpX* conditional mutant (Jenal and Fuchs 1998). Both strains lose viability around four hours after depletion of ClpX and expression of *clpX_{ATP}*, respectively; but induced UJ1249 cells apparently stop accumulating biomass slightly earlier than UJ200 (8-10 hours in UJ1249 vs. 8-14 hours in UJ200, Figure 3.5; Jenal and Fuchs 1998). Moreover, despite the presence of some residual ClpX activity in strain UJ1249, ClpX inactivation as evidenced by the observed stabilisation of CtrA and SsrA-tagged FlbD (see discussion 4.4) occurs very

rapidly. This establishes strain UJ1249 as an alternative strain to UJ200 in which ClpX activity can quickly be disrupted leading to ClpXP substrate stabilisation.

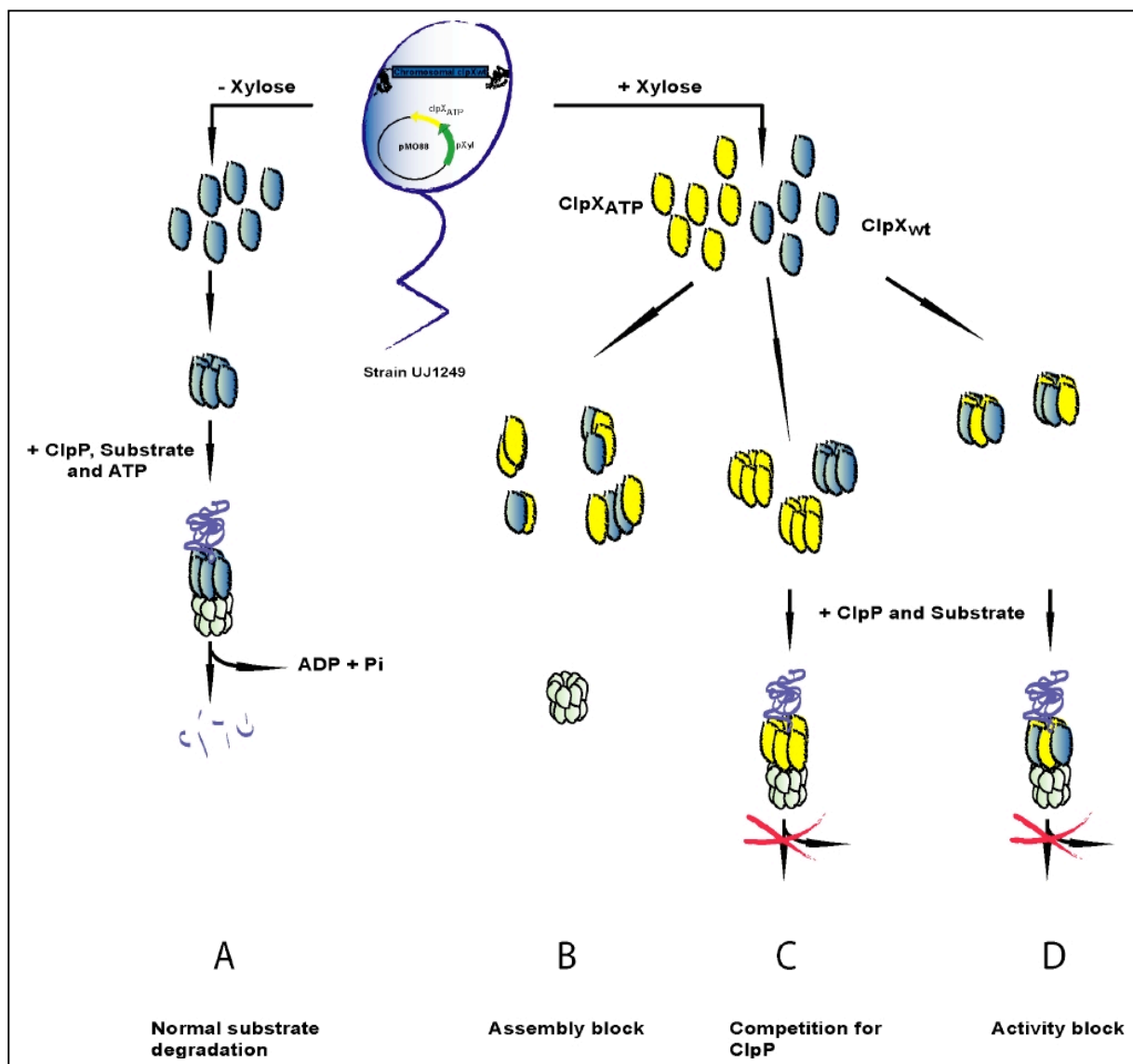


Figure 3.32. Model for inactivation of ClpXP activity in strain UJ1249. Plasmid *pMO88* carries the *clpX_{ATP}* allele under control of *P_{xyI}*. In the uninduced state, only *clpX_{wt}* is expressed from the chromosome (A). In the presence of xylose, expression of *clpX_{ATP}* results in substrate stabilisation and cell death. This could occur through a variety of mechanisms, not necessarily mutually exclusive (B-D). (B) ClpX_{wt} monomers are titrated by ClpX_{ATP} monomers into inactive oligomers that are incapable of forming ClpX rings and thus cannot bind ClpP. (C) The larger numbers of ClpX_{ATP} monomers result in the assembly of exclusively mutant hexamers that would bind to ClpP and out-compete wild-type ClpX rings. (D) Mixed oligomers between ClpX_{ATP} and ClpX_{wt} form that are unable to unfold and deliver substrates.

3.4.2 Identification of ClpX substrates in *C. crescentus*

We found nine spots to be degraded in the wild-type control but significantly stabilised in induced UJ1249 upon induction of *clpX_{ATP}* expression (Figure 3.15). Although all nine spots were stabilised in ClpX deficient cells, it is clear also that their synthesis is repressed as compared to the wild-type controls (Figure 3.14). It is possible, though unlikely, that all of those proteins are capable of repressing their own expression. This is at least true for CtrA, which negatively controls its own expression through binding to the P1 promoter (Domian et al. 1999). Alternatively, all of these proteins could be synthesised at a specific phase of the cell cycle and upon ClpX depletion, cells arrested in G1 would not proceed to this stage. As a result, overall synthesis in a non-synchronous population of cells would appear reduced. It remains possible that the stabilisation effect observed for those proteins is indirect, rather than being a direct consequence of ClpX depletion. If for instance degradation of any of these proteins would be limited to the S or G2 phase of the cell cycle, a G1 arrest would automatically result in overall stabilisation of the respective protein. This has to be considered for future analysis of these proteins (see below for CC2323).

The fact that CtrA and CheD have been found as ClpXP substrates using this proteomic screen is a positive indication of the system's specificity and accuracy since both have been independently identified as such (Jenal and Fuchs 1998; M.R.K. Alley, unpublished results). To identify the remainder of these unstable proteins, we conducted preparative scale 2D electrophoresis in order to enrich the spots for mass spectrometric analysis. Our experiments produced at least two candidate genes for most spots (Table 3.2). This uncertainty could have arisen from a variety of factors,

not least of which is excising the spots blindly was sometimes necessary and thus, spots could have been mis-excised at this stage of preparation. In addition, it is possible that two (or more) proteins could be positioned extremely close to, or at the same position of, the spot of interest hence leading to an ambiguous identification. To validate the MS results, we used an *in vivo* assay to test the dependence of each gene product on ClpX for degradation (see results section 3.2.3). Using this assay, only CtrA, CheD and the product of CC2323 have been found to be stabilised in the absence of ClpX activity. The fact that all three proteins were stabilised in both induced UJ1249 cells and repressed UJ200 cells points to them being genuine substrates.

As regarding the remaining spots, none were found to be degraded in the presence of ClpX in UJ200 cells using our *in vivo* assay. One possibility that could account for this is that tagging a potential ClpX substrate on the N-terminus could result in inhibition of its recognition by ClpX. Although most of the best studied examples of ClpXP substrates, such as LexA, λ O replication protein, the SsrA tag and MuA are degraded from the C-terminus (Gonciarz-Swiatek et al. 1999; Levchenko et al. 1997; Neher et al. 2003a; Neher et al. 2003b), work by Flynn et al. (2003) has shown that N-terminal signals also exist in a large number of identified ClpXP substrates. Thus, it is possible that the M2 tag we attached masked vital recognition signals in our candidates. To establish whether this is an effect due to N-terminal tagging, we tagged some substrates C-terminally and repeated the assay only to find that they were still stable in strain UJ200 under permissive conditions. It remains possible that through chance, all tested candidates require both N- and C-terminal domains for recognition by ClpX as previously shown for some substrates (Flynn et al. 2003). This could

explain why those proteins are apparently well degraded as seen on 2D gels but once tagged, they become stable.

Since degradation of all six proteins was tested in strain UJ200, it is formally possible that a reduced ClpX activity under permissive conditions in this strain leads to their stabilisation. To test this possibility, stability of the tagged proteins would have to be determined in NA1000 wild-type cells.

Two of the proteins for which specific degradation could not be verified with tagged proteins were Glyceraldehyde 3-phosphate dehydrogenase and GTP cyclohydrolase II. Homologues of both enzymes have been found to be ClpXP substrates in *E. coli* (Flynn et al. 2003). If indeed the same applies in *C. crescentus*, this could mean that both proteins require the C- and N-termini for recognition by ClpX. As for the remainder of the proteins tested, not only is this possibility open but it is also possible that they are false positives that our statistical analysis failed to eliminate.

3.4.3 CC2323, a potential novel ClpXP substrate

Our data in Results section 3.3 suggested that the product of the CC2323 gene might be highly unstable and likely to be a substrate for the ClpXP protease. From the data shown in Figure 3.29, it is evident that synthesis of M2-CC2323 and its overall levels correlate strongly suggesting that degradation of CC2323 is rapid and constitutive. This in turn would argue that the cellular concentrations of CC2323 are regulated only through synthesis during the cell cycle. However, the half life of M2-CC2323 is approximately 60 min, which is unexpectedly high for a model of constitutive degradation. Part of the explanation for this phenomenon might be that degradation of

M2-CC2323 is slightly slower than previously observed for untagged CC2323 on 2D gels (compare Figures 3.15 and 3.29). This would suggest that a N-terminal M2 tag partially stabilises CC2323 leading to this ambiguous result. Thus, from these experiments, the nature of the mechanisms regulating CC2323 levels during the cell cycle cannot be established. Further experiments using an antibody specific for CC2323 should be conducted to address this question.

The presence of the CC2323 protein in PD cells and its absence in SW and ST cells is reminiscent of the behaviour of the methyltransferase CcrM, which regulates the methylation state of the chromosome and is involved in correct initiation of DNA replication (Wright et al. 1996). CcrM is constitutively and rapidly degraded by the Lon protease suggesting that its levels in the cell are regulated primarily through expression (Wright et al. 1996). Unlike the product of CC2323, CcrM is essential for growth and viability. However, similar to CC2323, overexpression of *ccrM* leads to aberrant cell morphology and defects in cell division and chromosome replication (Zweiger et al. 1994). Due to the clearly toxic nature of high levels of CC2323, analysis of its overexpression was not possible. Mild and constitutive overexpression of CC2323 is already harmful to cells slowing their growth and causing cell elongation (see section 3.3.3). This suggests that the protein is normally maintained at low levels in the cell. Indeed, work with chromosomally expressed M2-CC2323 and untagged CC2323 suggests that this is true (see Results section 3.3.1). Alternatively, or in addition, the untimely presence of CC2323 in certain cellular compartments, or at other cell cycle stages, may be toxic for the cells. Taken together, our observations suggest that CC2323's role is confined to a limited window late in the cell cycle in G2 phase, immediately before cell division. As a first step in establishing the function of

the CC2323 protein in *C. crescentus*, a strain should be created that allows its conditional overexpression. Such a strain will be invaluable in establishing whether the protein has negative effects in G1- and/or S-phase, where it is normally not present. It is possible that CC2323 turnover provides the link between ClpXP and cell cycle progression.

The CC2323 gene is not essential. The reason for this is unclear but could be due to functional redundancy. Two paralogues of CC2323 (CC0948 and CC2637) exist in *C. crescentus*, both of which share significant identity with CC2323 (Figure 3.27). It is possible that they can substitute for the function of CC2323 in its absence. To test this, double and triple deletion mutants of the paralogues should be created. Alternatively, it is possible that CC2323 has an important role during the cell cycle without exhibiting an obvious phenotype under the conditions tested. An example of a protein behaving in this manner is Noc in *B. subtilis* (Wu and Errington 2004). Noc is a non-essential protein that non-specifically associates with the nucleoid in *B. subtilis* and prevents the formation of the division FtsZ ring all but in the centre of the nucleoid where its concentrations are lowest. When *noc* is deleted, the cell compensates for its absence using the Min system to achieve exact placement of cytokinesis. However, its overproduction results in a marked reduction in cell division, and an increase in cell length, both likely the result of blocking FtsZ ring assembly. Thus, Noc has a role as an important checkpoint for cell cycle progression. It would be interesting to see whether CC2323 has a similarly vital role for cell cycle progression in *C. crescentus*.

While this work was in progress, a new essential cell cycle master regulator, GcrA, was identified in *C. crescentus* (Holtzendorff et al. 2004). GcrA, directly or indirectly, controls the expression of approximately 125 genes as found by microarray analysis. It was also found that CtrA negatively regulates the expression of *gcrA* whilst GcrA seems to positively regulate the weak P1 promoter of *ctrA*. In the SW compartment where CtrA is present, *gcrA* expression is suppressed. When CtrA is proteolysed at the G1-to-S phase transition, GcrA levels begin to accumulate. It has been proposed that the spatial and temporal oscillation of the levels of both GcrA and CtrA leads to the coordinated and timed expression of specific cellular programs that ultimately result in cell cycle progression. Interestingly, one of the genes positively regulated by GcrA is CC2323. However, the synthesis of CC2323 begins approximately 60 min after that of GcrA, and when the levels of the latter already decline in the cell (Figure 3.33a; Holtzendorff et al. 2004). In contrast, CC2323 synthesis coincides exactly with the synthesis and presence of CtrA during the cell cycle (Figure 3.33a; Holtzendorff et al. 2004). This could suggest that while GcrA inhibits the expression of CC2323, CtrA overrides this inhibition and induces it. Further, as CtrA is proteolysed at the G1-to-S phase transition and GcrA is synthesised, CC2323 expression is inhibited. Nevertheless, such a regulatory mechanism would not explain why CC2323 is not expressed in SW cells - where CtrA is present but GcrA absent- and thus other regulatory elements must come into play.

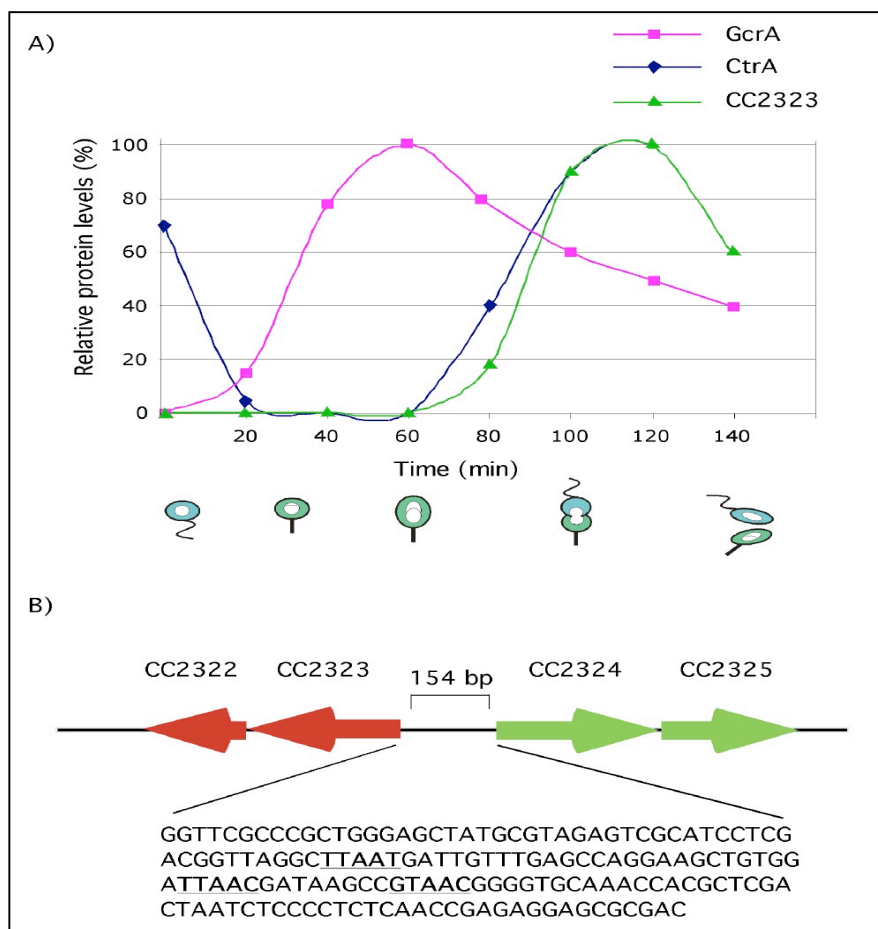


Figure 3.33. A) GcrA, CtrA and CC2323 protein levels as quantitated from immunoblots (GcrA and CtrA curves adapted from Holtzendorff et al., 2004)). The synthesis of CC2323 closely follows that of CtrA and is repressed in the presence of GcrA and the absence of CtrA. B) The chromosomal locus of CC2323. A short region of 154 bp separates the start of CC2323 and its neighbour, CC2324, and contains several putative CtrA-binding boxes (underlined)

A closer examination of the sequence upstream of CC2323 revealed that the intergenic region between CC2323 and CC2324, which has the opposite orientation, comprises only 154 bp (Figure 3.33b). CC2324 was found to be positively controlled by CtrA through microarray studies (Laub et al. 2000) and CtrA physically interacts with the region between CC2323 and CC2324 (Laub et al. 2002). The regulatory sequence(s) of GcrA are unknown, and while it is suspected that GcrA associates

directly with the DNA, it may also regulate gene expression indirectly through interaction with other proteins (Holtzendorff et al. 2004). Thus, it is possible the reduction of CC2323 expression observed in a conditional *gcrA* mutant is the result of an indirect secondary effect of the mutant. For instance, it is possible that the cell cycle block resulting from GcrA depletion could indirectly affect the expression of CC2323. Experiments to address this question and to clarify a possible direct involvement of CtrA in CC2323 cell cycle control are planned.

3.5 CONCLUDING REMARKS

We have generated an inactive *clpX* allele, *clpX_{ATP}*, and shown that it had a dominant negative effect leading to ClpX inactivation in *C. crescentus*. Our data suggests that this is due to the formation of mixed oligomers of ClpX_{ATP} and ClpX_{wt} monomers resulting in ClpX inactivation and subsequent substrate stabilisation. Despite the fact that our system does not completely inactivate ClpX, it rapidly reduces ClpXP activity making it an attractive tool for the identification of novel ClpXP substrates. Use of this new tool in a global *in vivo* proteomic screen for novel ClpXP substrates lead only to the identification of one protein, the product of the CC2323 gene. The reasons for the low yield of our screen are unknown but could be a combination of various factors, including technical problems as encountered in spot excision and protein preparation. Alternatively, a subset of the proteins identified might be *bona fide* ClpXP substrates, which our *in vivo* target validation assay failed to corroborate as such. Due to the complex nature of substrate recognition and dynamics of unfolding, biochemical means (such as *in vitro* degradation assays) are ultimately required to unequivocally identify and analyse ClpXP-dependent degradation. However, even such systems have their limitations; e.g., purified ClpX and ClpP have thus far failed to degrade CtrA, *in vitro*. This is likely due to the existence of (an) additional cofactor(s) that may be required for its efficient degradation. The requirement of such cofactors for some substrates substantially complicates *in vitro* analysis by biochemical assays.

The potential ClpXP substrate CC2323 was found to be present only in a narrow window of the cell cycle, namely in the late S- and G2-phase. Although CC2323 is a non-essential protein, its stabilisation and overproduction has a deleterious effect on cell proliferation and growth. Whether it is only the increased levels of CC2323, or its untimely presence at certain cell cycle points/cellular compartments, that is harmful to the cells remains to be elucidated. A number of experiments remain to be conducted in order to elucidate the function of CC2323 and the significance of its rapid degradation; chief of which is its conditional overexpression and analysis of the resultant phenotype. The generation of antibodies against CC2323 will also be critical for those studies as the presence of the M2 tag N-terminally may affect CC2323 turnover and generate distorted results. Such antibodies will be instrumental to establishing whether CC2323 degradation is constitutive or limited to a defined window of the cell cycle. Furthermore, analysis of suppressors of CC2323 overexpression may yield useful information on interaction partners and thus the function of CC2323 in cells. Finally, experiments to establish the roles of CtrA and GcrA in the control of CC2323 expression should clarify why it is synthesised in a cell cycle-dependent manner.

4 FUNCTIONAL ANALYSIS OF SSRA-DEPENDENT DEGRADATION IN *C. CRESCENTUS*

Abstract

SsrA is a highly hydrophobic protein-tag that targets proteins for degradation by ATP-dependent proteases. In *E. coli*, SsrA-tagged proteins are degraded primarily by the ClpXP protease. To establish whether the ClpXP protease degrades SsrA-tagged substrates in *C. crescentus*, we generated a recombinant hybrid protein by fusing the SsrA tag to the flagellar gene regulator FlbD. This hybrid protein was rapidly degraded and depletion of either ClpX or ClpP from cells resulted in its stabilisation. This suggests that in *C. crescentus*, as in *E. coli*, SsrA tagged substrates are degraded in a ClpXP-dependent manner.

Since FlbD induces the expression of Class III and IV flagellar genes, cells with unstable FlbD-SsrA variants were non-motile. To genetically dissect the requirements for SsrA-tagged protein degradation, we employed cells expressing *flbD-ssrA* in a selection for motile suppressors. The rationale was that cells would regain motility through the stabilisation of FlbD-SsrA by replacing important residues in the SsrA tag, or by inactivation of additional components required for SsrA-dependent degradation. Two motile suppressors with point mutations in *ssrA* were isolated, and indicated that the fourth and second-last residues of the SsrA tag are important for recognition by ClpXP. However, most of the suppressors had frame-shift mutations immediately preceding the *ssrA* that completely altered the C-terminus of FlbD. While these changes led to FlbD stabilisation, restoration of motility was, at

least in some instances, dependent on a second site mutation. This argued that while frame-shift mutations could stabilise FlbD-SsrA, they may have left the regulator inactive. It is possible that the motile suppressors have compensated for the lack of FlbD activity by a mutation(s) *in trans*.

To examine if the presence of FlbD is the sole requirement for motility, we generated a stable FlbD-SsrA variant (FlbD-SsrA_{DDD}). Surprisingly, cells expressing this stable protein were non-motile. Analysis of the FlbD-SsrA_{DDD} cellular concentrations showed that they are significantly higher than wild-type FlbD levels. Motile suppressors isolated from cells bearing a *flbD-ssrA_{DDD}* allele had no mutations *in cis* indicating that restoration of motility was due to a second site mutation *in trans*.

These results indicate that FlbD-SsrA can be stabilised by *cis* mutations in the SsrA tag. Most of these alterations, while stabilising FlbD to various degrees, seem to disrupt the activity of the FlbD transcriptional regulator. Mutants have been isolated that have second-site mutations that can compensate for this loss of activity. The mapping and analysis of these mutations will help reveal how FlbD senses an intermediate of the flagellar structure and how it activates the downstream genes in response to this checkpoint.

4.1 FlbD_{Δ13}-SsrA is a substrate for the ClpXP protease

To address the question of whether ClpXP is required for SsrA-tagged substrate degradation, we generated the artificial hybrid protein FlbD_{Δ13}-SsrA, encoded on pGR11 (pBGS18T::*flbD*_{Δ13}-*ssrA*). pGR11 is a suicide plasmid that contains 650 bp of the *flbD* 3' end, where the sequence coding for the last 13 AA was replaced with one encoding the SsrA tag (QVPPPQGGVGAAA → ANDNFAEEFAVAA). FlbD was largely chosen for our experiments for reasons that will be outlined in Section 4.2. We introduced pGR11 into NA1000 cells to create strain UJ1265. Plasmid pMO88 (*P*_{Xyl}::*clpX*_{ATP}) was then introduced into strain UJ1265 to create strain UJ1346. As a control for the effects of the SsrA tag, we created pGR8, a plasmid equivalent to pGR11 but with the 3' end of wild-type *flbD*, and introduced it into strain NA1000 creating strain UJ1262. We then introduced pMO88 into this strain to create strain UJ1347. We grew both strains UJ1346 and UJ1347 in the absence or presence of xylose in order to view the protein concentration in cells with or without ClpX activity. In the former case, ClpX activity would be unaffected and in the latter, ClpX activity would be depleted with time (see results section 3.1.4). Samples were collected every 30 minutes after xylose addition and immunoblots performed using anti-FlbD antibodies (Figure 4.1). FlbD_{Δ13}-SsrA is clearly a highly unstable protein as it is undetected in cells undisrupted for ClpX activity (Figure 4.1 c,d). However, within 60 minutes after xylose addition and ClpX inactivation, the protein begins to appear and subsequently accumulate in the cells.

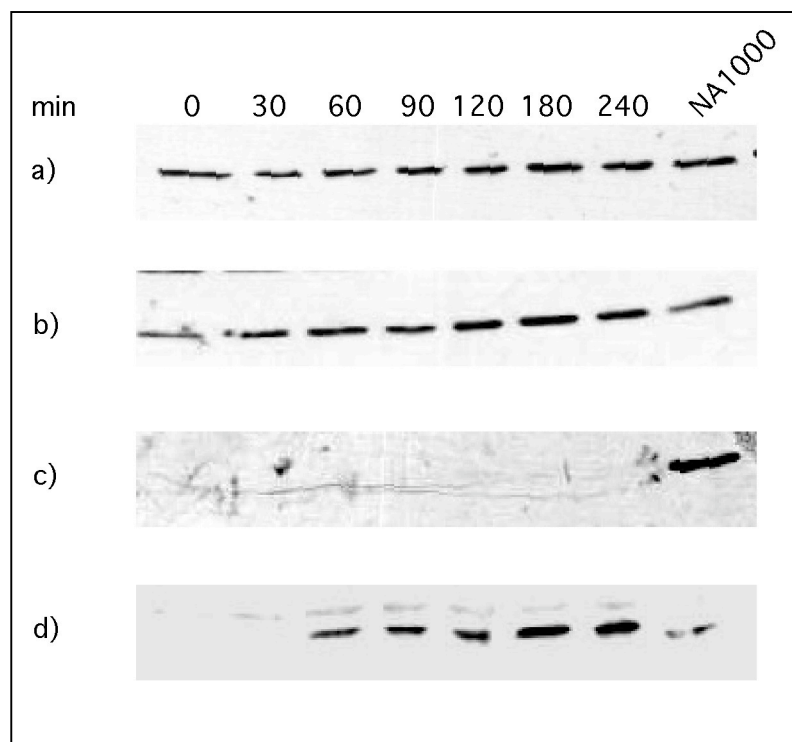


Figure 4.1. FlbD_{Δ13}-SsrA is an unstable protein that is a substrate of ClpXP. Strains UJ1346 and UJ1347 were grown in PYE media overnight to OD₆₆₀ 0.4-0.5. Cells of both strains were harvested and resuspended in fresh PYE medium with either xylose or glucose (t0) after which samples were collected for 240 min for immunoblots. a) and b) Strain UJ1347 grown in the presence and absence of xylose, respectively. c) and d) Strain UJ1346 grown with or without xylose, respectively. Depletion of ClpX activity in the cell leads to accumulation of FlbD_{Δ13}-SsrA.

To confirm that stabilization of FlbD_{Δ13}-SsrA in the absence of ClpX activity is directly linked to the ClpXP protease, we introduced pGR11 into strain UJ199 (*P_{xy}::clpP*) to produce strain UJ2502. Strain UJ2502 was grown in PYE-xylose overnight to OD₆₆₀ 0.5 after which cells were harvested, washed 3 times in fresh PYE medium and resuspended in either PYE-xylose (to deplete ClpP) or PYE-glucose (control). Samples were taken for 4 hours and FlbD_{Δ13}-SsrA levels were then assayed by immunoblots (Figure 4.2). In the presence of ClpP, FlbD_{Δ13}-SsrA is undetectable by immunoblots. However, after removal of xylose from the growth medium, ClpP is depleted and as a consequence, FlbD_{Δ13}-SsrA appears in the cells and accumulates over time.

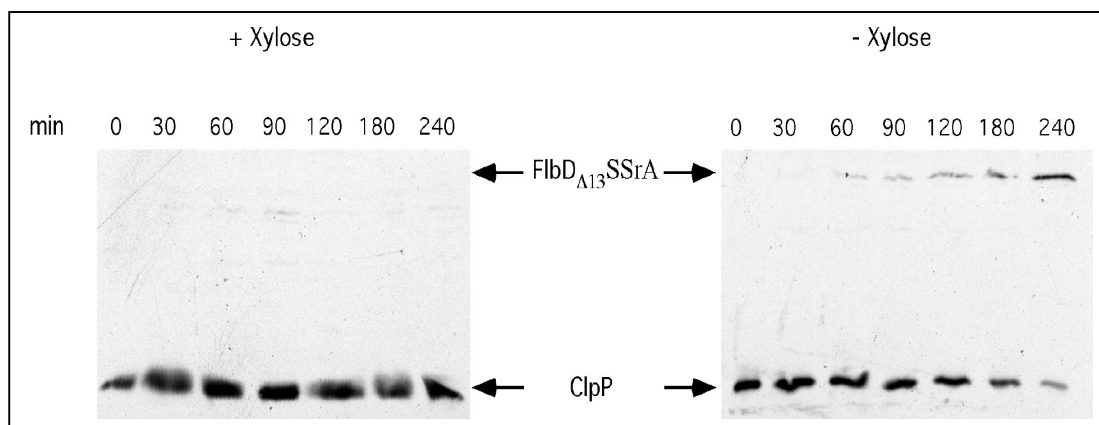


Figure 4.2. FlbD_{Δ13}-SsrA is dependent on ClpP for degradation. Strain U2502 was grown in the presence of xylose (left) and in its absence (right). Depletion of ClpP from the cell is coincident with accumulation of FlbD_{Δ13}-SsrA.

To determine FlbD_{Δ13}-SsrA stability in the presence and absence of ClpX, we conducted pulse/chase experiments on both strains UJ1346 (pMO88 *flbD-ssrA*) and UJ1347 (pMO88 *flbD_{wt}*). Both strains were grown in M2G overnight to OD₆₆₀ 0.3 after which the culture of the respective strain was split and either xylose or glucose added for 2 hours. A pulse/chase experiment was then conducted, immunoprecipitations with anti-FlbD antibodies performed (Figure 4.3) and the resulting bands quantitated (Figure 4.4).

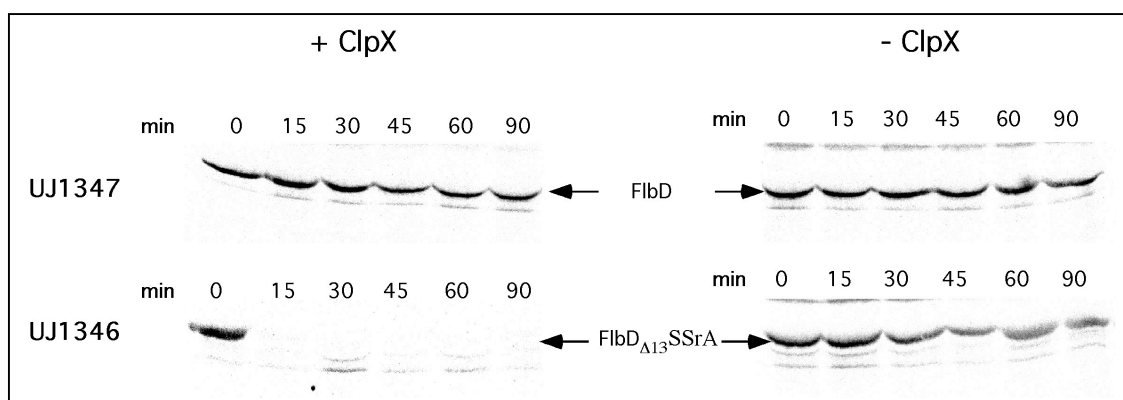


Figure 4.3. Stability of FlbD and FlbD-SsrA in the presence and absence of ClpX. FlbD_{Δ13}-SsrA is completely degraded within 15 min of its synthesis (UJ1346, + ClpX) but stabilised when ClpX is depleted (- ClpX). FlbD in strain UJ1347 is only weakly degraded. Disruption of ClpX activity by addition of xylose causes marked stabilization of FlbD_{Δ13}-SsrA.

FlbD_{Δ13}-SsrA was found to be rapidly degraded in cells with ClpX activity (Figure 4.3, UJ1346). Upon addition of xylose and consequently ClpX disruption, FlbD_{Δ13}-SsrA was dramatically stabilized, with a half life of approximately 90 min (vs. approximately 7.5 min in the presence of ClpX, Figure 4.4). In contrast, FlbD_{wt} was only slowly degraded with a half life of over 90 min and is unaffected by the depletion of ClpX activity from cells (Figure 4.4). These results lead us to conclude that FlbD_{Δ13}-SsrA is rapidly degraded by the ClpXP protease. Furthermore, our results suggest that in *C. crescentus*, like in other organisms, ClpXP is the main protease for SsrA-tagged substrates.

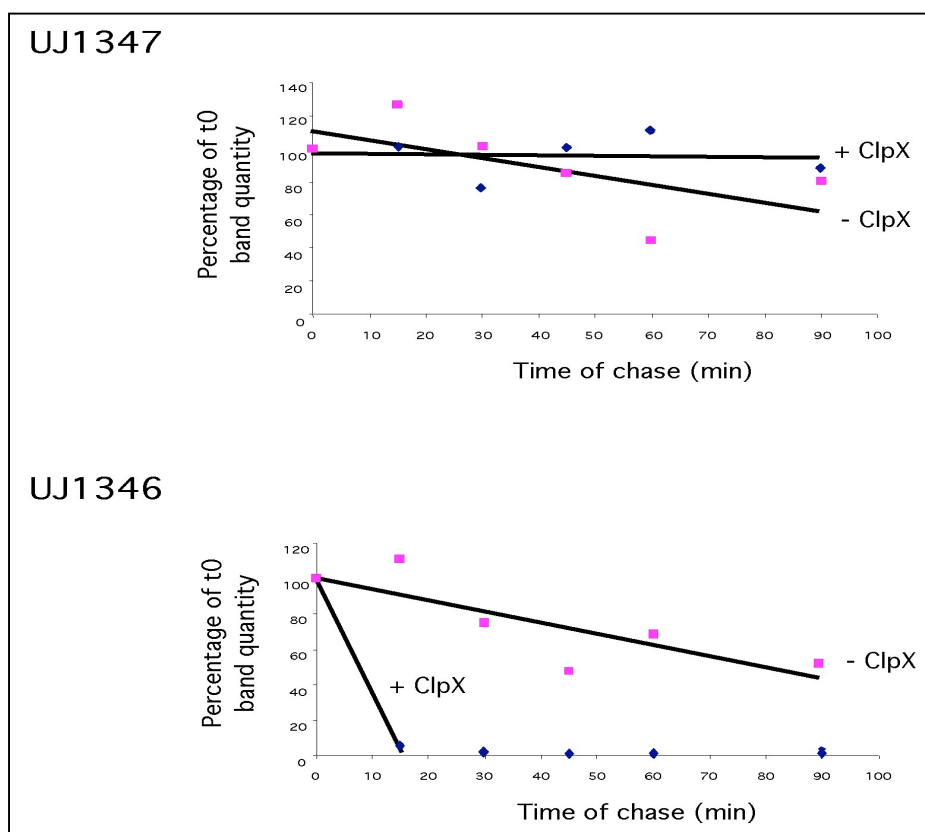


Figure 4.4. Quantitation of FlbD or FlbD_{Δ13}-SsrA stability in strains UJ1346 and UJ1347 in the presence (blue) and absence (pink) of ClpX. FlbD bands in the gels of Figure 3 were quantitated using the ImageQuantTM software (Molecular Dynamics).

4.2 Cells containing SsrA-tagged FlbD are non-motile and readily give rise to motile suppressors

Having established FlbD_{Δ13}-SsrA as a substrate for the ClpXP protease, we wanted to test whether we can use this recombinant protein to study functionally important residues in the SsrA tag. To do this, we employed a simple but elegant genetic screen relying on FlbD's essentiality for motility. Motility in *C. crescentus* depends on a single polar flagellum whose synthesis requires the expression of approximately 50 genes (England and Gober 2001). Those genes are divided into 4 classes of a transcriptional hierarchy. FlbD is required for the expression of Class III/IV genes (Wingrove et al. 1993). Class III genes encode proteins integral to the flagellar rod, hook protein and ring proteins; and Class IV genes encode the flagellar filament. It is worth noting that that flagellar assembly is a tightly regulated process intimately linked with the cell cycle and is governed by several checkpoints; that is, only when a class of genes in the hierarchy is expressed and sensed as functional can the next class be expressed. Details of this process are beyond the scope of this thesis but are reviewed extensively elsewhere (Brun et al. 1994; England and Gober 2001; Wu and Newton 1997). Suffice to say, expression of FlbD is imperative for flagellar assembly and therefore motility.

As we have demonstrated that FlbD_{Δ13}-SsrA is completely degraded within 15 minutes of its synthesis (see results section 4.1), we reasoned that cells harbouring this copy of FlbD as the activator of Class III/IV genes would be immotile. To test this, we streaked strain UJ1346 on semi-solid agar medium (hereafter named

Swarmer plates) side by side with NA1000 cells and indeed found that UJ1346 cells are non-motile (Figure 4.5).

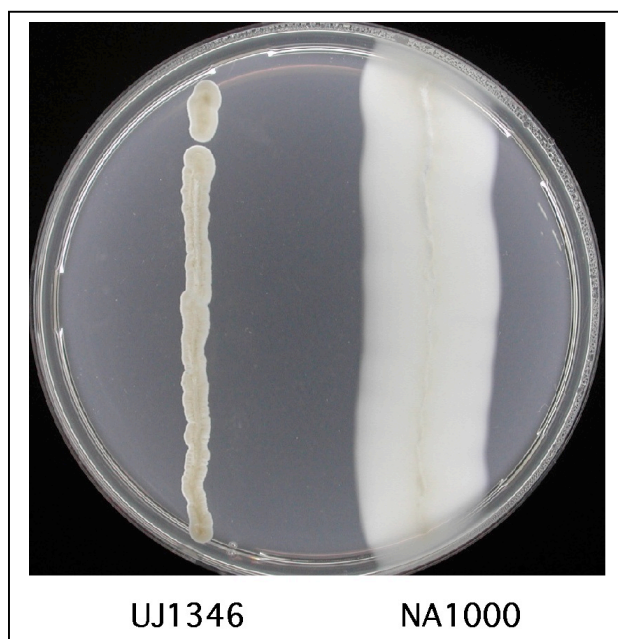


Figure 4.5. Strain UJ1346 is non motile. A colony of UJ1346 was streaked on PYE-Swarmer plates along with NA1000 and incubated for 3 days at room temperature.

pGR11 was designed so as to replace only the last 13 AA of FlbD. However, the SsrA tag is 14 AA with the sequence AANDNFAEEFAVAA. To screen for residues useful for SsrA-tagged FlbD degradation, we decided to recreate this allele with the full SsrA sequence replacing the last 13 AA of FlbD, finally creating an allele of FlbD that is only 1 AA longer than the original wild-type FlbD allele.

To create this allele, we used the λ -recombinase system to replace the end of *flbD* on pGR8 (pBGS18T with the 3' 650 bp of *flbD*) with the full length *ssrA* sequence (See Materials and Methods section 2.6.4). This procedure produced plasmids pST-30 and pST-39, the former with *flbD* _{Δ 13-*ssrA*} and the latter also with *flbD* _{Δ 13-*ssrA*} but that had accumulated a point mutation in the *ssrA* sequence converting the fourth amino acid

from Asp to Val. We decided to conduct further work with pST-39 as it could provide useful clues as to the role of this residue in SsrA tag recognition by ClpX. Both plasmids were transferred to NA1000 producing strains COH6 and COH7, respectively. When COH 6 and 7 were streaked onto Swarmer plates, initially they appeared as non motile as UJ1346 after 3 days of growth. However, when left for an additional day at room temperature, small flares became visible. An additional day later, the flares had grown substantially in size as motile cells multiplied giving the appearance almost of NA1000 cells grown on a swarmer plate, an example of which is shown in Figure 4.6.

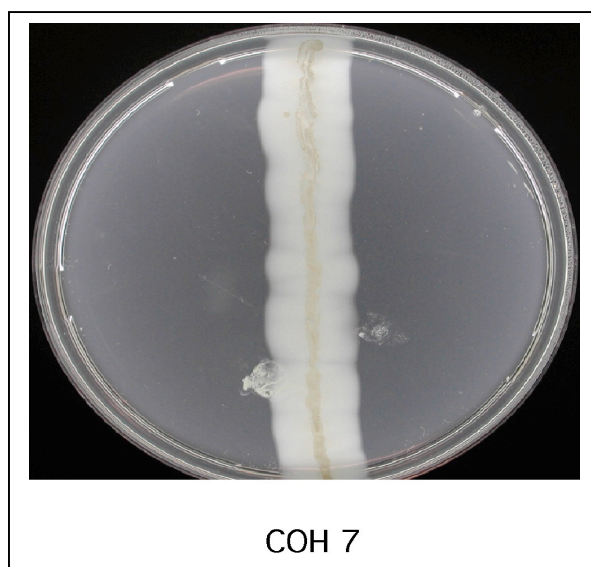


Figure 4.6. COH7 readily gives rise to motile suppressors. Motile suppressors appear as flares stemming from the central streak of a COH7 colony.

Four flares from either COH6 or COH7 were picked and re-streaked on PYE plates to isolate single colonies of each mutant. One clone from each plate was picked and grown overnight in liquid medium in order to assay for FlbD levels using immunoblot analysis. In addition, each suppressor was patched on a Swarmer plate along with the parent from which they were derived so as to quantitate their motility (Figure 4.7). Neither COH6 nor COH7 have detectable levels of FlbD as determined by

immunoblotting. However, unlike COH7, COH6 is able to swim, most likely as a result of the single point mutation found in the SsrA tag. Nevertheless, on Swarmer plates, COH6 is only about 50% as motile as the positive control, suggesting that though FlbD is still unstable, enough of it may remain to induce the expression of Class III/IV genes. As regarding the suppressors, while all eight regained motility to about the same extent, FlbD reached different levels in each one. This indicates that the suppressors isolated were genetically different.

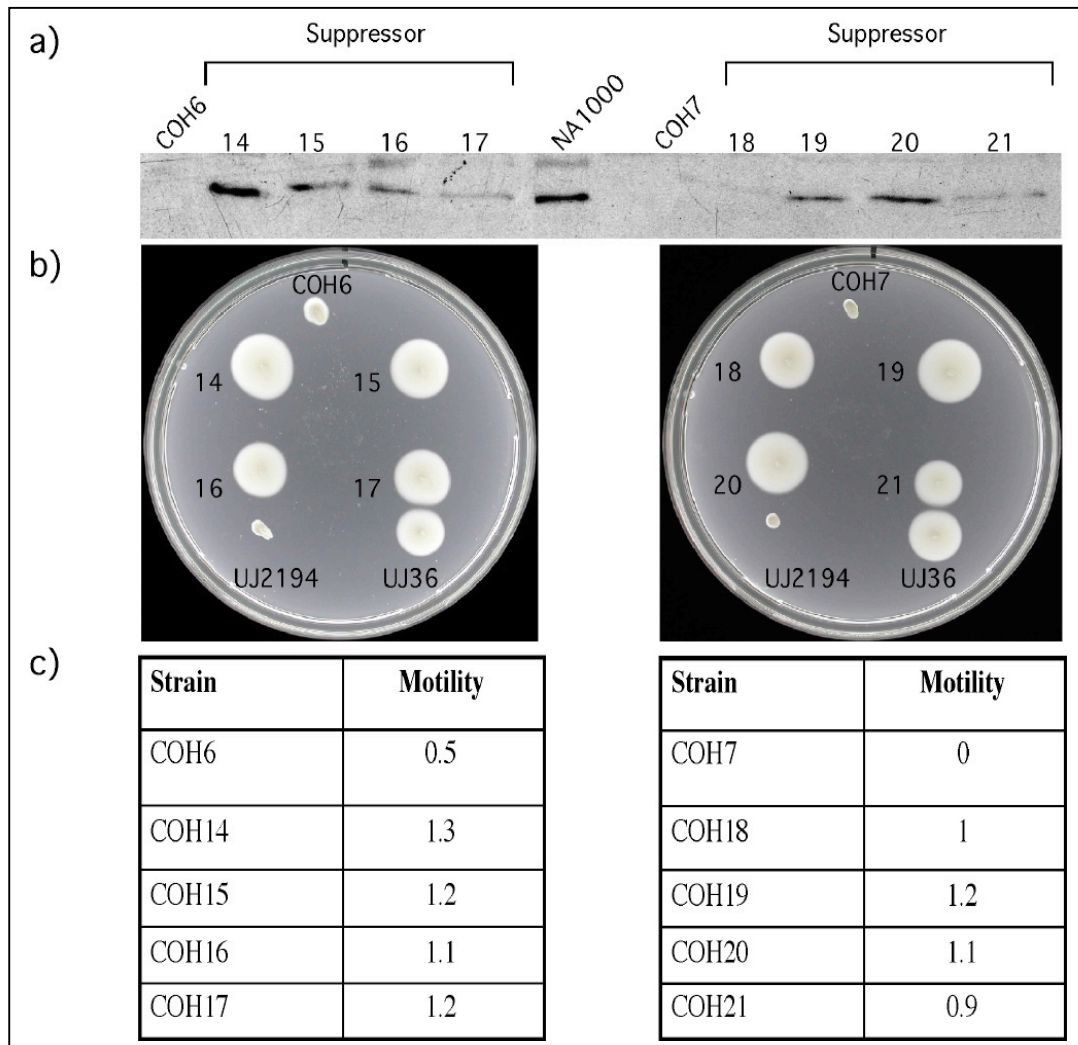


Figure 4.7. Analysis of motile suppressors derived from strains COH6 and COH7. a) Immunoblots with anti-FlbD antibody on cultures of the parent strains and derived suppressors. Levels of FlbD can directly be compared between strains as extracts were normalized by OD_{660} . Strains COH6 and COH7 have undetectable levels of FlbD whereas most of their derived suppressors have stabilised FlbD. b) Swarmer plates of both parents strains and derived suppressors. Included are also strains UJ2194 and UJ36, the negative and positive controls, respectively, which were selected for use based on them being two of the few *C. crescentus* strains with a CmR cassette. Liquid cultures of all strains were examined by light microscopy to verify their motility state. All strains, except COH7 but including COH6 were motile. c) Suppressor motility expressed as a ratio of the diameter of each suppressor colony to that of the positive control, UJ36 which was set to 1. The motility of COH7 and UJ2194 was set to 0, as they are non motile and did not spread on Swarmer plates.

To further characterize the motile suppressor mutants, we amplified a 1 kbp region containing the 3' end of *flbD* and the *ssrA* tag by PCR, and performed sequencing reactions (Figure 4.8). Both COH15 and COH18 have changed the SsrA tag completely due to frame shift mutations immediately upstream of the region coding for the tag. Interestingly, although the two new ends of both suppressors are closely related, only COH15 has detectable FlbD as evidenced by immunoblot analysis (Figure 4.7). Thus, even minor differences in the C-terminal sequences seem to affect FlbD's stability.

Strain COH14 has not only the highest motility value of all suppressors from both parents, but it is also the only suppressor with FlbD levels comparable to NA1000 wild-type cells. Yet the SsrA tag carried by strain COH14 is identical to that which causes FlbD instability in its progenitor, strain COH6. This is a significant result as it suggests that a mutation outside the SsrA sequence is responsible for the suppression and increased FlbD stability.

Strains COH16 and COH17 have single point mutations in the second last residue of the SsrA tag, suggesting that this is an area significant for SsrA tag recognition by ClpXP. The FlbD concentration in either mutant appears lower than in NA1000, though their motility is comparable. Finally, in strains COH19-21, in-frame mutations resulted in deletion of almost the entire SsrA tag, making a protein that is 11 AA shorter than the original construct in pST-30. The motility and FlbD abundance of both COH19 and COH20 are similar, but interestingly, COH21 has lower FlbD levels and is less motile. Together with our observations on strain COH14, it seems that the identity of the FlbD C-terminus may not be the sole determinant of its stability, or

indeed activity as estimated by motility. It is important to note that from these experiments, it cannot be ruled out that (a) second site mutation(s) is/are at least in part responsible for the motility phenotype and/or the increased FlbD levels in the suppressors analysed.

....DAGV AANVNFAEEFAVAA	COH6
....DAGV AANVNFAEEFAVAA	COH14
....DAGV QVPTSTSPRSSPWPPDI	COH15
....DAGV AANVNFAEEFAVVA	COH16
....DAGV AANVNFAEEFAVTA	COH17
....DAGV AANDNFAEEFAVAA	COH7
....DAG AWPPTTTSPRSSPWPPDI	COH18
....DAG VAA	COH19-21

Figure 4.8. C-terminal ends of motile suppressor mutants of COH6 and COH7. The last residues of FlbD are indicated in black. Red residues indicate the wild-type SsrA sequence while the blue residues are deviations thereof. COH6, 16 and 17 all have spontaneous point mutations (blue residues). COH15 has a replaced 5 bp (starting 2 bp upstream of the *ssrA*) with a new 7 bp sequence. COH18 has a 2 bp insertion at 2 bp upstream of the *ssrA* sequence. COH19-21 have deleted the entire *ssrA* sequence leaving only Ala-Ala at the end of the protein.

As it was not clear whether the C-terminal 13 amino acids of FlbD are required for its function, we repeated our experiments with a SsrA-tagged full length copy of FlbD. To do this, we created pST-32, which bears the 3' end *flbD* with a *ssrA* addition (see Materials and Methods section 2.6.4). pST-32 was introduced into NA1000 to produce strain COH33. Similar to strains COH6 and COH7, COH33 was non-motile. A colony of strain COH33 was streaked on a Swarmer plate and motile suppressors

isolated and examined as for COH6 and COH7 (Figure 4.9). The end of *flbD* was sequenced in each motile suppressor of COH33 as described for COH6 and 7 (Figure 4.10).

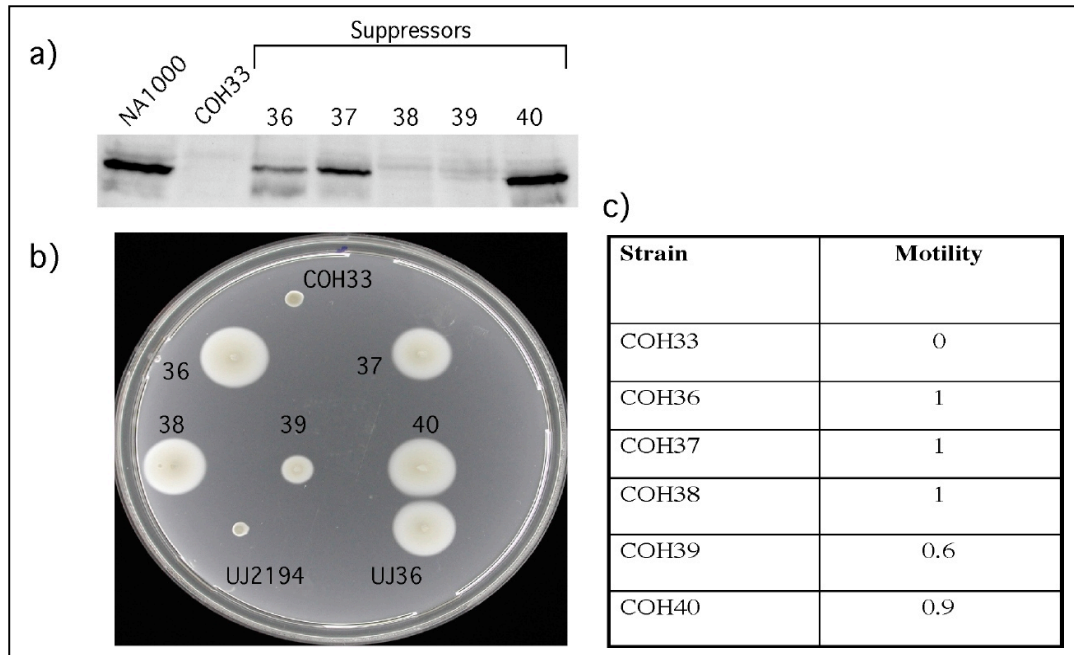


Figure 4.9. Analysis of motile suppressors derived from strain COH33. a) Immunoblots with anti-FliB antibodies on extracts from growing cultures of strain COH33 and the suppressors. Levels of FliB can be directly compared between strains as extracts were normalized by OD_{660} . COH33, 38 and 39 have no detectable FliB band. b) Swarmer plate of COH33 and the five derived suppressors. Included are also strains UJ2194 and UJ36, the negative and positive controls, respectively. Liquid cultures of all strains were examined by light microscopy to verify their motility state. All strains, except COH33 and UJ2194 were motile. c) Suppressor motility expressed as a ratio of the diameter of each suppressor colony to that of the positive control, UJ36, which was set to 1. The motility of COH33 and UJ2194 was set to 0, as they are non motile and did not spread on Swarmer plates.

....DAGVQVPPPQGGVGAAA AANDNFAEEFAVAA	COH33
....DAGVQVPPPQGGVG APTC DRSLRRINKSWCPC	COH36, 37
....DAGVQVPPPQ APACRCRRPRAGSARPLPPTTTSPRSSPWPPDI	COH38
....DAGVQVPPPQGGVGAAA AANDNFAEEFAVAA	COH39
....DAGVQVPPPQGGVGAAA APT TTSPRSSPWPPDI	COH40

Figure 4.10. C-terminal ends of strain COH33 and its derived suppressors. The residues of FlbD are indicated in black; the SsrA in red and deviations thereof in blue. Both COH36 and 37 have a deletion of 122 bp. COH38 has a 29 bp insertion 20 bp upstream of the first codon of the *ssrA* sequence. COH40 has an insertion of 2 bp after the first codon of *ssrA*, leading to a similar distal C-terminus end to that of COH38. COH39 has no mutations in the SsrA tag.

As for UJ1346 and COH7, COH33 had no detectable FlbD band (Figure 4.9). In contrast to two of the COH6 derived suppressors, and similar to those of COH7, none of strain COH33 derived suppressors had point mutations in the SsrA tag. Instead all the mutations are either insertions or deletions immediately upstream of the tag resulting in frame-shifts. Strain COH38 bears the longest tail thus far isolated in suppressors, has no detectable FlbD band and is slightly less motile than wild-type cells. Whether this is a direct effect of the tail identity/length of FlbD, or result of a second site mutation is unclear. The most interesting suppressor arising from strain COH33 is COH39, which has the SsrA tag intact, an undetectable FlbD band and is 60% as motile as wild-type cells. This mutant can be compared with COH14 that only has a mutation in the fourth residue of the SsrA tag. As mentioned above, COH14 is hyper-motile and has a strong FlbD band. Whether the effect on FlbD stability and motility is a direct effect of this mutation, or the length of FlbD is unknown. It

remains a formal possibility that none of the suppressor mutants, with or without an intact SsrA tag, are motile only due to FlbD stabilisation. Several mutants argue for this case (COH14, 18, 38 and 39) and point to the existence of a mutation *in trans* that restores motility.

To address this possibility, we transferred the *flbD* tails of strains COH18 and COH38 into wild-type NA1000 cells thus creating strains ST190 and ST191 (with the COH18 tail) and ST192 (with the COH38 tail) (See Materials and Methods section 2.6.5). Immunoblot analysis was then performed with anti-FlbD, anti-Flagellins and anti-FliF antibodies to address a series of questions. We expected that if the FlbD C-terminus alone is responsible for protein stability, the amount of FlbD in the original suppressors and derived strains should be identical. Regarding the expression of Flagellins, we wanted to test if FlbD in either suppressor was active purely on merit of its new C-terminus, and if so it should allow the expression of Class III/IV flagellar genes in the suppressor-derived strains. Lastly, we tested the levels of FliF in the suppressor-derived strains as a second measure of FlbD activity. One of the functions of FlbD is to suppress the expression of Class II genes, one of which is *fliF*. We reasoned that if FlbD is active by virtue of the acquired C-termini, its ability to repress *fliF* expression should be identical in the original suppressors and their derivatives (Figure 4.11)

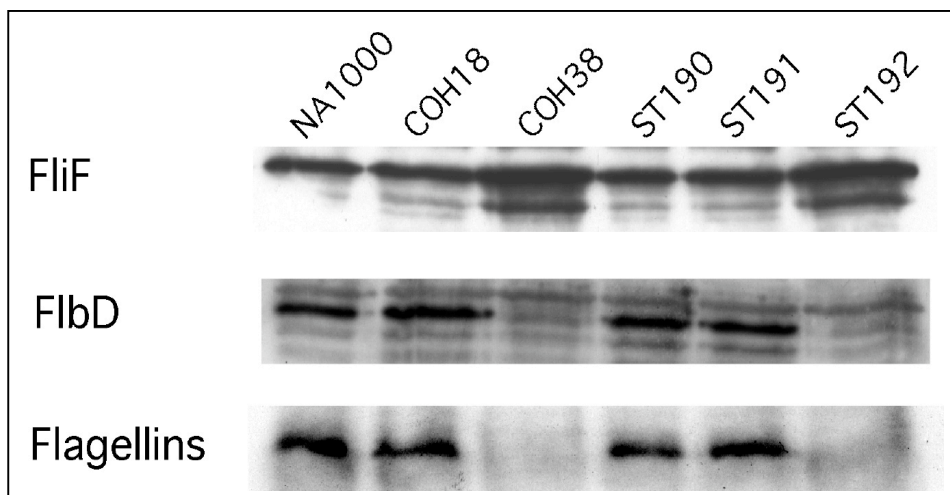


Figure 4.11. Immunoblot analysis of extracts of COH18, COH38 and derivative strains ST190-192 with anti-FlbD, anti-Flagellins and anti-FliF antibodies. Unlike figure 4.7, COH18 has a marked FlbD band that is close in intensity to NA1000 FlbD. The transfer of the FlbD tail from either suppressor to NA1000 carries with it the same behaviour of FliF, FlbD and Flagellins.

In all three strains, the behaviour of FlbD seems to be inherited from the suppressor confirming that tail identity alone governs protein stability. However, strain COH18 should be treated with caution as a previous experiment has shown it to contain no FlbD (Figure 4.7). Concerning FliF, COH18 has comparable levels to its derivatives ST190/191 and NA1000 suggesting that repression of Class II expression functions normally. Furthermore, all three strains synthesise Flagellins. Taken together, these observations argue strongly that the FlbD in COH18 is a functional protein. Consistent with this result is the fact that ST190/191 are both motile as evidenced by light microscopy. In contrast, the levels of FliF are elevated in both COH38 and its derivative ST192, and Flagellins are not produced. This fact is in agreement with the relative absence of FlbD from either strain. Surprisingly, neither COH38 nor ST192 produce Flagellin proteins, at least not in any detectable quantity. It should be noted

that the anti-Flagellin antibody we used is a polyclonal antibody and is likely to largely recognize FljK, as it is the predominant subunit of the flagellum. Thus, COH38 seems to lack FljK, yet it is able to swim; a phenomenon observed independently by A. Levi (personal communication). However, the hypothesis that COH38 is motile because it only lacks FljK but synthesises the other flagellins is hampered by the obvious lack of FliD in this strain. An alternative explanation is that cells have regained Class III/IV gene expression through a FliD-independent mechanism. The observation that strain ST192 is unable to swim and also lacks one or several of the flagellins indicates that a second site mutation is responsible for the suppression of the motility defect in strain COH38 *in trans*. Thus, moving the FliD C-terminus of strain COH38 into NA1000 uncouples FliD from a second site mutation that must have occurred to restore motility in this strain.

These observations lead us to conclude that the identity of the FliD C-terminus alone is not the sole determinant for motility, at least in strain COH38. A second site mutation clearly seems to be responsible for the regain of motility in this strain. This might also be the case for other suppressors and has to be tested. In contrast, FliD's instability in strain COH38 seems to rely on the FliD C-terminus only. Similarly, suppressor strains COH16 and COH17 argue that FliD stabilisation is the result of a single mutation (additional to that of their progenitor, COH6) in the SsrA tag. If this is indeed the case and FliD stability in general is determined by its C-terminus remains to be demonstrated by allele transfer experiments. The only exception to this is strain COH14 where FliD stabilisation does not seem to be limited to a mutation *in cis*.

4.3 Cells bearing an undegradable version of SsrA-tagged FlbD are non-motile

Some of the above experiments suggested that stabilisation alone of FlbD might not be sufficient for motility. To determine if a stable FlbD-SsrA variant would support motility, we mutated the last three residues of the SsrA tag from AAA to DDD based on previous studies (Flynn et al. 2001; Gottesman et al. 1998; Keiler et al. 2000; Roche and Sauer 1999). The FlbD variants FlbD_{Δ13}-SsrA_{DDD} and FlbD-SsrA_{DDD} (on pST-31 and pST-33, respectively) were transferred into NA1000 wild-type cells, thus creating strains COH12/13 and COH34/35, respectively (see Materials and Methods section 2.6.4). All four strains were examined for FlbD stability and motility, and the 3' ends of *flbD* were sequenced as described above (Figure 4.12-14).

To our surprise, COH12/13 and COH34/35 were non motile even though the levels of FlbD in all four strains were elevated above those of NA1000 (Figures 4.12 and 4.13). Why these *flbD* alleles do not support motility is not clear. It is possible that elevated levels of FlbD could somehow inhibit motility. Alternatively, the C-terminal tag could disturb or annul FlbD function making the cells non motile. It is also possible that the failure to swim results from a combination of these reasons. To analyse the molecular basis of the motility defect in strains COH12/13 and COH34/35, motile suppressors were isolated and their motility behaviour, FlbD levels, and the FlbD C-terminus were analysed (Figures 4.12-4.14).

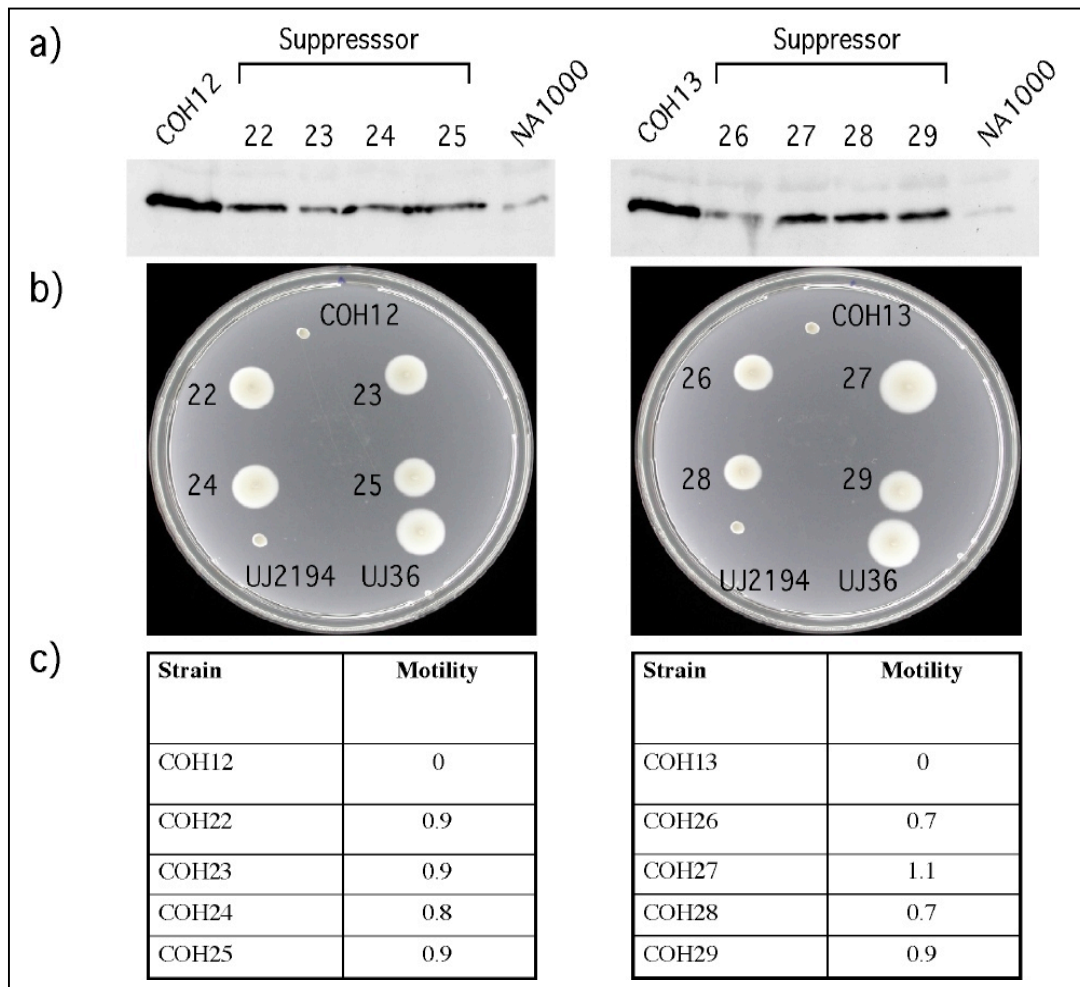


Figure 4.12. Analysis of suppressors derived from strains COH12/13. a) Immunoblots with anti-F1bD antibody on extracts of growing cultures of COH12/13 and the suppressors. Levels of F1bD can be directly compared between strains as extracts were normalized by OD_{660} . COH12/13 both have elevated F1bD levels as compared to NA1000, and their derived suppressors appear to have reduced levels of F1bD. b) Swarmer plate of COH12/13 and derived suppressors. Included also are strains UJ2194 and UJ36, the negative and positive controls, respectively. Liquid cultures of all strains were examined by light microscopy to verify their motility state. All strains, except COH12 and COH13 were motile. c) Suppressor motility expressed as a ratio of the diameter of each suppressor colony to that of the positive control, UJ36 which was set to 1. The motility of COH12/13 and UJ2194 was set to 0, as they are non motile and did not spread on Swarmer plates.

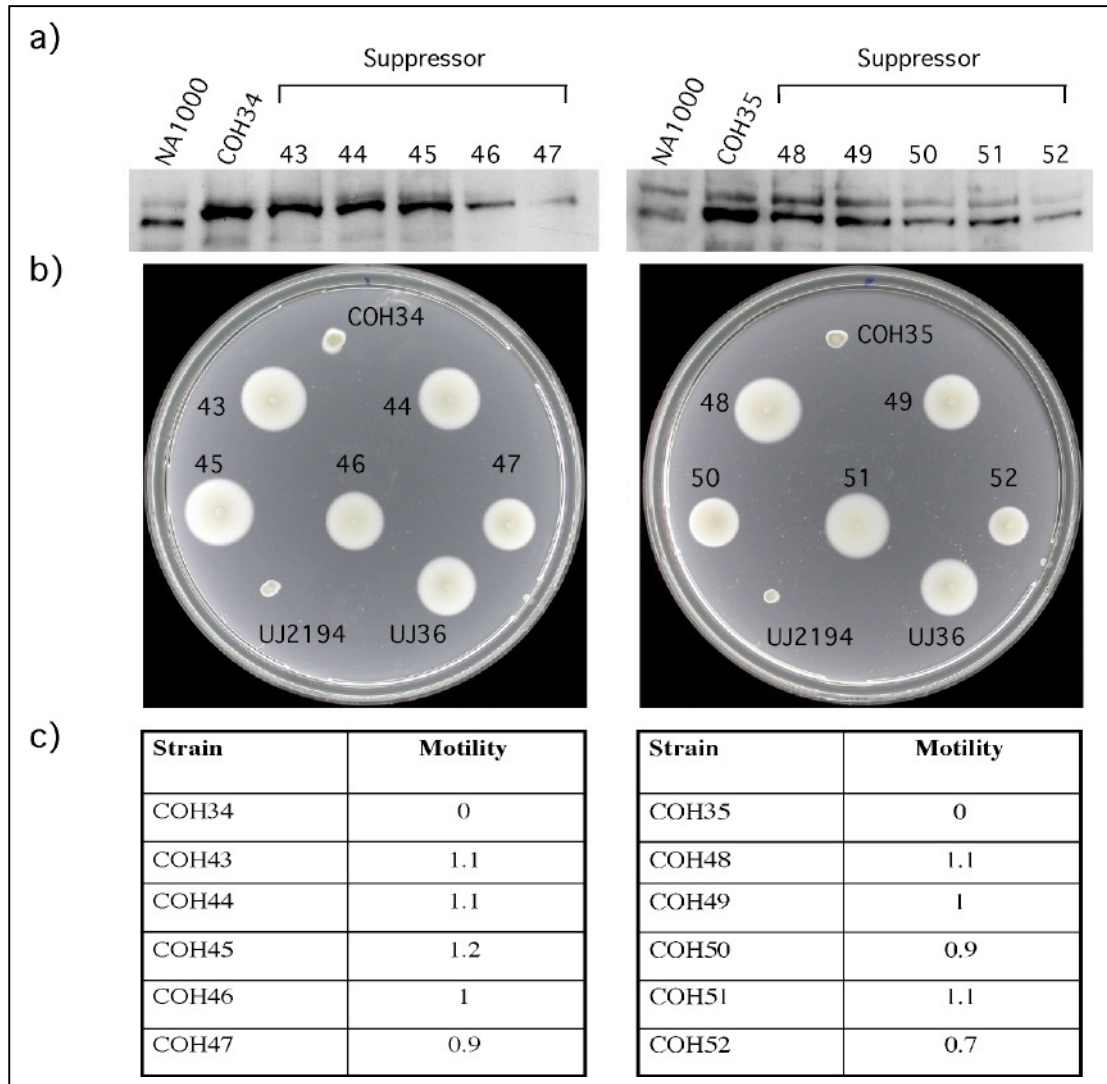


Figure 4.13. Analysis of suppressors derived from strains COH34/35. a) Immunoblots with anti-F1bD antibody on extracts of growing cultures of COH34/35 and the suppressors. Levels of F1bD can be directly compared between strains as extracts were normalized by OD_{660} . COH34/35 both have elevated F1bD levels as compared to NA1000 and their derived suppressors appear to have reduced levels of F1bD. b) Swarmer plate of COH34/35 and derived suppressors. Included also are strains UJ2194 and UJ36, the negative and positive controls, respectively. Liquid cultures of all strains were examined by light microscopy to verify their motility state. All strains, except COH34 and COH35 were motile. c) Suppressor motility expressed as a ratio of the diameter of each suppressor colony to that of the positive control, UJ36 which was set to 1. The motility of COH34/35 and UJ2194 was set to 0, as they are non motile and did not spread on Swarmer plates.

....DAGV AANDNFAEEFADDD	COH12/13
....DAGQ VPTTSPRSSPTT DI	COH27
....DAGV AANDNFAEEFADDD	COH22-26, 28-29
....DAGVQVPPPQGGVGAAA AANDNFAEEFADDD	COH34/35
....DAGVQVPPPQGGVGAAA AANDNFAEEFADDD	COH43-52

Figure 4.14. C-terminal tail identity of COH12/13 and COH34/35 derived suppressors. The residues of FlbD are indicated in black; the SsrA in red and deviations thereof in blue. With the exception of COH27, all derived suppressors from the 4 parents have an intact SsrA_{DDD} tag. COH27 has a 2bp insertion before the start of the *ssrA* sequence.

A striking difference in motility between suppressors derived from strains COH12/13 (FlbD_{Δ13}-SsrA_{DDD}) and those derived from strains COH34/35 (FlbD-SsrA_{DDD}) was observed (Figure 4.12-4.13). Suppressors of strains COH12/13 are generally less motile than the wild-type control, with the exception of strain COH27. Interestingly, strain COH27 is the only suppressor derived from a FlbD_{Δ13}-SsrA_{DDD} with a mutation *in cis* (Figure 4.14). Suppressors derived from strains COH34/35 generally showed a higher degree of motility than the wild-type control, with the exception of COH46, COH47, COH50 and COH52. The reason for the difference in motility between suppressors derived from either FlbD_{Δ13}-SsrA_{DDD} or FlbD-SsrA_{DDD} could be related to the overall length of the FlbD C-terminus; or to the fact that in the latter, the 13 amino acids of the FlbD C-terminus are still present.

The FlbD C-termini in all suppressors of strains COH34/35 and COH12/13 is identical to their parent strains, with the exception of strain COH27. This argues that

the differences observed in motility, and possibly FlbD stability, must be due to a second site mutational event(s) acting *in trans*. The results obtained for these strains confirm our earlier observation that the presence of FlbD alone is not sufficient for motility. Furthermore, the length or final 13 amino acids of FlbD may be factors that could affect motility of cells.

To establish whether the presence of the last 13 amino acids of FlbD is important for motility, we constructed pST-35 (pBGS18T::*flbD*_{Δ13}) and transferred it to NA1000 cells producing strain ST198. Strain ST198 was patched on a Swarmer plate and an extract from an overnight exponentially growing culture was tested for FlbD levels by immunoblotting (Figure 4.15). It is interesting to note that strain ST198 is more motile than the wild-type control but has FlbD levels comparable to those of NA1000 (Figure 4.15). It therefore appears that the last 13 amino acids of FlbD are not required for motility and their removal may even increase it.

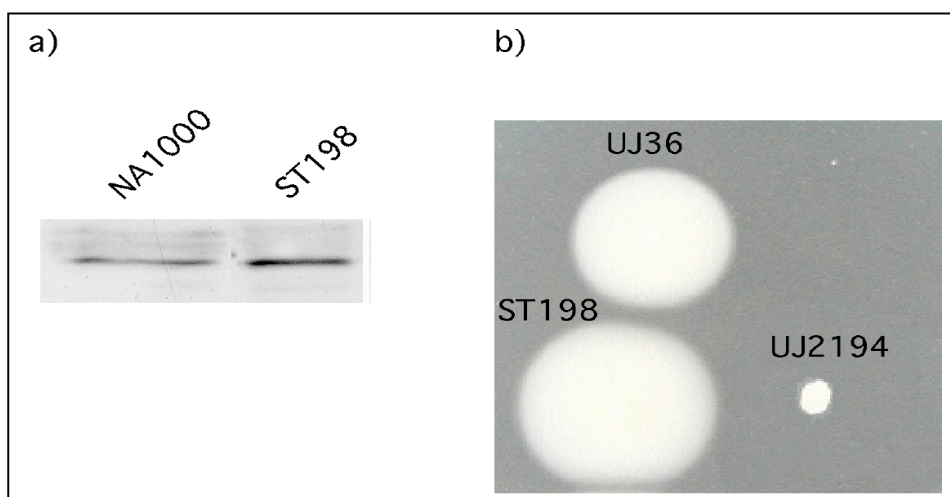


Figure 4.15. The last 13 amino acids of FlbD are not required for motility. a) Immunoblot of extracts of strain ST198 (NA1000::*flbD*_{Δ13}) standardised for OD₆₆₀ for comparison with NA1000. FlbD levels are comparable in both strains. b) Swarmer plate with strain ST198, UJ36 (positive control) and UJ2194 (negative control). Strain ST198 has a motility value of 1.2 relative to strain UJ36.

4.4 DISCUSSION

4.4.1 SsrA-tagged FlbD variants as targets for the ClpXP protease

The data presented in this chapter show that a SsrA-tagged copy of FlbD is degraded in a ClpXP dependent manner. To demonstrate this, we have used the dominant negative *clpX_{ATP}* allele (see Chapter 3) to disrupt ClpX activity and ask if the unstable FlbD_{Δ13}-SsrA becomes stable as a result. Indeed, this was observed and FlbD_{Δ13}-SsrA became stable within 60 min of *clpX_{ATP}* expression (Figure 4.1). This result is confirmed by pulse chase analysis of strain UJ1346 (pMO88::*flbD_{Δ13}-SsrA*) where FlbD_{Δ13}-SsrA is degraded within 15 min of its synthesis, and upon *clpX_{ATP}* induction is significantly stabilised (Figure 4.4). This observation is in agreement with the kinetics of CtrA stabilisation upon ClpX inactivation, hence lending more proof that *clpX_{ATP}* expression rapidly inactivates ClpX activity. Thus, in *C. crescentus*, like in *E. coli*, SsrA-tagged substrates are rapidly degraded by the ClpXP protease *in vivo*.

4.4.2 Degradation determinants in the SsrA tag

To study useful *cis* and *trans* degradation determinants for SsrA-tagged substrates, we devised a genetic selection regime taking advantage of SsrA-tagged FlbD. We showed that cells bearing *flbD_{Δ13}-ssrA* as the only *flbD* copy are non-motile (Figure 4.5). We assumed that this results from the marked instability of SsrA-tagged FlbD, and as a consequence, class III and IV genes would not be expressed. Using this

allele, we developed a powerful selection for spontaneous mutations arising in motile cells, presumably due to stabilisation of FlbD. We expected to find mutations altering the SsrA tag rendering it inaccessible to ClpXP. In previous research, this task has been conducted using site-directed mutagenesis of residues thought to be important for recognition of SsrA tag recognition. Such work has revealed that ClpX recognises the three nonpolar residues Leu-Ala-Ala at the C-terminus of the tag (Flynn et al. 2001; Levchenko et al. 1997). Flynn et al. (2001) have also identified a binding site for SspB in the first half of the SsrA tag. SspB acts as a specificity enhancer of the ClpXP protease for the SsrA tag (Levchenko et al. 2000; Wah et al. 2002). No SspB homologue exists in *C. crescentus* but the existence of a functional homologue cannot be ruled out. We therefore decided to use our motility screen in order to obtain more information about specific recognition determinants in the SsrA tag.

Surprisingly, the majority of suppressors derived from cells bearing *flbD*_{Δ13}-*ssrA* or *flbD*-*ssrA* alleles did not contain point mutations in the *ssrA* portion of the tag, but rather frame-shift mutations (insertions or deletions) that completely altered the amino acid sequence of the tag (Figures 4.8 and 4.10). The only two mutants with amino acid substitutions in the SsrA tag were COH16 and COH17. Worthy of note is that both mutants were derived from COH6, a strain containing *flbD*_{Δ13}-*ssrA* with a spontaneous point mutation at position four of the SsrA tag (Asp→Val). As a result of this mutation, strain COH6 is slightly motile while its FlbD levels are undetectable by immunoblots. No such suppressors were derived from the other parent strains, which contained the wild-type SsrA-tagged FlbD and were non-motile. This suggests that single point mutations in SsrA that stabilise FlbD can only be obtained if the original mutant form shows a basic level of protein activity and/or abundance. These

two mutations potentially alter ClpX recognition and by that stabilise FlbD-SsrA partially. It is not clear whether the resulting increase in motility is the direct result of this stabilisation or if a second site mutation is involved.

Our observations with strains COH6, 16 and 17 lead us to conclude that we have identified two critical determinants for SsrA tag recognition by the ClpXP protease. The first determinant is an Asp residue at position four of the SsrA tag whose replacement with Val seems to allow cells to regain some motility, yet not significant FlbD stability. This residue has been shown by Flynn et al. (2001) to specifically interact with ClpX in *E. coli*. The other determinant is the second last residue of the tag (Ala) whose replacement with Val or Thr leads to increased FlbD stability and possibly motility. Whether or not stabilisation of FlbD in these mutants is the direct cause for motility is unclear and is discussed in details below in light of other data.

4.4.3 Motile suppressors with an intact SsrA tag

Two suppressors, COH14 and COH39, were isolated that contained a SsrA tag indistinguishable from their non-motile progenitors. COH14 is a suppressor of *flbD*_{Δ13}-*ssrA* (from COH6) that has a high FlbD concentration, and a high motility value. This mutant suggests that a mutation *in trans* must have occurred to lead to this marked FlbD stability and possibly the restoration of motility. In contrast, COH39, derived from a *flbD-ssrA* bearing strain (COH33), has a low motility value and undetectable FlbD. The difference between COH39 and COH14 is that the former contains the original FlbD C-terminus followed by an intact SsrA tag, while the latter lacks the 13 C-terminal amino acids of FlbD and is followed by a SsrA tag with a

single point mutation at position four. Whether FlbD levels directly correlate with motility in these strains remains to be shown. In light of the above presented data, it is likely that the *in trans* mutations in COH14 and COH39 are genetically distinct.

It is formally possible that one of these second site mutations would map to a functional homologue of SspB. An alternative possibility is a mutation in ClpX itself that reduces its affinity for the SsrA tag. Finally, mutations that sequester or protect FlbD-SsrA from access by the protease would also lead to the observed phenotype.

4.4.4 Novel FlbD C-termini and motility

Our attempts to isolate motile suppressors with point mutations in the SsrA tag were largely unsuccessful for reasons that are unclear. One explanation could be that frame-shift mutations are more frequent than point mutations. Alternatively, other than those identified, point mutations in the *ssrA* tag may not restore motility and thus not be detected by our selection method. We have, however, obtained a variety of interesting mutants that could shed light on the regulation of motility in *C. crescentus*. Most of the suppressors obtained from *flbD_{Δ13}-ssrA* or *flbD-ssrA* bearing strains contained frame-shift mutations in the *ssrA* tag producing novel FlbD C-termini. Whether it is the nature of the FlbD C-terminus that directly controls FlbD stability and motility is not clear. The observation that the *flbD* locus of suppressor COH38 was not able to confer motility when transferred into a clean genetic background suggested that, at least in this strain, a second site mutation is required to restore motility. Also, the fact that identical FlbD C-termini do not always endow the cells with the same motility value, or even FlbD stability (eg. COH19 vs. COH21,

Figure 4.7) suggests that motility, and may be FlbD stability, is dependent on a genetic change *in trans*. Furthermore, FlbD levels do not seem to directly correlate with motility in several suppressors (e.g. COH18 vs. COH38 and COH40), again arguing for the presence of second site mutations. It is thus possible that, for unknown reasons, in most cases two mutational events are necessary to restore motility in cells with a FlbD-SsrA protein: the first to stabilise FlbD to appropriate cellular concentrations, and the second to restore motility, possibly through the activation of an otherwise inactive SsrA-tagged FlbD. It has to be noted though, that despite double mutational events being rare, the selective pressure applied in our regime is high. A step-wise restoration of motility through two mutational events could therefore explain the observed genetic pattern.

To address whether the presence of the SsrA tag C-terminally inactivates FlbD and whether FlbD's levels control motility, we created the stable *flbD* alleles *flbD*_{Δ13}-*ssrA*_{DDD} and *flbD*-*SsrA*_{DDD}. Interestingly, cells harbouring either allele were non-motile. It is possible that this particular SsrA tag destroys FlbD function or that the resulting increase in FlbD levels above those of wild-type cells inhibits motility. Of 18 suppressors derived from strains bearing either allele, only one suppressor had a frame-shift mutation whilst the remainder left the *SsrA*_{DDD} tag unchanged (Figure 4.14). When compared with suppressors derived from COH6, 7 and COH33, this is a significantly different outcome. This might reflect the fact that in a strain containing *flbD*_{Δ13}/*flbD*-*ssrA*_{DDD} though FlbD is present, it is inactive, or present in concentrations disruptive to motility. *In trans* suppressors of this allele would therefore have to either restore FlbD activity or reduce its overall cellular concentrations. Indeed, we have some evidence to support the latter possibility and that is suppressors derived from

COH12, 13 and COH34, 35 all show reduced levels of FlbD (Figures 4.12 and 4.13). This argues that high FlbD levels might be inhibitory to motility and must somehow be reduced. One possible mechanism by which this could be achieved is to reduce expression of the gene. Though, considering that the motility of the different suppressors is not identical yet their FlbD C-termini are, whatever mutations occurred to restore reduce FlbD levels and regain motility are likely different.

It has been shown recently that the cell division checkpoint exerted by the first structural intermediate of the flagellum (composed of Class II proteins) is mediated by FlbD (Muir and Gober 2001). It is not known how FlbD transfers the information regarding the assembly status of the flagellum to the cell division apparatus, but it is possible that too much FlbD could block cell division at an early stage. In agreement with this, we have preliminary evidence suggesting that overexpression of *flbD-ssrA_{DDD}* is not tolerated by cells (plasmid pST-36, not shown). However, strains COH12/13 and COH34/35 have no such division defect and cell morphology appears normal (not shown). This suggests that though the increased FlbD levels in these strains may inhibit motility, they remain below the threshold for cell division-inhibition.

Given earlier work we suspected that the second mutation (s) would lie in FlbD (Mangan et al. 1995). It is known that in order for the cell to express Class III/IV genes, it must first sense that Class II genes are expressed and correctly assembled. However, mutants that could bypass this requirement for Class II gene expression and assembly (*bfa*, bypass of flagellar assembly) were isolated and found to reside in *flbD* (Muir et al. 2001). We sequenced the *flbD* gene in all our suppressors and found none

bearing any mutations. We then turned our attention to FliX, a trans-acting factor that acts as both an activator and a repressor of FlbD activity (Muir and Gober 2001; Muir et al. 2001). FliX is a 14 kDa protein of unknown biochemical function that is essential for motility due to its interaction with FlbD (direct, or otherwise). Furthermore, a *bfa*-like mutation in *fliX* was isolated from other Class II gene mutants that incurred motility in the absence of Class II assembly (Muir and Gober 2001). In addition, high levels of FliX in the cell repress motility, and hence the negative effect on FlbD. Taken together, this data opened the possibility that our *bfa*-like mutation(s) in the suppressors could reside in *fliX*. We sequenced the gene encoding FliX in all suppressors and found no mutations. It remains likely that the lack of motility in COH12/13 and COH34/35 is due to titration of FliX from the cell by the increased levels of FlbD. This idea suggests that FliX has a FlbD-independent activity that is also required for motility. The fact that FlbD levels are reduced in suppressors of strains bearing a stable FlbD protein could argue in favour of this hypothesis.

We have divided all suppressors into four categories based on the identity of their FlbD C-termini (Table 4.1). Examination of the data in Table 4.1 immediately shows that within each category, further divisions could be made based on the FlbD concentration or the motility. Therefore, our results strongly argue that there are independent genetic events that have led to the restoration of motility in a situation where FlbD is rapidly degraded, or stable but inactive or over produced. Considering class C suppressors, we presume that if the same mutation occurred in all strains, then they should all regain motility to the same degree. This indicates the suppressors in this class are genetically distinct.

Table 4.1. Motile suppressors derived from *ssrA/ssrA_{DDD}* tagged *flbD_{Δ13}/flbD* bearing strains are divided into four categories based on the nature of the FlbD C-terminus. Class C strains are derived either from *flbD_{Δ13}-ssrA_{DDD}* bearing strains (top sequence) or from *flbD-ssrA_{DDD}* bearing strains (bottom sequence). For ease of reference, relative motility values are indicated by '+/-' signs, where '-' is non-motile, '+' is ≤ 0.8 , '++' = 0.9, '+++ = 1, or wild-type value, and '++++' is ≥ 1.1 . The intensity of the FlbD band is compared to that of NA1000 and expressed symbolically where '-' is no FlbD band visible, '+' is a weak FlbD band, '++' is comparable to NA1000 and '++++' is more FlbD per cell than NA1000. The FlbD tail identity is shown in the central column where the original FlbD residues are coloured in black, SsrA residues in red and deviations thereof in blue.

Strain	FlbD C-terminus	Motility	FlbD band
Wild-typeDAGVQVPPPQGGVGAAA	+++	++
A) Strains with point mutations in the SsrA tag			
COH6DAGV AANVNFAEEF AVAA	+	-
COH14DAGV AANVNFAEEF AVAA	++++	++
COH16DAGV AANVNFAEEF AVVA	++++	+
COH17DAGV AANVNFAEEF AVTA	++++	+
B) Strains with intact SsrA on FlbD C-terminus			
COH39VPPPQGGVGAAA AANDNFAEEF AVAA	+	-
C) Strains with intact SsrA_{DDD} on FlbD C-terminus			
COH26,52		+	+
COH28DAGV ANDNFAEEF ADDD	+	++
COH47PPPQGGVGAAA AANDNFAEEF ADDD	++	+
COH23,25,29,50		++	+++
COH22,24,46,49		+++	+++
COH43-45,48,51		++++	+++
D) Strains with Novel FlbD C-termini			
COH21DAGV AA	++	+
COH40PPPQGGVGAAA AAPTTTSPRSSPWPPDI	++	++
COH18DAG AWPPTTTSPRSSPWPPDI	+++	++
COH38VPPPQ APACRCRRPRAGSARLPPTTTS PRSSPWPPDI	+++	-
COH36,37PPPQGGVG APTCDGRSLRRINKSWCPC	+++	+
COH15DAGV QVPTTSPRSSPWPPDI	++++	+
COH19DAGV AA	++++	+
COH20DAGV AA	++++	++
COH27DAG QVPTTSPRSSPTT DI	++++	+++

4.5 CONCLUDING REMARKS

We have shown for the first time that SsrA-tagged FlbD, and by extension SsrA-tagged substrates, in *C. crescentus* is rapidly in a ClpX- and ClpP-dependent manner. Our results indicate two positions in the SsrA tag that appear to influence degradation of the tagged substrate, namely, the fourth and second-last residue. A change in the fourth position from the charged residue Asp to the non-polar Val may be directly responsible for partial stabilisation of FlbD, and thus for regaining motility. A clearer picture is seen with two further suppressors, COH16 and COH17 that point to the second-last residue of the SsrA tag as being involved in SsrA-tagged substrate recognition by ClpX. It seems likely that the combination of these two point mutations is responsible for FlbD stabilisation. It would be interesting to isolate more motile suppressors from strain COH6 as it seems to offer a platform from which suppressors with defined amino acid substitutions in the SsrA tag may be isolated, possibly due to the partial stabilisation of FlbD in this strain.

While the C-terminus of FlbD seems to be tolerant to a large number of mutations that either extend or reduce its length, and/or completely change its nature, it is not clear if these mutations only increase stability of FlbD or if they also restore its activity. We have some evidence to suggest that the last 13 amino acids of FlbD are not required for motility, suggesting that FlbD variants with altered C-termini might in principle be functional.

The remainder of our results suggested the existence of a diverse range of mutations that could restore motility in cells producing stable FlbD proteins or FlbD with novel

C-termini. The *trans*- mutations must be genetically distinct as the motility values in strains bearing similar or identical C-termini are sometimes different. We may have inadvertently stumbled upon mutations in proteins that either regulate the activity of FlbD or interact with it. It will be interesting to locate these mutations as they may provide useful information about FlbD and its regulation of flagellar assembly in *C. crescentus*. The challenge for future work will be to map the second site mutation(s) and to define the exact contributions of *cis*- and *trans*- mutations for FlbD stability and/or activity.

5 IDENTIFICATION OF THE PROTEASE AND THE TURNOVER SIGNAL RESPONSIBLE FOR CELL CYCLE- DEPENDENT DEGRADATION OF THE *CAULOBACTER* FLIF MOTOR PROTEIN

Björn Grünenfelder, Sherif Tawfilis, Stefanie Gehring, Magne Østeras, Daniel Eglin
and Urs Jenal

This chapter was published as an article in the Journal of Bacteriology in August
2004, Vol. 186 (15), p. 4960-4971.

REFERENCES

Banecki, B., K. Liberek, D. Wall, A. Wawrzynow, C. Georgopoulos, E. Bertoli, F. Tanfani and M. Zylicz (1996). "Structure-function analysis of the zinc finger region of the DnaJ molecular chaperone." *J Biol Chem* **271**(25): 14840-8.

Banecki, B., A. Wawrzynow, J. Puzewicz, C. Georgopoulos and M. Zylicz (2001). "Structure-function analysis of the zinc-binding region of the ClpX molecular chaperone." *J Biol Chem* **276**(22): 18843-8.

Bochtler, M., C. Hartmann, H. K. Song, G. P. Bourenkov, H. D. Bartunik and R. Huber (2000). "The structures of HsIU and the ATP-dependent protease HsIU-HsIV." *Nature* **403**(6771): 800-5.

Brun, Y., G. Marczyński and L. Shapiro (1994). "The expression of asymmetry during *Caulobacter* cell differentiation." *Ann Rev Biochem* **63**: 419-50.

Burton, R. E., S. M. Siddiqui, Y. I. Kim, T. A. Baker and R. T. Sauer (2001). "Effects of protein stability and structure on substrate processing by the ClpXP unfolding and degradation machine." *Embo J* **20**(12): 3092-100.

Datsenko, K. A. and B. L. Wanner (2000). "One-step inactivation of chromosomal genes in *Escherichia coli* K-12 using PCR products." *Proc Natl Acad Sci U S A* **97**(12): 6640-5.

Domian, I. J., K. C. Quon and L. Shapiro (1997). "Cell type-specific phosphorylation and proteolysis of a transcriptional regulator controls the G1-to-S transition in a bacterial cell cycle." *Cell* **90**(3): 415-24.

England, J. C. and J. W. Gober (2001). "Cell cycle control of cell morphogenesis in *Caulobacter*." *Curr Opin Microbiol* **4**(6): 674-80.

Farr, G. W., K. Furtak, M. B. Rowland, N. A. Ranson, H. R. Saibil, T. Kirchhausen and A. L. Horwich (2000). "Multivalent binding of nonnative substrate proteins by the chaperonin GroEL." *Cell* **100**(5): 561-73.

Flynn, J. M., I. Levchenko, M. Seidel, S. H. Wickner, R. T. Sauer and T. A. Baker (2001). "Overlapping recognition determinants within the *ssrA* degradation tag allow modulation of proteolysis." *Proc Natl Acad Sci U S A* **98**(19): 10584-9.

Flynn, J. M., S. B. Neher, Y. I. Kim, R. T. Sauer and T. A. Baker (2003). "Proteomic discovery of cellular substrates of the ClpXP protease reveals five classes of ClpX-recognition signals." *Mol Cell* **11**(3): 671-83.

Goldberg, A. L. and A. C. St John (1976). "Intracellular protein degradation in mammalian and bacterial cells: Part 2." *Annu Rev Biochem* **45**: 747-803.

Gonciarz-Swiatek, M., A. Wawrzynow, S. J. Um, B. A. Learn, R. McMacken, W. L. Kelley, C. Georgopoulos, O. Sliemers and M. Zylicz (1999). "Recognition, targeting, and hydrolysis of the lambda O replication protein by the ClpP/ClpX protease." J Biol Chem **274**(20): 13999-4005.

Gottesman, S. (1996). "Proteases and their targets in Escherichia coli." Annu Rev Genet **30**: 465-506.

Gottesman, S. (2003). "Proteolysis in bacterial regulatory circuits." Annu Rev Cell Dev Biol **19**: 565-87.

Gottesman, S., W. P. Clark, V. de Crecy-Lagard and M. R. Maurizi (1993). "ClpX, an alternative subunit for the ATP-dependent Clp protease of Escherichia coli. Sequence and in vivo activities." J Biol Chem **268**(30): 22618-26.

Gottesman, S. and M. R. Maurizi (1992). "Regulation by proteolysis: energy-dependent proteases and their targets." Microbiol Rev **56**(4): 592-621.

Gottesman, S., E. Roche, Y. Zhou and R. T. Sauer (1998). "The ClpXP and ClpAP proteases degrade proteins with carboxy-terminal peptide tails added by the SsrA-tagging system." Genes Dev **12**(9): 1338-47.

Grimaud, R., M. Kessel, F. Beuron, A. C. Steven and M. R. Maurizi (1998). "Enzymatic and structural similarities between the Escherichia coli ATP-dependent proteases, ClpXP and ClpAP." J Biol Chem **273**(20): 12476-81.

Grünenfelder, B., S. Gehrig and U. Jenal (2003). "Role of the cytoplasmic C-terminus of the FliF motor protein in flagellar assembly and rotation." J. Bacteriol. **185**: 1624-1633.

Grünenfelder, B., G. Rummel, J. Vohradsky, D. Röder, H. Langen and U. Jenal (2001). "Proteomic analysis of the bacterial cell cycle." Proc Natl Acad Sci U S A **98**(8): 4681-4686.

Grünenfelder, B., S. Tawfilis, S. Gehrig, O. S. M, D. Eglin and U. Jenal (2004). "Identification of the protease and the turnover signal responsible for cell cycle-dependent degradation of the Caulobacter FliF motor protein." J Bacteriol **186**(15): 4960-71.

Hoskins, J. R., S. K. Singh, M. R. Maurizi and S. Wickner (2000). "Protein binding and unfolding by the chaperone ClpA and degradation by the protease ClpAP." Proc Natl Acad Sci U S A **97**(16): 8892-7.

Hoskins, J. R., K. Yanagihara, K. Mizuuchi and S. Wickner (2002). "ClpAP and ClpXP degrade proteins with tags located in the interior of the primary sequence." Proc Natl Acad Sci U S A **99**(17): 11037-42.

Hwang, B. J., K. M. Woo, A. L. Goldberg and C. H. Chung (1988). "Protease Ti, a new ATP-dependent protease in Escherichia coli, contains protein-activated ATPase and proteolytic functions in distinct subunits." J Biol Chem **263**(18): 8727-34.

Jenal, U. and T. Fuchs (1998). "An essential protease involved in bacterial cell-cycle control." EMBO J **17**(19): 5658-5669.

Jenal, U. and R. Hengge-Aronis (2003). "Regulation by proteolysis in bacterial cells." Curr Opin Microbiol **6**: 163-172.

Jenal, U. and L. Shapiro (1996). "Cell cycle-controlled proteolysis of a flagellar motor protein that is asymmetrically distributed in the Caulobacter predivisive cell." EMBO J **15**(10): 2393-406.

Johnson, R. C. and B. Ely (1977). "Isolation of spontaneously derived mutants of *Caulobacter crescentus*." Genetics **86**(1): 25-32.

Joshi, S. A., T. A. Baker and R. T. Sauer (2003). "C-terminal domain mutations in ClpX uncouple substrate binding from an engagement step required for unfolding." Mol Microbiol **48**(1): 67-76.

Joshi, S. A., G. L. Hersch, T. A. Baker and R. T. Sauer (2004). "Communication between ClpX and ClpP during substrate processing and degradation." Nat Struct Mol Biol **11**(5): 404-11.

Katayama, Y., S. Gottesman, J. Pumphrey, S. Rudikoff, W. P. Clark and M. R. Maurizi (1988). "The two-component, ATP-dependent Clp protease of *Escherichia coli*. Purification, cloning, and mutational analysis of the ATP-binding component." J Biol Chem **263**(29): 15226-36.

Keiler, K. C. and L. Shapiro (2003). "tmRNA is required for correct timing of DNA replication in *Caulobacter crescentus*." J Bacteriol **185**(2): 573-80.

Keiler, K. C., L. Shapiro and K. P. Williams (2000). "tmRNAs that encode proteolysis-inducing tags are found in all known bacterial genomes: A two-piece tmRNA functions in *Caulobacter*." Proc Natl Acad Sci U S A **97**(14): 7778-83.

Keiler, K. C., P. R. Waller and R. T. Sauer (1996). "Role of a peptide tagging system in degradation of proteins synthesized from damaged messenger RNA." Science **271**(5251): 990-3.

Kenniston, J. A., T. A. Baker, J. M. Fernandez and R. T. Sauer (2003). "Linkage between ATP consumption and mechanical unfolding during the protein processing reactions of an AAA+ degradation machine." Cell **114**(4): 511-20.

Kim, D. Y. and K. K. Kim (2003). "Crystal structure of ClpX molecular chaperone from *Helicobacter pylori*." J Biol Chem **278**(50): 50664-70.

Kim, Y. I., R. E. Burton, B. M. Burton, R. T. Sauer and T. A. Baker (2000). "Dynamics of substrate denaturation and translocation by the ClpXP degradation machine." Mol Cell **5**(4): 639-48.

Kim, Y. I., I. Levchenko, K. Fraczkowska, R. V. Woodruff, R. T. Sauer and T. A. Baker (2001). "Molecular determinants of complex formation between Clp/Hsp100 ATPases and the ClpP peptidase." Nat Struct Biol **8**(3): 230-3.

Komine, Y., M. Kitabatake, T. Yokogawa, K. Nishikawa and H. Inokuchi (1994). "A tRNA-like structure is present in 10Sa RNA, a small stable RNA from Escherichia coli." Proc Natl Acad Sci U S A **91**(20): 9223-7.

Laub, M. T., S. L. Chen, L. Shapiro and H. H. McAdams (2002). "Genes directly controlled by CtrA, a master regulator of the *Caulobacter* cell cycle." Proc Natl Acad Sci U S A **99**(7): 4632-7.

Laub, M. T., H. H. McAdams, T. Feldblyum, C. M. Fraser and L. Shapiro (2000). "Global analysis of the genetic network controlling the *Caulobacter* cell cycle." Science **290**: 2144-2148.

Levchenko, I., M. Seidel, R. T. Sauer and T. A. Baker (2000). "A specificity-enhancing factor for the ClpXP degradation machine." Science **289**(5488): 2354-6.

Levchenko, I., M. Yamauchi and T. A. Baker (1997). "ClpX and MuB interact with overlapping regions of Mu transposase: implications for control of the transposition pathway." Genes Dev **11**(12): 1561-72.

Mangan, E. K., M. Bartamian and J. W. Gober (1995). "A mutation that uncouples flagellum assembly from transcription alters the temporal pattern of flagellar gene expression in *Caulobacter crescentus*." J Bacteriol **177**(11): 3176-84.

Maurizi, M. R. (1992). "Proteases and protein degradation in *Escherichia coli*." Experientia **48**(2): 178-201.

Maurizi, M. R., W. P. Clark, Y. Katayama, S. Rudikoff, J. Pumphrey, B. Bowers and S. Gottesman (1990a). "Sequence and structure of Clp P, the proteolytic component of the ATP-dependent Clp protease of *Escherichia coli*." J Biol Chem **265**(21): 12536-45.

Maurizi, M. R., W. P. Clark, S. H. Kim and S. Gottesman (1990b). "Clp P represents a unique family of serine proteases." J Biol Chem **265**(21): 12546-52.

Meisenzahl, A. C., L. Shapiro and U. Jenal (1997). "Isolation and characterization of a xylose-dependent promoter from *Caulobacter crescentus*." J Bacteriol **179**(3): 592-600.

Muir, R. E. and J. W. Gober (2001). "Regulation of late flagellar gene transcription and cell division by flagellum assembly in *Caulobacter crescentus*." Mol Microbiol **41**(1): 117-30.

Muir, R. E., T. M. O'Brien and J. W. Gober (2001). "The *Caulobacter crescentus* flagellar gene, *fliX*, encodes a novel trans-acting factor that couples flagellar assembly to transcription." Mol Microbiol **39**(6): 1623-37.

Neher, S. B., J. M. Flynn, R. T. Sauer and T. A. Baker (2003a). "Latent ClpX-recognition signals ensure LexA destruction after DNA damage." Genes Dev **17**(9): 1084-9.

Neher, S. B., R. T. Sauer and T. A. Baker (2003b). "Distinct peptide signals in the UmuD and UmuD' subunits of UmuD/D' mediate tethering and substrate processing by the ClpXP protease." Proc Natl Acad Sci U S A **100**(23): 13219-24.

Neuwald, A. F., L. Aravind, J. L. Spouge and E. V. Koonin (1999). "AAA+: A class of chaperone-like ATPases associated with the assembly, operation, and disassembly of protein complexes." Genome Res **9**(1): 27-43.

Oh, B. K. and D. Apirion (1991). "10Sa RNA, a small stable RNA of Escherichia coli, is functional." Mol Gen Genet **229**(1): 52-6.

Ortega, J., H. S. Lee, M. R. Maurizi and A. C. Steven (2002). "Alternating translocation of protein substrates from both ends of ClpXP protease." Embo J **21**(18): 4938-49.

Osteras, M. and U. Jenal (2000). "Regulatory circuits in Caulobacter." Curr Opin Microbiol **3**(2): 171-6.

Osteras, M., A. Stotz, S. Schmid Nuoffer and U. Jenal (1999). "Identification and transcriptional control of the genes encoding the *Caulobacter crescentus* ClpXP protease." J. Bacteriol. **181**(10): 3039-3050.

Parsell, D. A., A. S. Kowal, M. A. Singer and S. Lindquist (1994). "Protein disaggregation mediated by heat-shock protein Hsp104." Nature **372**(6505): 475-8.

Potocka, I., M. Thein, M. Osteras, U. Jenal and M. R. Alley (2002). "Degradation of a Caulobacter soluble cytoplasmic chemoreceptor is ClpX dependent." J. Bacteriol. **184**(23): 6635-41.

Quon, K. C., G. T. Marczyński and L. Shapiro (1996). "Cell cycle control by an essential bacterial two-component signal transduction protein." Cell **84**: 83-93.

Quon, K. C., B. Yang, I. J. Domian, L. Shapiro and G. T. Marczyński (1998). "Negative control of bacterial DNA replication by a cell cycle regulatory protein that binds at the chromosome origin." Proc Natl Acad Sci USA **95**(1): 120-5.

Rabilloud, T. (2000). Proteome Research: Two-Dimensional Gel Electrophoresis and Identification Methods, Springer Verlag.

Roche, E. D. and R. T. Sauer (1999). "SsrA-mediated peptide tagging caused by rare codons and tRNA scarcity." Embo J **18**(16): 4579-89.

Ryan, K. R., E. M. Judd and L. Shapiro (2002). "The CtrA Response Regulator Essential for *Caulobacter crescentus* Cell-cycle Progression Requires a Bipartite Degradation Signal for Temporally Controlled Proteolysis." J Mol Biol **324**(3): 443-55.

Sambrook, J., E. F. Fritsch and T. Maniatis (1989). Molecular cloning. A laboratory manual, Cold Spring Harbor Laboratory Press.

Seol, J. H., S. H. Baek, M. S. Kang, D. B. Ha and C. H. Chung (1995a). "Distinctive roles of the two ATP-binding sites in ClpA, the ATPase component of protease Ti in *Escherichia coli*." J Biol Chem **270**(14): 8087-8092.

Seol, J. H., K. M. Woo, M. S. Kang, D. B. Ha and C. H. Chung (1995b). "Requirement of ATP hydrolysis for assembly of ClpA/ClpP complex, the ATP-dependent protease Ti in *Escherichia coli*." Biochem Biophys Res Commun **217**(1): 41-51.

Singh, S. K., R. Grimaud, J. R. Hoskins, S. Wickner and M. R. Maurizi (2000). "Unfolding and internalization of proteins by the ATP-dependent proteases ClpXP and ClpAP." Proc Natl Acad Sci U S A **97**(16): 8898-903.

Singh, S. K. and M. R. Maurizi (1994). "Mutational analysis demonstrates different functional roles for the two ATP-binding sites in ClpAP protease from *Escherichia coli*." J Biol Chem **269**(47): 29537-29545.

Singh, S. K., J. Rozycki, J. Ortega, T. Ishikawa, J. Lo, A. C. Steven and M. R. Maurizi (2001). "Functional domains of the ClpA and ClpX molecular chaperones identified by limited proteolysis and deletion analysis." J Biol Chem **9**: 9.

Smith, C. K., T. A. Baker and R. T. Sauer (1999). "Lon and Clp family proteases and chaperones share homologous substrate- recognition domains." Proc Natl Acad Sci U S A **96**(12): 6678-82.

Straus, D. B., W. A. Walter and C. A. Gross (1988). "*Escherichia coli* heat shock gene mutants are defective in proteolysis." Genes Dev **2**(12B): 1851-8.

Sutton, M. D., B. T. Smith, V. G. Godoy and G. C. Walker (2000). "The SOS response: recent insights into umuDC-dependent mutagenesis and DNA damage tolerance." Annu Rev Genet **34**: 479-497.

Thompson, M. W., S. K. Singh and M. R. Maurizi (1994). "Processive degradation of proteins by the ATP-dependent Clp protease from *Escherichia coli*. Requirement for the multiple array of active sites in ClpP but not ATP hydrolysis." J Biol Chem **269**(27): 18209-15.

Tsai, J. W. and M. R. Alley (2001). "Proteolysis of the *Caulobacter* McpA chemoreceptor is cell cycle regulated by a ClpX-dependent pathway." J Bacteriol **183**(17): 5001-7.

Turgay, K., J. Hahn, J. Burghoorn and D. Dubnau (1998). "Competence in *Bacillus subtilis* is controlled by regulated proteolysis of a transcription factor." EMBO J **17**(22): 6730-6738.

Wah, D. A., I. Levchenko, T. A. Baker and R. T. Sauer (2002). "Characterization of a specificity factor for an AAA+ ATPase: assembly of SspB dimers with ssrA-tagged proteins and the ClpX hexamer." Chem Biol **9**(11): 1237-45.

Walker, J. E., M. Saraste, M. J. Runswick and N. J. Gay (1982). "Distantly related sequences in the alpha- and beta-subunits of ATP synthase, myosin, kinases and other ATP-requiring enzymes and a common nucleotide binding fold." Embo J **1**(8): 945-51.

Wang, J., J. A. Hartling and J. M. Flanagan (1997). "The structure of ClpP at 2.3 Å resolution suggests a model for ATP-dependent proteolysis." Cell **91**(4): 447-56.

Wingrove, J. A., E. K. Mangan and J. W. Gober (1993). "Spatial and temporal phosphorylation of a transcriptional activator regulates pole-specific gene expression in *Caulobacter*." Genes Dev **7**(10): 1979-92.

Withey, J. H. and D. I. Friedman (2003). "A salvage pathway for protein structures: tmRNA and trans-translation." Annu Rev Microbiol **57**: 101-23.

Wonnacott, T. H. and R. J. Wonnacott (1990). Introductory statistics, Fifth edition, John Wiley and Sons, Inc.

Wright, R., C. Stephens, G. Zweiger, L. Shapiro and M. R. Alley (1996). "*Caulobacter* Lon protease has a critical role in cell-cycle control of DNA methylation." Genes Dev **10**(12): 1532-42.

Wu, J. and A. Newton (1997). "Regulation of the *Caulobacter* flagellar gene hierarchy; not just for motility." Mol Microbiol **24**(2): 233-239.

Wu, L. J. and J. Errington (2004). "Coordination of cell division and chromosome segregation by a nucleoid occlusion protein in *Bacillus subtilis*." Cell **117**(7): 915-25.

Zweiger, G., G. Marczyński and L. Shapiro (1994). "A *Caulobacter* DNA methyltransferase that functions only in the predivisional cell." J Mol Biol **235**(2): 472-85.

Curriculum Vitae

Name Sherif Tawfilis
Nationality Australian
Date of Birth 27.06.1979
Family Status Single

Languages Spoken English, Arabic and German (/Swiss German)

Address Jägerstrasse 15
4058 Basel
Switzerland (Until November 2004, and thereafter,

10 Jacobs Drive
South Clayton, VIC 3169
Australia)

Email Sherif.Tawfilis@unibas.ch

Academic Background

September 2000 – September 2004

Postgraduate PhD student in Prof. Dr. U. Jenal's group (partly supervised by Dr. Magne Østeras)

Biozentrum der Universität Basel, Molekulare Mikrobiologie,
Klingelbergstrasse 50-70, CH-4056 Basel, Switzerland

My research focused on substrate identification of the essential ClpXP protease in *Caulobacter crescentus*, a dimorphic non-pathogenic alpha proteobacterium. *C. crescentus* offers an excellent model system through which important questions pertaining to bacterial development can be addressed. The ClpXP protease is required for survival and G1 cell cycle progression, and its activity is therefore intimately linked with bacterial development. My research has provided several clues as to the role of proteolysis in the cell cycle through the degradation of certain novel proteins. One of my secondary interests was the regulation of motility in *C. crescentus*, through the flagellar regulator FlbD. Much of the work I had conducted suggested the existence of motility regulatory pathways/factors previously uncharacterised.

September 1999 – August 2000

Research Assistant in Dr. C. Gray's group

F.Hoffmann La-Roche AG, PRPI
Grenzacherstrasse 124, 4070 Basel, Switzerland

My research was largely focused on drug resistant strains of *Haemophilus influenzae* and *Moraxella cattharalis*, and the examination of their transcriptomes under various conditions by Affymterix chips.

March 1999 – July 1999

Research Assistant in Dr. F. Köntgen's group

The Walter and Eliza Hall Institute of Medical Research
1G Royal Parade, Parkville, VIC 3050, Australia

I worked as part of a team that was interested in the generation of catalytic antibodies in a small biotechnology company, CATAB.

February 1998 – November 1998

Bachelor of Science (Honours) research in Dr. L. Corcoran's group

Department of Medical Microbiology (The University of Melbourne)
The Walter and Eliza Hall Institute of Medical Research
1G Royal Parade, Parkville, Victoria 3050, Australia

Thesis title: Identification of Oct-2 target genes in murine B-cells

1995 – 1997

Bachelor of Science (Biomedical), with majors in Microbiology and Immunology

Monash University
Wellington Road, Clayton, VIC 3800, Australia

Employment History

2001 –

Private party-catering service (Middle Eastern/Asian Cuisine)

October 2001 – February 2002

Assistant Chef at Restaurant Cantina Don Camillo

Burgweg 7, 4058 Basel, Switzerland

October 2000 – March 2001

Casual service assistant at Coop Supermarkets

Centralbahnplatz 4, 4051 Basel, Switzerland

January 1999 – March 1999

Summer student (Praktikant) in Dr. C. Grays's group

F.Hoffmann La-Roche AG, PRPI

Grenzacherstrasse 124, 4070 Basel, Switzerland

November 1998 – January 1999

Summer student in Dr. F. Köntgen's group

The Walter and Eliza Hall Institute of Medical Research

1G Royal Parade, Parkville, VIC 3050, Australia

November 1997 – January 1998

Summer student in Prof. Dr. J. W. Goding's group

Monash Medical School, The Alfred Hospital

Commercial Road Prahran, VIC 3181, Australia

August 1994 – October 1998

Casual service assistant at Coles Supermarkets

Oakleigh Central Shopping Centre

Oakleigh, VIC 3166

Specialised Technical Experience

- * Extensive knowledge of proteomic and 2D gel techniques
- * Large scale protein preparation/enrichment for 2D gels
- * *Caulobacter* genetics
- * Transduction, transposition and gene manipulation
- * PCR, cloning, site-directed mutagenesis
- * Protein purification

- * Protein-DNA interaction techniques
- * Cell culture and transfection
- * Some confocal microscopy and FACS experience
- * PDQuest 2D gel analysis software, and general web based DNA/protein analysis programs

Academic Scholarships

September 2000 Awarded a four year scholarship by the Schweizer National Fonds to conduct my doctoral research

1997 Awarded life-time membership to the Golden Key National Honour Society

Teaching Experience

I annually took part in a practical Microbiology one-week course (Blockkurs) held at the Biozentrum for graduating Bachelor of Science students. The course was designed to introduce the students to bacterial genetics using *Caulobacter* as a model system

During my PhD studies at the Biozentrum, I planned and supervised the Honours degree project of Daniel Eglin, part of which was published recently along with some of my work (Grünenfelder et al., 2004). This experience was not only valuable scientifically. It allowed me to help develop the creative skills and confidence of a young scientist; this was one of the most rewarding experiences during my PhD.

Publication List

Grünenfelder, B., **Tawfilis, S.**, Gehring, B., Østeras, M., Eglin, D., and Jenal, U. (2004). Identification of the protease and the turnover signal responsible for cell cycle-dependent degradation of the *Caulobacter* FliF motor protein. *Journal of Bacteriology* **186**: 4960-71.

Corcoran, L.M., **Tawfilis, S.** and Barlow, L. (1999). Generation of B lymphoma cell lines from knockout mice by transformation in vivo with E μ -myc transgene. *Journal of Immunological Methods* **228**: 131-138.

Tawfilis, S., Suwaki, N., Edwards-Ingram, L.C., Jenal, U., and Alley, M. R. K. (2004). The application of the nitrate assimilation operon promoter to control gene expression in *Caulobacter* (In preparation).

Interests

My main passion is Flamenco dancing, which I have been learning for several years now. One of my personal goals is to perfect certain styles of Flamenco and fuse them with other dances. I also enjoy dancing to other music such as Street Latin and Jazz. Since coming to Europe, I began to realise my love of travelling and experiencing other cultures. I am an avid cook and enjoy experimenting and creating cross-cultural dishes. Subjects such as psychology, instinct, behaviour and philosophy have always fascinated me and I try to learn more about them as often as I can.

References

Prof. Dr. U. Jenal
Division of Molecular Microbiology
Biozentrum der Universität Basel
Klingelbergstrasse 70,
CH-4056 Basel, Switzerland

Email : Urs.Jenal@unibas.ch

Dr. Magne Osteras
Scientific Director
Fasteris SA
P.O. Box 28
109 ch. du Pont-du-Centenaire
1228 Plan-les-Ouates
Switzerland

Email: Magne.Osteras@fasteris.com

Dr. Frank Köntgen
Director & CEO
OZGENE Pty Ltd
PO BOX 1128
Bentley DC, WA 6983
Australia

Email : Koentgen@ozgene.com

